



UTeV - 2004



The Physics of Calorimetry

Dan Green

Fermilab

US CMS Program Manager



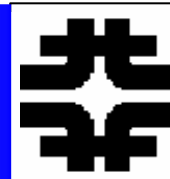
Outline



- **Units and orders of magnitude**
- **Ionization and dE/dx , Multiple Scattering**
- **Photon interactions**
 - Photoelectric effect
 - Compton scattering
 - Pair Production
- **Electron interactions**
 - Bremsstrahlung
 - Critical energy



References



- *General References - A*

Mechanics, Electricity and Magnetism and Quantum Mechanics

- [1] The Feynman Lectures in Physics, R. Feynman, R. Leighton, M. Sands, Addison-Wesley Publishing Co., Inc. (1963).
- [2] Classical Mechanics, H. Goldstein, Addison-Wesley Publishing Co., Inc. (1950).
- [3] Classical Electricity and Magnetism, W.K.H. Panofsky and M. Phillips, Addison-Wesley Publishing Co., Inc. (1962).
- [4] Quantum Mechanics, E. Merzbacher, John Wiley & Sons, Inc. (1961).

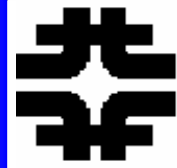
- *General References - B*

Textbooks on Particle Detectors

- [1] Detectors for Particle Radiation, K. Kleinknecht, Cambridge University Press (1987).
- [2] Experimental Techniques in High Energy Physics, T. Ferbel, Addison-Wesley Publishing Co., Inc. (1987).
- [3] Instrumentation in High Energy Physics, Ed. F. Sauli, World Scientific (1992).
- [4] Instrumentation in Elementary Particle Physics, J.C. Anjos, D. Hartill, F. Sauli, M. Sheaf, Rio de Janeiro, 1990, World Scientific Publishing Co. (1992).
- [5] Instrumentation in Elementary Particle Physics, C.W. Fabjan, J.E. Pilcher, Trieste 1987, World Scientific Publishing Co. (1988).
- [6] "Particle Detectors" C.W. Fabjan, H.F. Fisher, Repts. Progr. Phys. 43, 1003 (1980).



Fundamental Constants



$$\hbar c = 0.2 \text{ GeV fm}, 1 \text{ GeV} = 10^9 \text{ eV}$$

$$= 2000 \text{ eV } \overset{\circ}{\text{A}}$$

$$1 \overset{\circ}{\text{A}} = 10^{-8} \text{ cm}, 1 \text{ fm} = 10^{-13} \text{ cm}$$

$$= 10 \text{ nm.}$$

$$M_e = 0.51 \text{ MeV}$$

$$M_p = 938 \text{ MeV}$$

$$\alpha = 1/137$$

$$\lambda = 1/m$$

$$a = \lambda / \alpha$$

$$kT = 1/40 \text{ eV}$$

Quantity	Symbol, equation	Value	Uncert. (ppm)
speed of light in vacuum	c	299 792 458 m s ⁻¹	exact*
Planck constant	h	6.626 075 5(40) × 10 ⁻³⁴ J s	0.60
Planck constant, reduced	$\hbar \equiv h/2\pi$	1.054 572 66(63) × 10 ⁻³⁴ J s = 6.582 122 0(20) × 10 ⁻²² MeV s	0.60 0.30
electron charge magnitude	e	1.602 177 33(49) × 10 ⁻¹⁹ C = 4.803 206 8(15) × 10 ⁻¹⁰ esu	0.30, 0.30
conversion constant	$\hbar c$	197.327 053(59) MeV fm	0.30
conversion constant	$(\hbar c)^2$	0.389 379 66(23) GeV ² mbarn	0.59
electron mass	m_e	0.510 999 06(15) MeV/c ² = 9.109 389 7(54) × 10 ⁻³¹ kg	0.30, 0.59
proton mass	m_p	938.272 31(28) MeV/c ² = 1.672 623 1(10) × 10 ⁻²⁷ kg = 1.007 276 470(12) u = 1836.152 701(37) m_e	0.30, 0.59 0.012, 0.020
deuteron mass	m_d	1875.613 39(57) MeV/c ²	0.30
unified atomic mass unit (u)	(mass ¹² C atom)/12 = (1 g)/(N _A mol)	931.494 32(28) MeV/c ² = 1.660 540 2(10) × 10 ⁻²⁷ kg	0.30, 0.59
permittivity of free space	ϵ_0	8.854 187 817 ... × 10 ⁻¹² F m ⁻¹	exact
permeability of free space	μ_0	4π × 10 ⁻⁷ N A ⁻² = 12.566 370 614 ... × 10 ⁻⁷ N A ⁻²	exact
fine-structure constant	$\alpha = e^2/4\pi\epsilon_0\hbar c$	1/137.035 989 5(61) [†]	0.045
classical electron radius	$r_e = e^2/4\pi\epsilon_0 m_e c^2$	2.817 940 92(38) × 10 ⁻¹⁵ m	0.13
electron Compton wavelength	$\lambda_e = \hbar/m_e c = r_e \alpha^{-1}$	3.861 593 23(35) × 10 ⁻¹³ m	0.089
Bohr radius ($m_{\text{nucleus}} = \infty$)	$a_{\infty} = 4\pi\epsilon_0\hbar^2/m_e e^2 = r_e \alpha^{-2}$	0.529 177 249(24) × 10 ⁻¹⁰ m	0.045
wavelength of 1 eV/c particle	$\hbar c/e$	1.239 842 44(37) × 10 ⁻⁶ m	0.30
Rydberg energy	$\hbar c R_{\infty} = m_e e^4/2(4\pi\epsilon_0)^2 \hbar^2 = m_e c^2 \alpha^2/2$	13.605 698 1(40) eV	0.30
Thomson cross section	$\sigma_T = 8\pi r_e^2/3$	0.665 246 16(18) barn	0.27
Bohr magneton	$\mu_B = e\hbar/2m_e$	5.788 382 63(52) × 10 ⁻¹¹ MeV T ⁻¹	0.089
nuclear magneton	$\mu_N = e\hbar/2m_p$	3.152 451 66(28) × 10 ⁻¹⁴ MeV T ⁻¹	0.089
electron cyclotron freq./field	$\omega_{\text{cycl}}^e/B = e/m_e$	1.758 819 62(53) × 10 ¹¹ rad s ⁻¹ T ⁻¹	0.30
proton cyclotron freq./field	$\omega_{\text{cycl}}^p/B = e/m_p$	9.578 830 9(29) × 10 ⁷ rad s ⁻¹ T ⁻¹	0.30
gravitational constant	G_N	6.672 59(85) × 10 ⁻¹¹ m ³ kg ⁻¹ s ⁻² = 6.707 11(86) × 10 ⁻³⁹ $\hbar c$ (GeV/c ²) ⁻²	128 128
standard grav. accel., sea level	g	9.806 65 m s ⁻²	exact
Avogadro constant	N_A	6.022 136 7(36) × 10 ²³ mol ⁻¹	0.59
Boltzmann constant	k	1.380 658(12) × 10 ⁻²³ J K ⁻¹ = 8.617 385(73) × 10 ⁻⁵ eV K ⁻¹	8.5 8.4
molar volume, ideal gas at STP	$N_A k(273.15 \text{ K})/(101 325 \text{ Pa})$	22.414 10(19) × 10 ⁻³ m ³ mol ⁻¹	8.4
Wien displacement law constant	$b = \lambda_{\text{max}} T$	2.897 756(24) × 10 ⁻³ m K	8.4
Stefan-Boltzmann constant	$\sigma = \pi^2 k^4/60\hbar^3 c^2$	5.670 51(19) × 10 ⁻⁸ W m ⁻² K ⁻⁴	34
Fermi coupling constant [†]	$G_F/(\hbar c)^3$	1.166 39(2) × 10 ⁻⁵ GeV ⁻²	20
weak mixing angle	$\sin^2 \hat{\theta}(M_Z)$ (\overline{MS})	0.2319(5)	2200
W^{\pm} boson mass	m_W	80.22(26) GeV/c ²	3200
Z^0 boson mass	m_Z	91.187(7) GeV/c ²	77
strong coupling constant	$\alpha_s(m_Z)$	0.116(5)	43000
$\pi = 3.141 592 653 589 793 238$		$e = 2.718 281 828 459 045 235$	$\gamma = 0.577 215 664 901 532 861$
1 in ≡ 0.0254 m		1 G ≡ 10 ⁻⁴ T	1 eV = 1.602 177 33(49) × 10 ⁻¹⁹ J
1 Å ≡ 10 nm		1 dyne ≡ 10 ⁻⁵ N	1 eV/c ² = 1.782 662 70(54) × 10 ⁻³⁶ kg
1 barn ≡ 10 ⁻²⁸ m ²		1 erg ≡ 10 ⁻⁷ J	2.997 924 58 × 10 ⁹ esu = 1 C
			1 atmosphere ≡ 760 torr ≡ 101 325 Pa

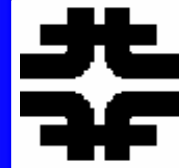
* The meter is defined to be the length of path traveled by light in vacuum in 1/299 792 458 s. See B.W. Petley, Nature 303, 373 (1983).

† At $Q^2 = 0$. At $Q^2 \approx m_W^2$ the value is approximately 1/128.

‡ See discussion in Sec. 26 "Standard Model of electroweak interactions."



Properties of Materials



$$Z/A \sim 1/2$$

$$V \sim A \sim a^3$$

$$\sigma_T \sim A^{2/3}$$

$$[N_0 \rho / A] \langle L \rangle \sigma = 1$$

[# targets(nuclei)/volume]

longitudinal distance (transverse distance²)

$$\rho \langle L \rangle = A / \sigma$$

$$\sim A^{1/3}$$

$$dE/d(\rho x) \sim 1.5 \text{ MeV}/(\text{gm}/\text{cm}^2)$$

$$\rho X_0 \sim 1/Z$$

ATOMIC AND NUCLEAR PROPERTIES OF MATERIALS

Table revised June 1994. Gases are evaluated at 20°C, 1 atm, (in parentheses) or at STP [square brackets].

Material	Z	A	Nuclear ^a total cross section σ_T [barn]	Nuclear ^b inelastic cross section σ_I [barn]	Nuclear ^c collision length λ_T [g/cm ²]	Nuclear ^c interaction length λ_I [g/cm ²]	dE/dx_{min} ^d [MeV g/cm ²] () is for gas	Radiation length ^e X_0 [cm] () is for gas	Density ^f [g/cm ³] () is for gas	Refractive index n^f () is for gas () is (n-1) × 10 ⁶ for gas	
H ₂ gas	1	1.01	0.0387	0.033	43.3	50.8	(4.103)	61.28	865	(0.0838)[0.090]	[140]
H ₂ (B.C., 26K)	1	1.01	0.0387	0.033	43.3	50.8	4.045	61.28	865	0.0708	1.112
D ₂	1	2.01	0.073	0.061	45.7	54.7	(2.052)	122.6	757	0.162[0.177]	1.128
He	2	4.00	0.133	0.102	49.9	65.1	(1.937)	94.32	755	0.125[0.178]	1.024[35]
Li	3	6.94	0.211	0.157	54.6	73.4	1.639	82.76	155	0.534	—
Be	4	9.01	0.268	0.199	55.8	75.2	1.594	65.19	35.3	1.848	—
C	6	12.01	0.331	0.231	60.2	86.3	1.745	42.70	18.8	2.265 ^g	—
N ₂	7	14.01	0.379	0.265	61.4	87.8	(1.825)	37.99	47.0	0.808[1.25]	1.205[300]
O ₂	8	16.00	0.420	0.292	63.2	91.0	(1.801)	34.24	30.0	1.14[1.43]	1.22[266]
Ne	10	20.18	0.507	0.347	66.1	96.6	(1.724)	28.94	24.0	1.207[0.900]	1.092[67]
Al	13	26.98	0.634	0.421	70.6	106.4	1.615	24.01	8.9	2.70	—
Si	14	28.09	0.660	0.440	70.6	106.0	1.664	21.82	9.36	2.33	—
Ar	18	39.95	0.868	0.566	76.4	117.2	(1.519)	19.55	14.0	1.40[1.782]	1.233[283]
Ti	22	47.88	0.995	0.637	79.9	124.9	1.476	16.17	3.56	4.54	—
Fe	26	55.85	1.120	0.703	82.8	131.9	1.451	13.84	1.76	7.87	—
Cu	29	63.55	1.232	0.782	85.6	134.9	1.403	12.86	1.43	8.96	—
Ge	32	72.59	1.365	0.858	88.3	140.5	1.371	12.25	2.30	5.323	—
Sn	50	118.69	1.967	1.21	100.2	163	1.264	8.82	1.21	7.31	—
Xe	54	131.29	2.120	1.29	102.8	169	(1.255)	8.48	2.77	3.057[5.858]	[705]
W	74	183.85	2.767	1.65	110.3	185	1.145	6.76	0.35	19.3	—
Pt	78	195.08	2.861	1.708	113.3	189.7	1.129	6.54	0.305	21.45	—
Pb	82	207.19	2.960	1.77	116.2	194	1.123	6.37	0.56	11.35	—
U	92	238.03	3.378	1.98	117.0	199	1.082	6.00	≈0.32	≈18.95	—
Air, (20°C, 1 atm.), [STP]					62.0	90.0	(1.815)	36.66	[30420]	(1.205)[1.29]	(273)[293]
H ₂ O					60.1	84.9	1.991	36.08	36.1	1.00	1.33
CO ₂					62.4	90.5	(1.819)	36.2	[18310]	[1.977]	[410]
Shielding concrete ^h					67.4	99.9	1.711	26.7	10.7	2.5	—
Borosilicate glass (Pyrex) ^l					66.2	97.6	1.695	28.3	12.7	2.23	1.474
SiO ₂ (fused quartz) ^m					67.0	99.2	1.697	27.05	11.7	2.32 ^m	1.458
Methane (CH ₄)					54.7	74.0	(2.417)	46.5	[64850]	0.423[0.717]	[444]
Ethane (C ₂ H ₆)					55.73	75.71	(2.304)	45.66	[34035]	0.509(1.356) ⁿ	(1.038) ⁿ
Propane (C ₃ H ₈)					—	—	(2.262)	—	—	(1.879)	—
Isobutane ((CH ₃) ₂ CHCH ₃)					56.3	77.4	(2.239)	45.2	[16930]	[2.67]	[1900]
Octane, liquid (CH ₃ (CH ₂) ₆ CH ₃)					—	—	2.123	—	—	0.703	—
Paraffin wax (CH ₃ (CH ₂) _n CH ₃ , (n) ≈ 25)					—	—	2.087	—	—	0.93	—
Nylon, type 6					—	—	1.974	—	—	1.14	—
Polycarbonate (Lexan)					—	—	1.886	—	—	1.200	—
Polyethylene terephthalate (Mylar) (C ₁₀ H ₈ O ₂)					60.2	85.7	1.848	39.95	28.7	1.39	—
Polyethylene (monomer CH ₂ =CH ₂)					56.9	78.8	2.076	44.8	≈47.9	0.92-0.95	—
Polyimide film (Kapton)					—	—	1.820	—	—	1.420	—
Polymethylmethacrylate (Lucite, Plexiglas) (monomer (CH ₂ =C(CH ₃)CO ₂ CH ₃))					59.2	83.6	1.929	40.55	≈34.4	1.16-1.20	≈1.49
Polystyrene, scintillator (monomer C ₆ H ₅ CH=CH ₂)					58.4	82.0	1.936	43.8	42.4	1.032	1.581
Polytetrafluoroethylene (Teflon) (monomer CF ₂ =CF ₂)					—	—	1.671	—	—	2.20	—
Polyvinyltoluene, scintillator (monomer 2-CH ₃ C ₆ H ₄ CH=CH ₂)					—	—	1.956	—	—	1.032	—
Barium fluoride (BaF ₂)					92.1	146	1.303	9.91	2.05	4.89	1.56
Bismuth germanate (BGO) (Bi ₄ Ge ₃ O ₁₂)					97.4	156	1.251	7.98	1.12	7.1	2.15
Cesium iodide (CsI)					—	—	1.243	—	—	4.51	—
Lithium fluoride (LiF)					62.00	88.24	1.614	39.25	14.91	2.632	1.392
Sodium fluoride (NaF)					66.78	97.57	1.69	29.87	11.68	2.558	1.336
Sodium iodide (NaI)					94.8	152	1.305	9.49	2.59	3.67	1.775
Silica Aerogel ^o					65.5	95.7	1.83	29.85	≈150	0.1-0.3	1.0+0.25 _p
NEMA G10 plate ^p					62.6	90.2	1.87	33.0	19.4	1.7	—



Properties of Materials



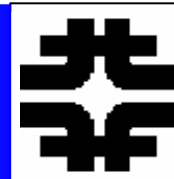
Table 1: Physical properties of some materials used in calorimeters.

	Z	ρ g.cm ⁻³	I/Z eV	(1/ ρ)dT/dx MeV/g.cm ⁻³	ϵ MeV	X ₀ cm	λ_{int} cm
C	6	2.2	12.3	1.85	103	~ 19	38.1
Al	13	2.7	12.3	1.63	47	8.9	39.4
Fe	26	7.87	10.7	1.49	24	1.76	16.8
Cu	29	8.96		1.40	~ 20	1.43	15.1
W	74	19.3		1.14	~ 8.1	0.35	9.6
Pb	82	11.35	10.0	1.14	6.9	0.56	17.1
U	92	18.7	9.56	1.10	6.2	0.32	10.5

Ionization energy
~ E₀ = 13.6 eV
critical energy ~ 1/Z
X₀ ~ (A/Z)(1/Z) ~ 1/Z
<L> ~ A^{1/3}/ ρ



Energy, Size, Coupling



Electromagnetic and Strong Coupling

$$\alpha = e^2 / \hbar c \sim 1/137$$

$$\alpha_s = g_s^2 / \hbar c \sim (1/10 - 1) \text{ (Table 1.1)}$$

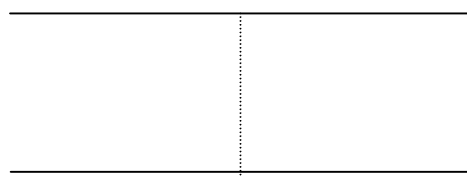
$$E_o = -mc^2 \alpha^2 / 2 \text{ (Table 1.1, Rydberg)}$$

$$m_e c^2 = 0.51 \text{ MeV}, E_o = 13.6 \text{ eV}$$

$$a_o \sim \lambda / \alpha = 0.56 \text{ Angstroms}$$

$$E_n = E_o / n^2$$

$$a_n = a_o / n^2$$

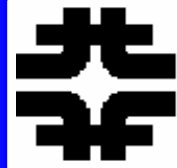


Amplitude $\sim \alpha$

Binding Energy $\sim \alpha^2$



Atoms - Ionization Energy and Size



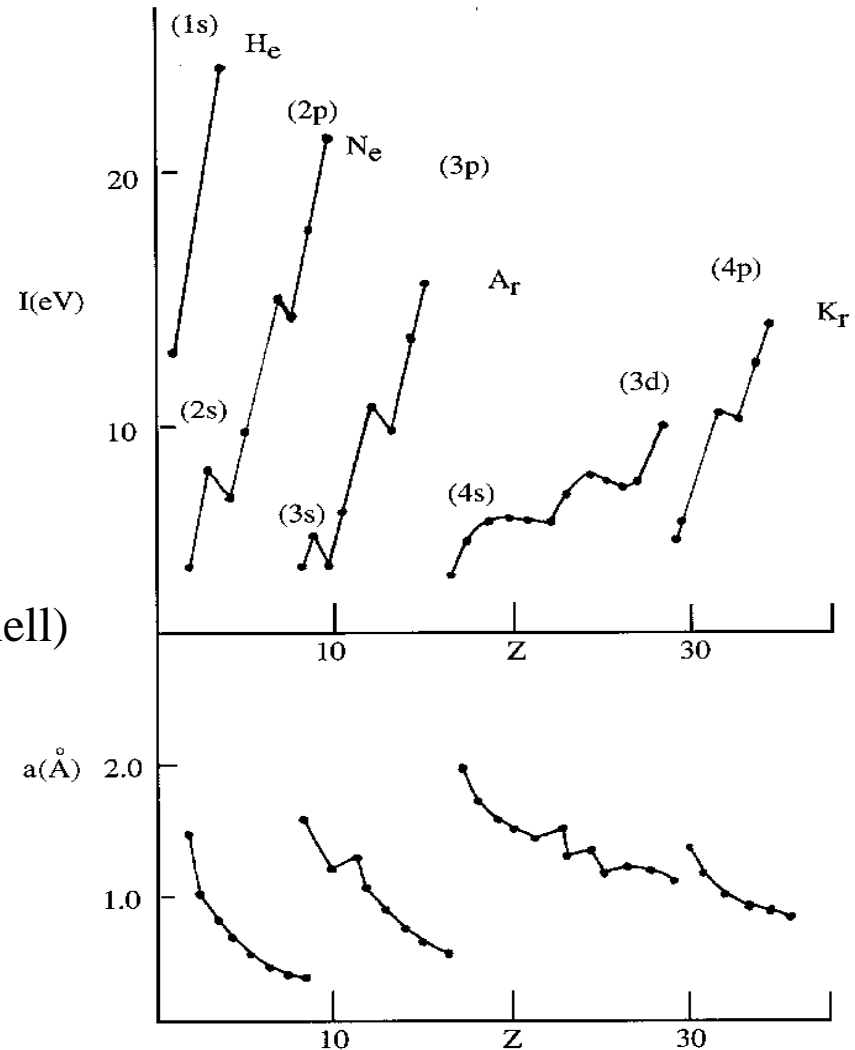
$n = 1, l = 0, m_l = 1, \text{spin} = 2$
 $n = 2, l = 0, 2 \text{ states}$
 $l = 1, 6 \text{ states } [(2l+1)2]$

metals \rightarrow noble gases

centrifugal repulsive potential
 $U \sim L^2/r^2$
Lower l fills first

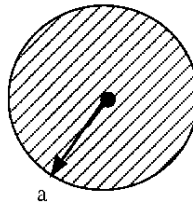
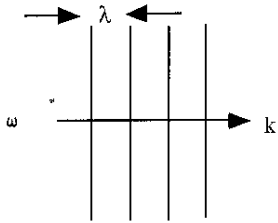
Metals “see” 1 e of charge (closed shell)

Lightly bound, $E \sim 1/n^2, a \sim n^2$





Cross Sections



$$N(x) = N(0) \exp(-N_o \rho x \sigma / A)$$

$$\langle L \rangle^{-1} = [N_o \rho \sigma / A] (cm)^{-1}$$

$$\langle L \rho \rangle^{-1} = [N_o \sigma / A] (gm / cm^2)^{-1}$$

$$\sigma_{atom} \sim \pi a_o^2 \sim 3 \times 10^8 b, a_o \sim 1 \text{ \AA}$$

$$\sigma_{nuc} \sim \pi a_N^2 \sim 31 mb, a_N \sim 1 fm$$

$$(\hbar c)^2 = 0.4 GeV^2 mb$$

$$1 mb = 10^{-27} cm^2, 1 b = 10^{-24} cm^2$$

$$\sigma_N \sim \pi a_N^2$$

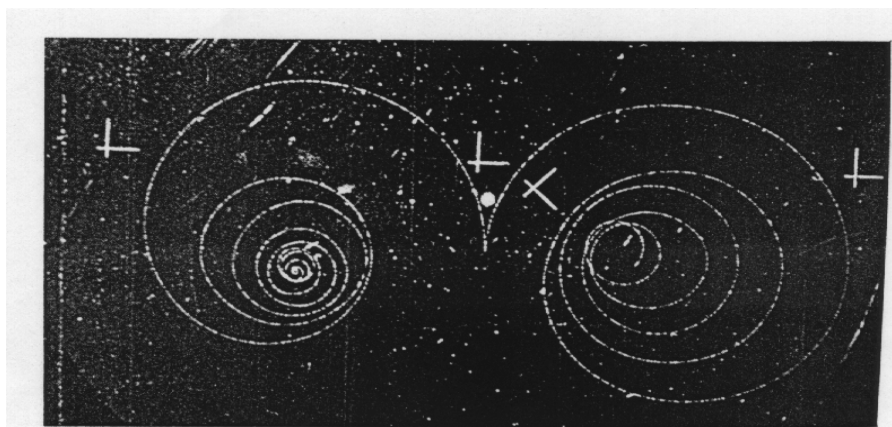
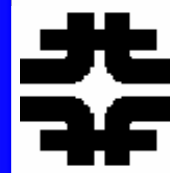
$$\sim A^{2/3}$$

$$\langle L \rangle \sim A^{1/3} \quad (Eq. 1.8)$$

$$\lambda_I \sim (35 gm / cm^2) A^{1/3}$$



Nuclear vs EM Cross Sections



$$\sigma_N \sim A^{2/3} \lambda_p^2$$

$$\sigma_B \sim (Z\alpha)^2 \alpha \lambda_e^2$$

$$\lambda_1 / X_o \sim (Z / A) / [5.1 A^{2/3}]$$

see Properties

cross at $Z \sim 3$

at high Z , $X_o \ll \lambda$, Why

basis of calorimetric particle ID



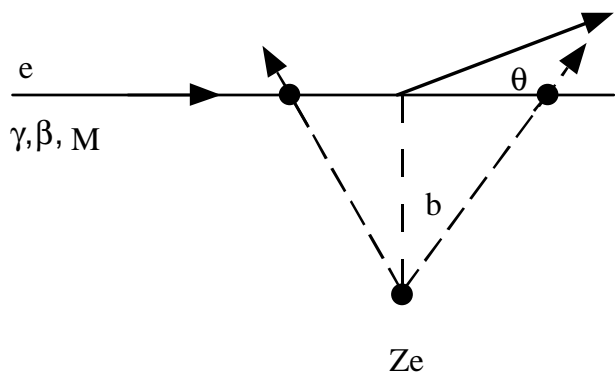
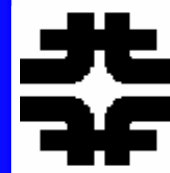
Ionization and dE/dx



- **Coulomb Collisions**
- **Multiple Scattering**
- **“Radiation” Length**
- **Recoil Energy Distribution**
- **dE/dx**
- **Minimum Ionizing Particles**
- **Range and Momentum**



Coulomb Scattering



$$dP \sim d\vec{b} = d\sigma \quad \text{Can't aim}$$

$$d\sigma \sim b db d\phi = \frac{d\sigma}{d\Omega} d\Omega, \quad d\Omega = \sin\theta d\theta d\phi$$

$$\frac{d\sigma}{d\Omega} = \frac{b}{\sin\theta} \left(\frac{db}{d\theta} \right)$$

$$F(b) = Ze^2 / b^2$$

$$\Delta t = 2b / v$$

$$\Delta p_T \sim F(b)\Delta t, \quad \vec{F} \equiv d\vec{p} / dt$$

$$\theta \sim \Delta p_T / p, \quad \Delta p_T = 2Z\alpha / bv$$

$$\theta_R \sim 2Z\alpha / pvb$$

$$\Delta p_T \rightarrow 2Z\alpha/bc$$

independent of incident particle mass, velocity

→ MIP

$$\frac{d\sigma_R}{d\Omega} \sim \left(\frac{Z\alpha}{Mv^2} \right)^2 / \theta^4$$

Rutherford scattering off the nucleus

$$\sigma \sim \int_{\theta_{\min}}^{\infty} \left(\frac{d\sigma}{d\Omega} \right) 2\pi\theta d\theta = \int_0^{a_0} 2\pi b db =$$

$$\sim \pi a_0^2 \sim 1 / \theta_{\min}^2 \sim \int_{\theta_{\min}}^{\infty} d\theta / \theta^3$$



Multiple Scattering



Mean square scattering angle

$$\langle \theta^2 \rangle \equiv \frac{\int \theta^2 \frac{d\sigma}{d\Omega} d\Omega}{\int \frac{d\sigma}{d\Omega} d\Omega} \sim \frac{\int (d\theta / \theta)}{\int (d\theta / \theta^3)}, \text{ Eq.5.4}$$
$$\sim 2\theta_{\min}^2 [\ln(\theta_{\max} / \theta_{\min})]$$

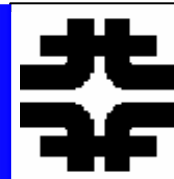
$$\langle \theta_{MS}^2 \rangle = N \langle \theta^2 \rangle$$

$$N = (N_o \rho \sigma / A) dx, \text{ (Section 1)}$$
$$= dx / \langle L \rangle$$

$$\langle \theta_{MS}^2 \rangle = \left[\frac{N_o \rho dx}{A} \right] 2\pi \left[\frac{2Z\alpha}{p\beta c} \right]^2 [\ln(\cdot)]$$



Multiple Scattering - II



$$\langle \theta_{MS}^2 \rangle = \frac{dx}{X_o} m^2 / (\alpha \beta^2 p^2)$$

$$X_o^{-1} = \frac{16}{3} \left(\frac{N\rho}{A} \right) (Z^2 \alpha) (\alpha^2 / m^2) [\ln O]$$

$$E_s \equiv \sqrt{\frac{4\pi}{\alpha}} (mc^2) = 21 MeV$$

Define for now, see brem later

Radiation length

$$\sqrt{\langle \theta_{MS}^2 \rangle} = \frac{E_s}{p\beta} \sqrt{\frac{dx}{X_o}}$$

Stochastic process – e.g. diffusion goes as \sqrt{x}

$$\theta_{MS} = (\Delta p_T)_{MS} / p, (\Delta p_T)_{MS} = \frac{E_s}{\beta} \sqrt{\frac{dx}{X_o}} = \frac{E_s}{\beta} \sqrt{t}$$



Recoil Energy Distribution



$$\Delta p_T \sim 2\alpha / bv, Z = 1$$

$$\Delta \varepsilon \sim \Delta p_T^2 / 2m$$

$$\Delta \varepsilon \sim 2\alpha^2 / b^2 v^2 m$$

Incoherent

$$d\sigma = d\vec{b} = b db d\phi = (d\sigma / dT) dT$$

$$\frac{d\sigma_\delta}{dT} = 2\pi b \left(\frac{db}{dT} \right) = \left[\frac{2\pi\alpha^2}{\beta^2 c^2 T^2 m} \right]$$

Relabel $b \rightarrow T$

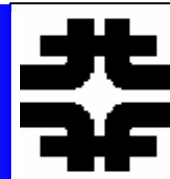
Energy given to recoil

(n.b. e here not the nucleus since $\sim 1/m$)

ionize the e , kick out of the atom – I



Energy Loss in Scattering



$$d\varepsilon \sim \int 2\pi b db (d\varepsilon / d\vec{b})$$

$$\sim \frac{4\pi\alpha^2}{mv^2} \left[\ln(b_{\max} / b_{\min}) \right]$$

$$\frac{dE_1}{d(\rho x)} \sim \left(\frac{N_o Z}{A} \right) d\varepsilon$$

$$\frac{dE_1}{d(\rho x)} \sim 4\pi \left(\frac{N_o Z}{A} \right) (\alpha^2 \lambda_e) \left(\frac{1}{\beta^2} \right) \left[\ln() \right]$$

$$\ln(b_{\max} / b_{\min}) \sim \left[\ln(T_{\max} / \langle I \rangle) \right]$$

$$T_{\max} = 2m(\beta\gamma)^2$$

$$\sim 2m \sim 1 \text{ MeV (MIP)}$$

$$\langle I \rangle \sim 10 \text{ eV}$$

$$\ln(T_{\max} / \langle I \rangle) = 11.5$$

$$d\varepsilon \rightarrow 4\pi\alpha^2 / (mc^2) (1/\beta^2) (11.5)$$

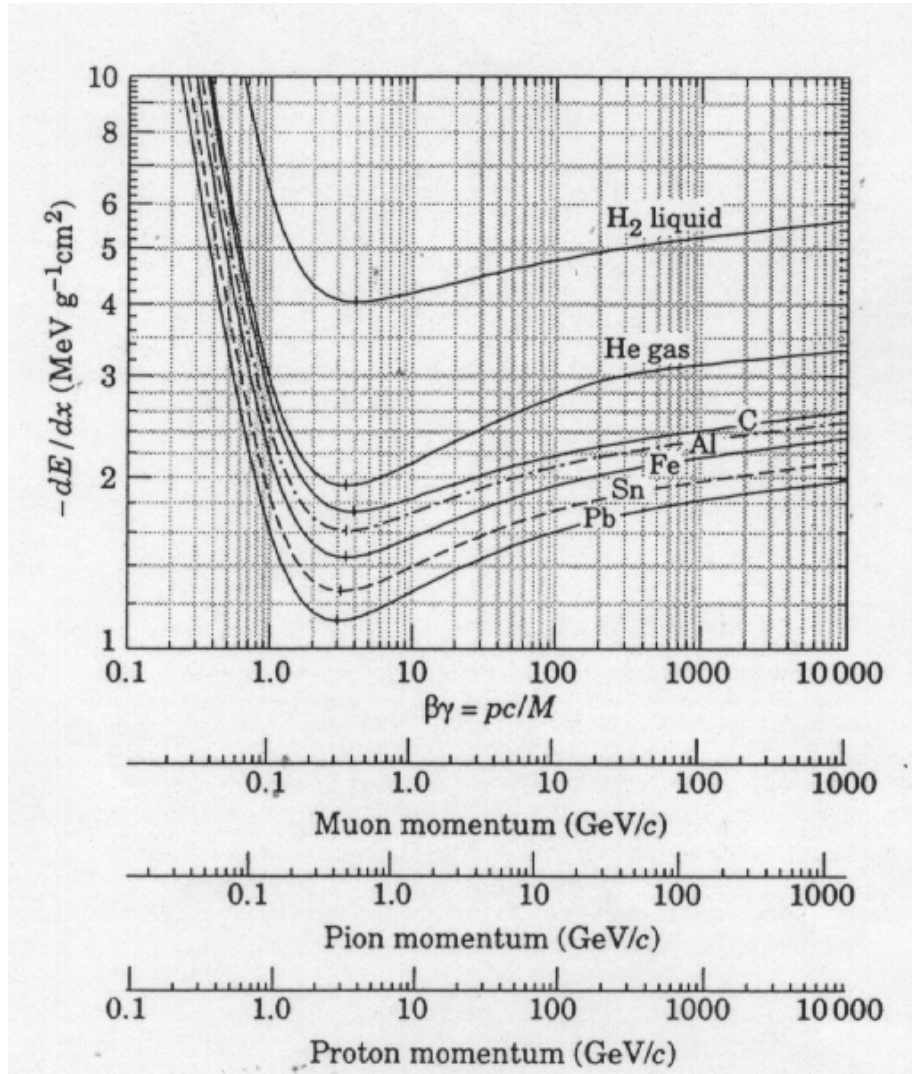
$$\sim 3.0 [Z/A] [\text{MeV/gm/cm}^2] (1/\beta^2)$$

numerically

medical uses of the Bragg peak



dE/dx and Momentum - MIP



$$\frac{dE_1}{dx} \sim \frac{1}{\beta^2} \sim \frac{M^2}{p^2}$$

$$T = \frac{p^2}{2M}$$

$$\frac{dE_1}{dx} \sim \frac{1}{p^2} \sim \frac{1}{T} \sim \frac{dT}{dx}$$



Range and Momentum



Ultra-relativistic

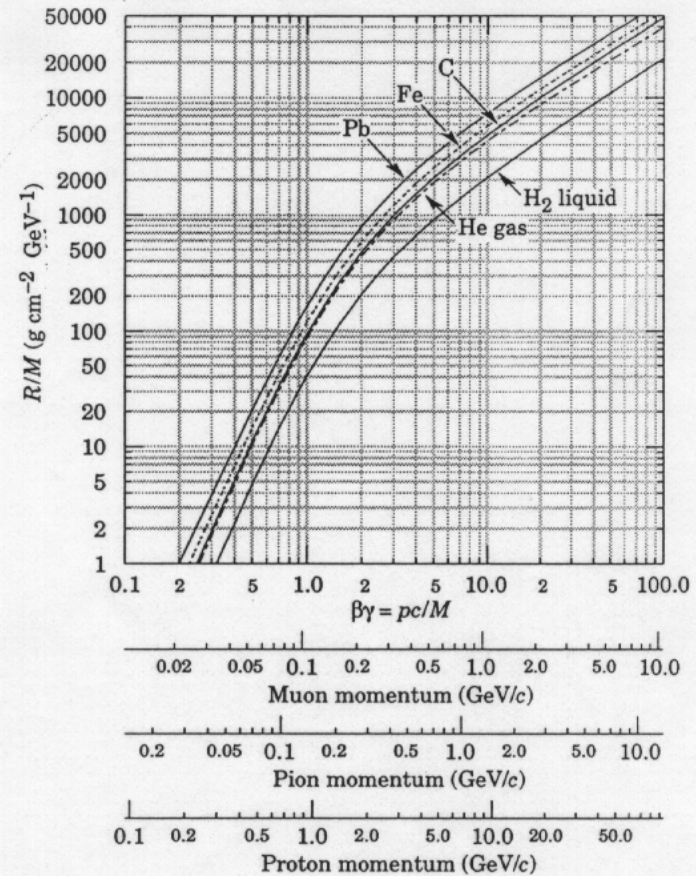
and

Non - relativistic

$$\left(\frac{dE_I}{d(\rho x)} \right)_{MIP} \underline{R} \sim T_o \sim \epsilon_o \sim \gamma$$

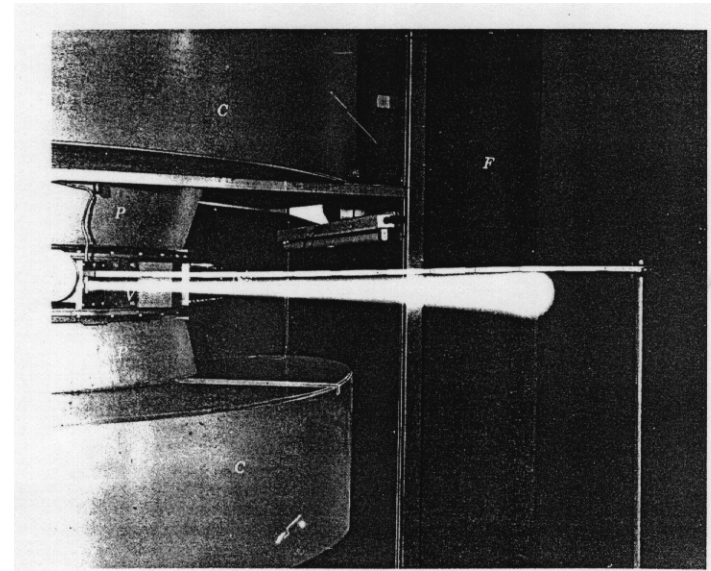
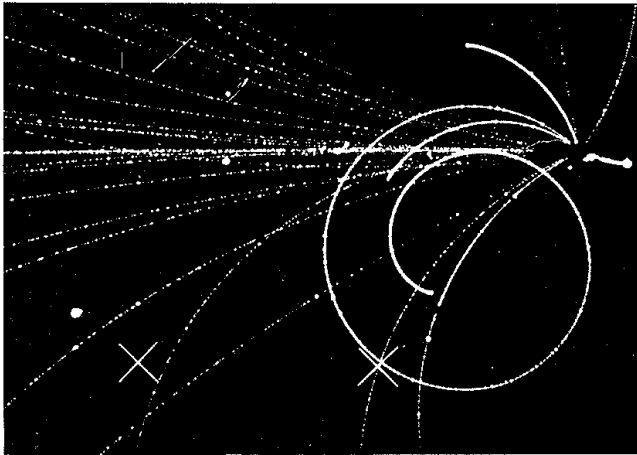
$$\int_{T_o}^o T dT = \int_o^R dx$$

$$\underline{R} \sim T_o^2 \sim p_o^4 \sim \beta_o^4$$





Range and Incident Charge



if $\Delta p_T \sim F(b)\Delta t \sim z\alpha$
then $dE/dx \sim z^2(Z/A)$
i.e. 1, 4, 9, bubble density

slow down toward the end of range
multiple scattering has $\theta \sim 1/p\beta$



Photon Interactions



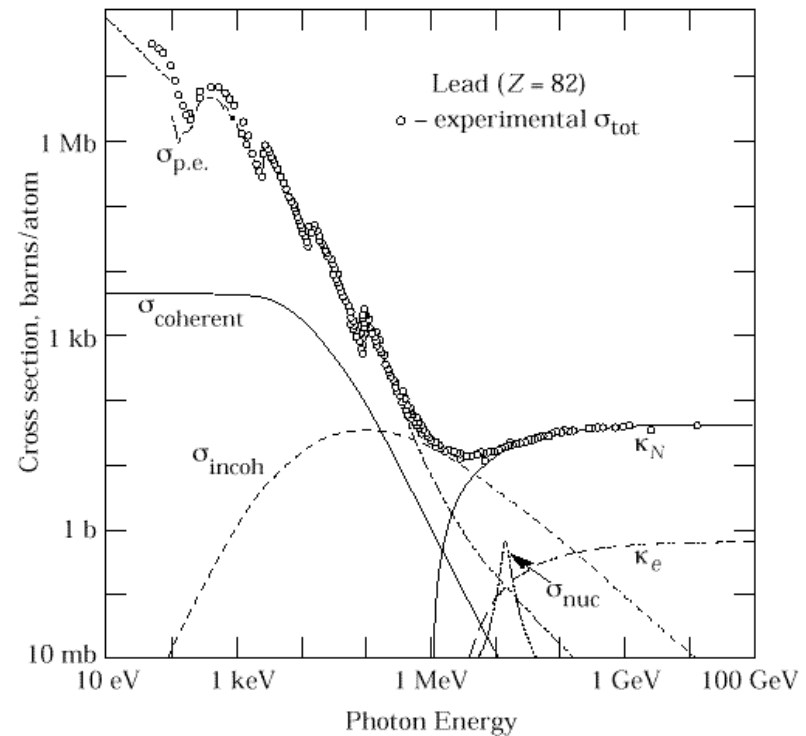
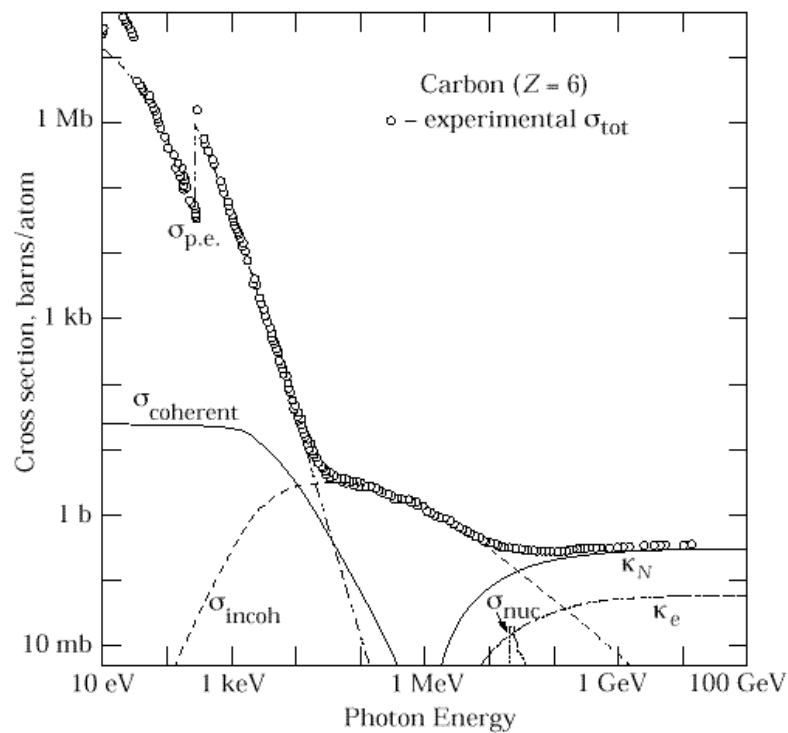
- **Cross section as a function of photon energy**
- **Photoelectric Effect**
- **Thompson Scattering**
- **Relativistic Photon Scattering**
- **Compton Effect**
- **Pair Production by Photons**



Photon Cross Sections

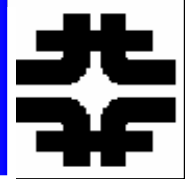


There are 3 regimes and a strong Z dependence

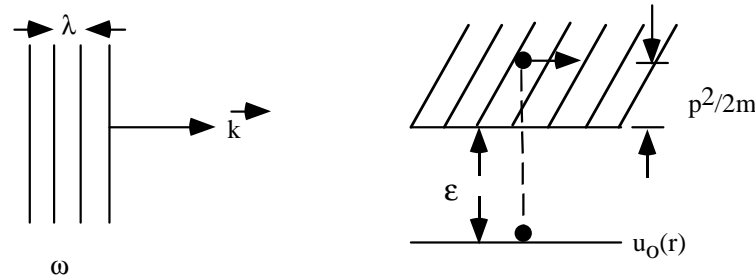




Photoelectric Effect



Photoeffect dominates for photon energy $< (10-100)$ keV



The inner e “see” the full electron charge Z

$$u_0(r) \sim \frac{1}{\sqrt{\pi a^3}} e^{-r/a}$$

$$a_0 = \hbar / \alpha, a \sim a_0 / Z$$

$$E_n = - \left[\frac{mc^2}{2} (Z\alpha)^2 \right] / n^2$$

$$= -13.6 eV Z^2 / n^2$$

$$\sigma_{PE} \sim \alpha \hat{\lambda}^2 \left[\frac{mc^2}{\hbar \omega} \right] \left[\lambda_{DB} / a \right]^5$$

$$\sim 1 / \omega^{7/2}$$

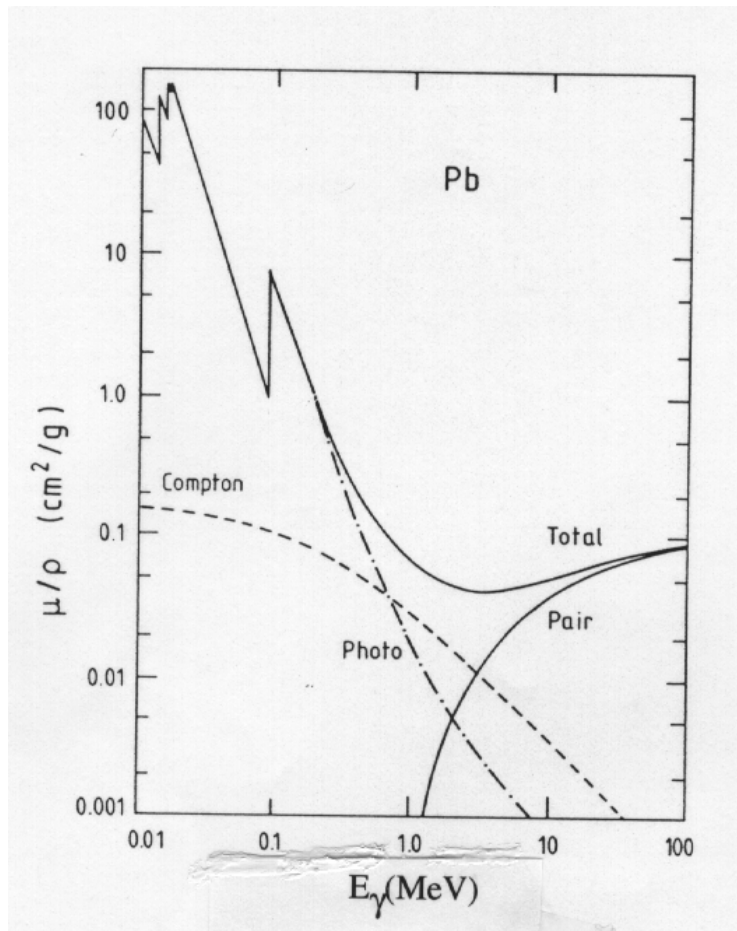
$$\hbar \omega \sim p^2 / 2m \text{ (Eq. 2.2)}$$



Photoelectric Effect - II



Inverse mean free path $1/[\rho\langle L\rangle]$



$$\sigma_{PE} \sim \frac{32\pi}{3} \sqrt{2} (Z\alpha)^4 Z \left(\frac{m}{\hbar\omega}\right)^{7/2} (\alpha\lambda)^2$$

$$\sigma_T \sim \frac{8\pi}{3} Z (\alpha\lambda)^2$$

$$\sigma_{PE} / \sigma_T \sim 4\sqrt{2} (Z\alpha)^4 (m_e c^2 / \hbar\omega)^{7/2}.$$

$$\sigma \sim Z^5$$

Compare Thompson (γ - e non-relativistic)

If $(Z\alpha) \sim 1$ - Pb then the cross sections cross at $\sim m_e = 0.51$ MeV

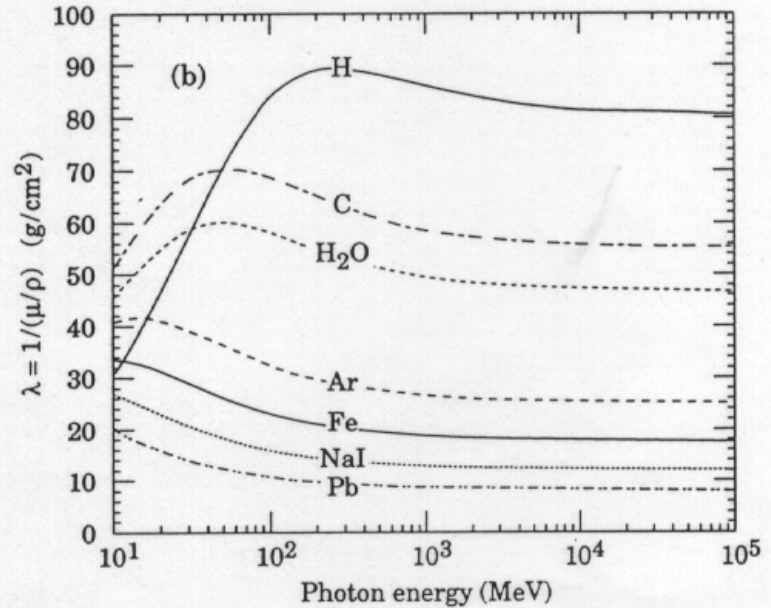
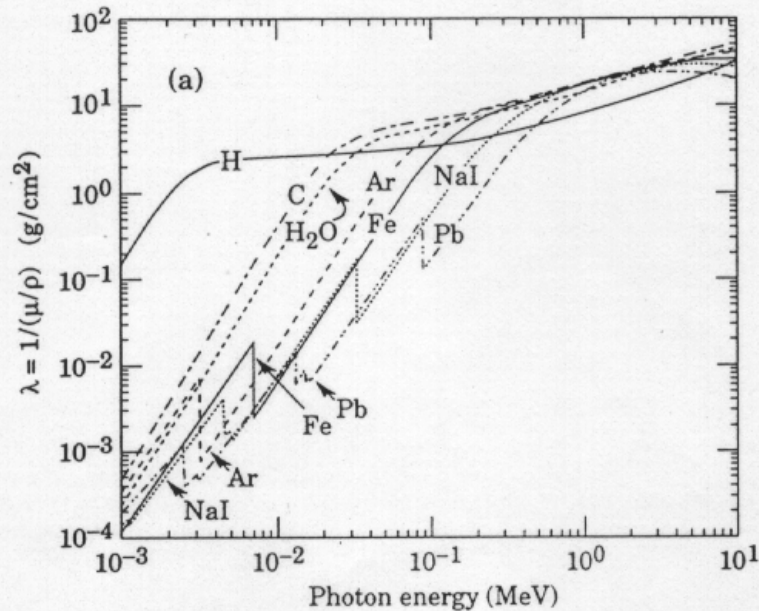


Photon Mean Free Path



PHOTON AND ELECTRON ATTENUATION

Photon Attenuation Length



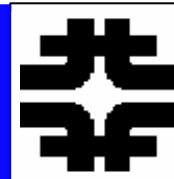
Dominated by the photoeffect
 Z^5 and $1/\omega^{7/2}$

Thompson/Compton \sim constant $\rho \langle L \rangle$
 Energy independent

Pair production goes as $X_0 \sim 1/Z$
 Energy independent



Photon - e Scattering



Dipole – Larmor, Non-relativistic

$$\frac{dP}{d\Omega} = \frac{e^2}{4\pi c^3} |a|^2 \sin^2 \theta$$

$$a = eE_o / m$$

$$\sigma_{KN} \sim \frac{3}{8} \sigma_T \left(\frac{m}{\sqrt{s}} \right)^2 [1 + \ln()] \sim \alpha^2 / s$$

$$\frac{d\sigma_T}{d\Omega} = (e^2 / mc^2)^2 \sin^2 \theta \equiv \langle dP / d\Omega \rangle / \langle |\vec{S}| \rangle$$

$$\sigma_T = \frac{8\pi}{3} (\alpha \hat{\lambda})^2$$

$$N \rho \langle L \rangle Z \sigma_T / A \sim 1$$

$$\sigma_T = \frac{8}{3} [\pi a_0^2] \alpha^4$$

$$\rho \langle L \rangle \sim (A/Z) \sim \text{const}$$

$$a_0 = \hat{\lambda} / \alpha \text{ (Section 1)}$$

see photon cross section figure

$$\sigma_T / \pi a_0^2 \sim \alpha^4 \sim 10^{-8}$$

Reduced by α^4 w.r.t. atomic geometric cross section



Compton Scattering - Kinematics

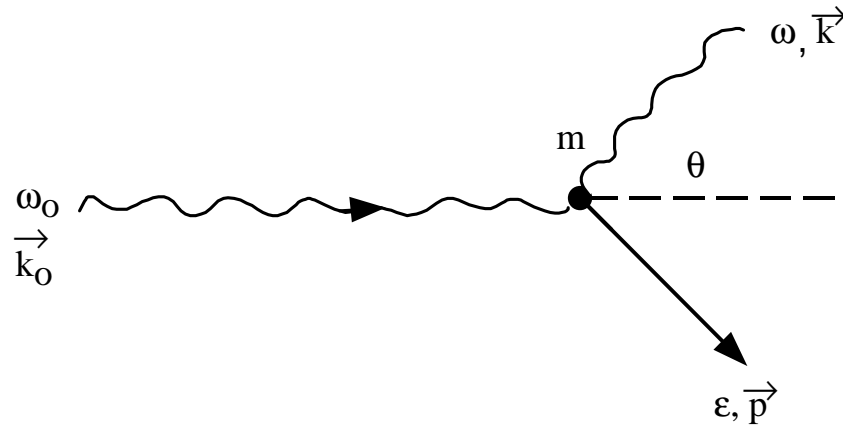


$$\omega_o + m = \varepsilon + \omega$$

$$\vec{k}_o = \vec{p} + \vec{k}$$

$$\left(\frac{1}{\omega} - \frac{1}{\omega_o} \right) = \frac{1}{m} (1 - \cos \theta)$$

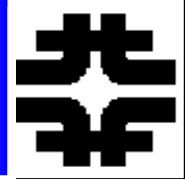
$$\lambda - \lambda_o = 2\pi\lambda(1 - \cos \theta)$$



dynamics \rightarrow e takes off most of the energy

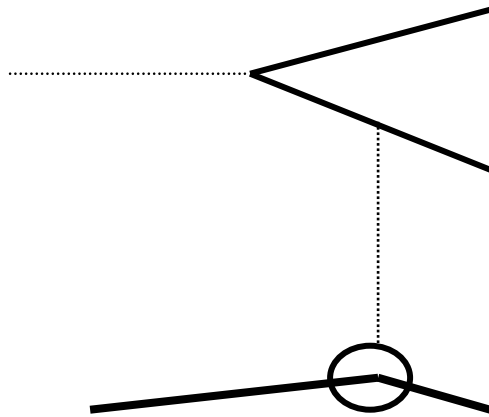


Pair Production

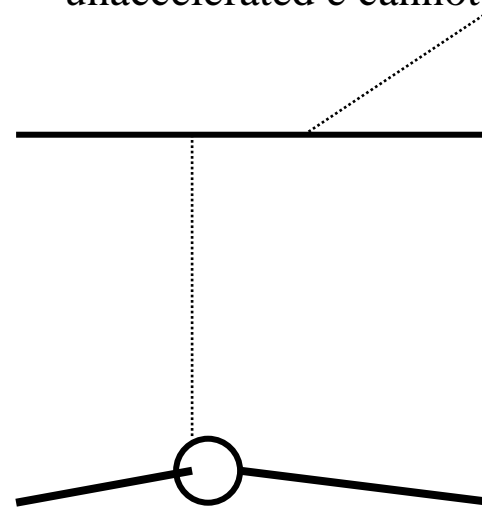


isolated photon cannot “decay” into an e^+e^- pair

unaccelerated e cannot radiate a photon



$$\gamma + Z \rightarrow e^+e^- + Z$$



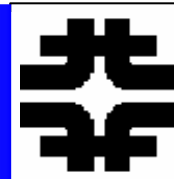
$$e + Z \rightarrow e + Z + \gamma$$

Pair Production and Bremsstrahlung are topologically similar.

Defer the cross section discussion until radiation by charged particles in accelerated motion.



Electron Interactions



- **Radiation in relativistic motion**
- **Linear and Circular acceleration**
- **Angular distributions**
- **Bremsstrahlung as the scattering off virtual photons of the target by the projectile**
- **Radiation length**
- **Critical energy**



Relativistic Radiation



$$\begin{aligned}\underline{P} &= \frac{2}{3} \frac{e^2}{c^3} A_{\mu} A^{\mu} \\ &= \frac{2}{3} (e^2 / c^3) \gamma^6 \left[|\vec{a}|^2 - |\vec{\beta} \times \vec{a}|^2 \right]\end{aligned}$$

Linear

$$(\underline{P})_{\circ} = \frac{2}{3} \frac{e^2}{c^3} \gamma^4 |\vec{a}|^2$$

Circular

$$A_{\mu} = \left(\frac{\gamma \beta}{m} \right) \frac{d}{dx} \left[\varepsilon(\vec{\beta}, 1) \right], \quad dx = \beta c dt$$

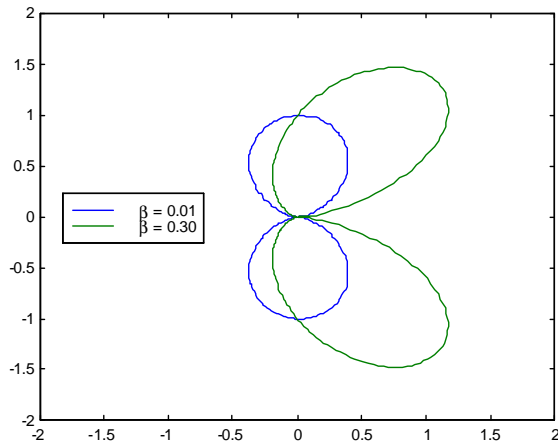
$$(\underline{P})_{LIN} = \frac{2}{3} \frac{e^2}{m^2 c^3} \left(\frac{d\varepsilon}{dx} \right)^2$$

generalize Larmor

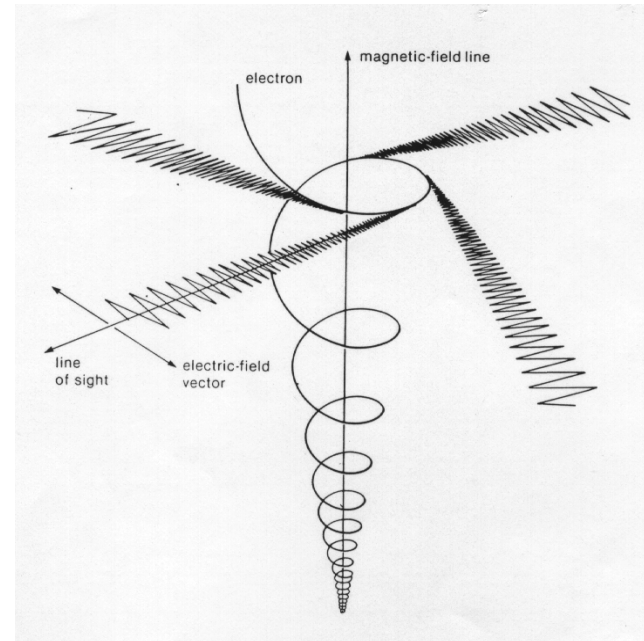
- strong γ dependence
- radiation is important at high energies



Angular Distributions



dipole tips forward at high γ



Linear Acceleration
Circular

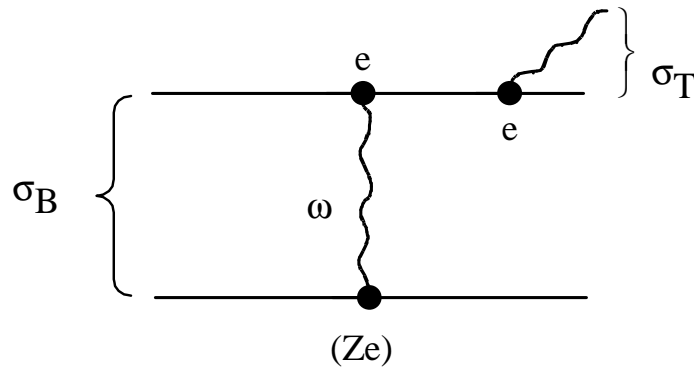
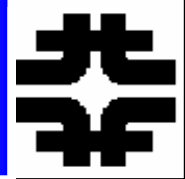
Synchrotron Radiation -

complex in general but
 $\langle \theta \rangle \sim 1/\gamma$ - “searchlight effect”

→ calorimetry is approximately 1 dimensional



Bremsstrahlung



**The Thompson scattering
of the virtual quanta of
the target by the projectile**

in a Coulomb collision we can decompose the fields of a charged particle into a distribution of “virtual quanta”

$$\begin{aligned} \frac{dN_\gamma(\omega)}{d\omega} &\sim \frac{\alpha}{\beta^2} \left(\frac{1}{\omega} \right) [\ln(\cdot)] \\ &= \frac{2\alpha}{\pi} \left(\frac{1}{\beta^2} \right) \left(\frac{1}{\omega} \right) [\ln(\cdot)] \end{aligned}$$

but coherent!

Recall $d\varepsilon \sim \alpha/\beta^2 [\ln(\cdot)] (Z^2)$

$$\begin{aligned} \frac{d\sigma_B}{d\omega} &\sim Z^2 \frac{dN_\gamma}{d\omega} \sigma_T \\ \frac{d\sigma_B}{d\omega} &\sim \frac{(Z^2 \alpha)}{\omega} (\alpha \lambda)^2 [\ln(\cdot)] \end{aligned}$$

coherent because the nucleus ~ 1 fm is small on the scale of the projectile deBroglie wavelength. Thus no phase change over nucleus, amplitude $\sim Z$, cross section $\sim Z^2$



Radiation Length



$$dE \sim \int_0^E (\hbar\omega) \left(\frac{N_o \rho dx}{A} \right) \left(\frac{d\sigma_B}{d\omega} \right) d\omega$$

$$\frac{1}{E} \left(\frac{dE}{\rho dx} \right) \equiv \frac{1}{X_o}, E(x) = E(o) e^{-\rho x / X_o}$$

By definition X_o is the bremsstrahlung mean free path

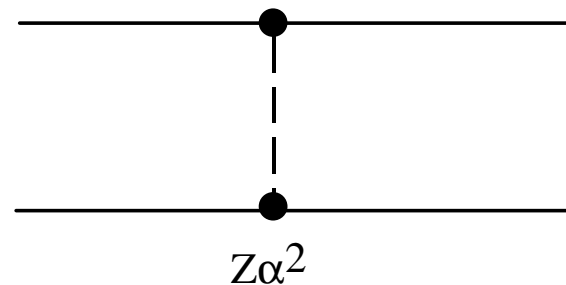
Look at the photon cross section table

It is the projectile because that acceleration cause the radiation

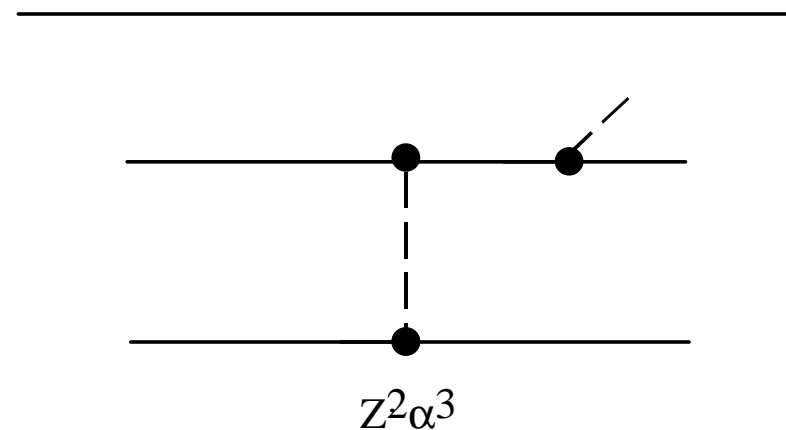
$$X_o^{-1} = \frac{16}{3} \left(\frac{N_o}{A} \right) (Z^2 \alpha) (\alpha \hat{\lambda}_p)^2 [\ln(\)]$$
$$\sim (Z / A) Z \sim Z$$



Critical Energy - Ionization and Bremsstrahlung



radiation rises with E (relativity)
 $(Z\alpha)$ coherence vs coupling
 ionization transfers energy to the atomic e
 radiation accelerates the projectile



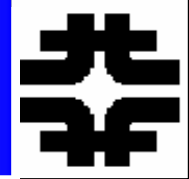
$$E_c \sim \frac{3\pi}{4} \left(\frac{m_p}{m_T} \right) \left[\frac{m_p c^2}{Z\alpha} \right]$$

$$\sim 165 \text{ MeV} / Z$$

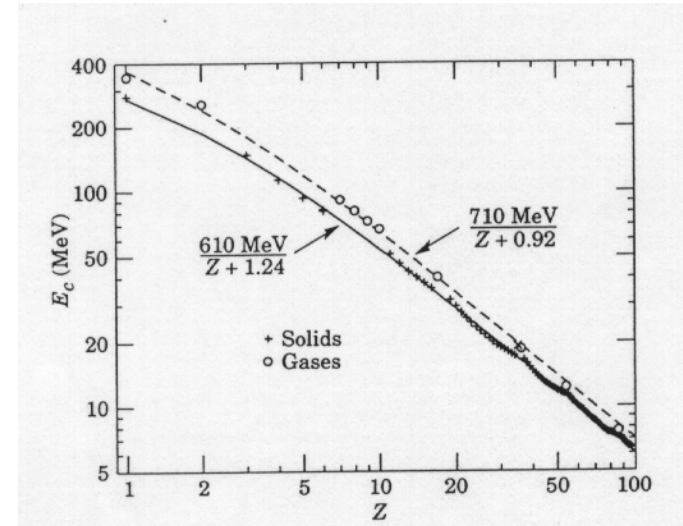
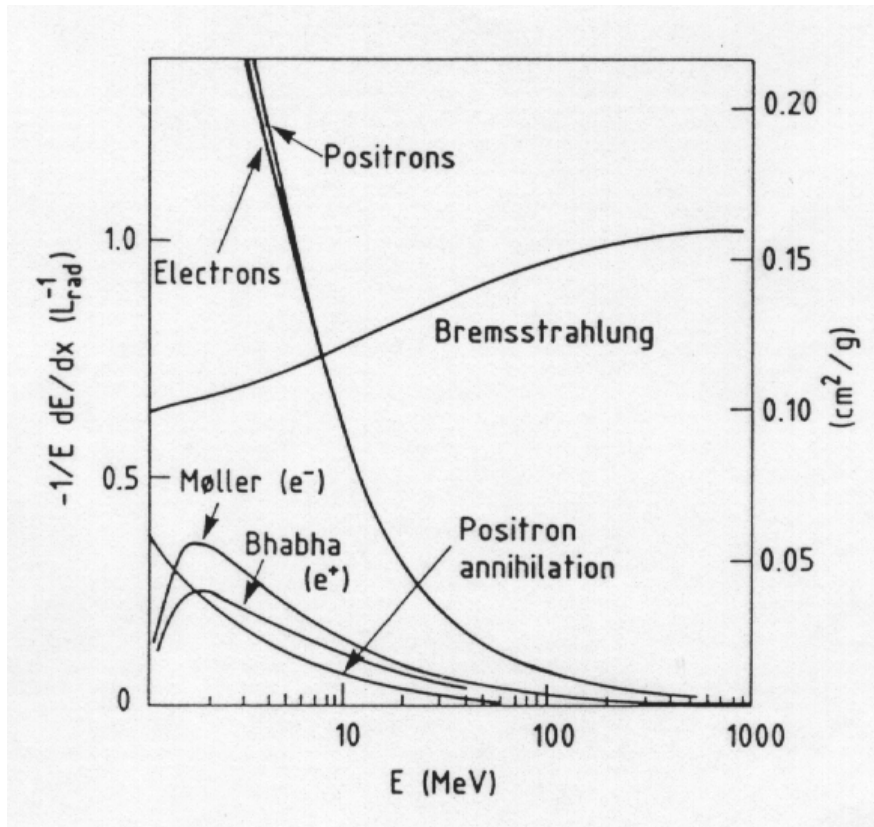
incoherent ionization – 2 vertices
 coherent brems – 3 vertice



Critical Energy



Pb



$\sim 1/Z$ behavior of E_c

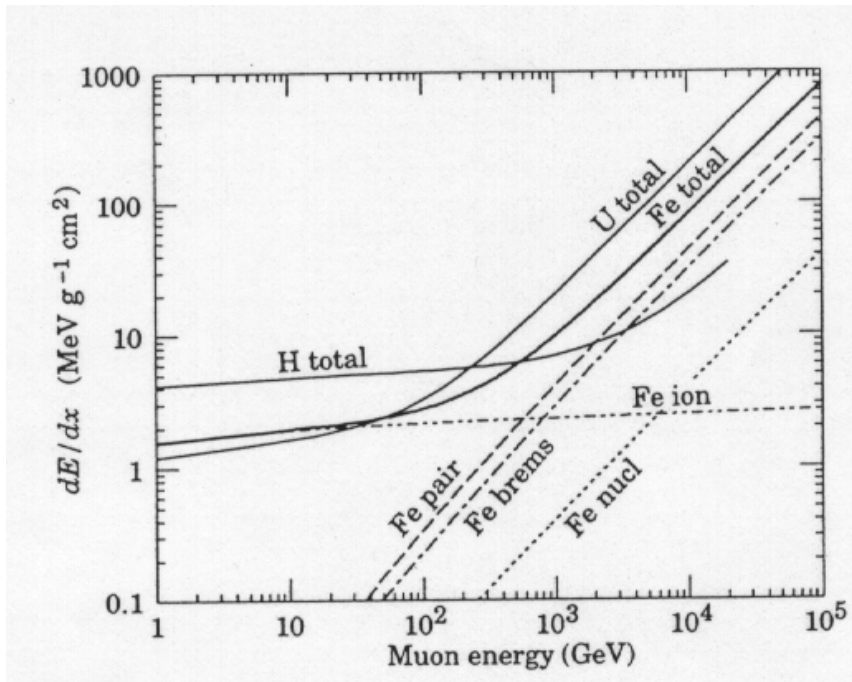
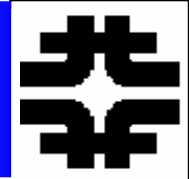
EM cascade stops multiplying at E_c and begins to die out by ionization and photoeffect.

$$1/E[dE/dx] \sim 1/X_0$$

$$E_c \sim 7 \text{ MeV}$$



Critical Energy for Muons



Same forces on μ and e
 But accel $\sim 1/m$
 And radiation $\sim a^2$
 So much less muon radiation

$$E_c \sim (m_p^2)$$

So if 24 MeV for e on Fe
 Then $\sim (200) \cdot (200)$ or ~ 1 TeV
 For muon

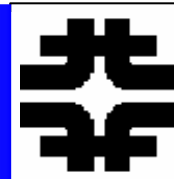
Another process



$$\sigma_{\text{pair}} \sim \sigma_B$$



EM Calorimetry



- **Basic parameters**
- **The EM Cascade**
- **Energy Resolution**
- **Sampling Fluctuations**
- **Nobel Liquids - Pulse Formation**
- **Crystals**
- **Transverse Size**
- **Leakage**
- **Calibration**



Basic Parameters



$$(dE_B / E) \sim (\rho dx) / X_o$$

$$X_o \sim [180 \text{ gm} / \text{cm}^2] [A / Z^2]$$

$$t = x / X_o$$

Radiation Length

[Basic EM Length Unit]

$$(dE / dx) \sim - E_C / X_o$$

$$E_C \sim [550 (\text{MeV})] / Z$$

$$y = E / E_C$$

Critical Energy

[EM Energy Unit]

$$dE_I / dx \sim [3 (\text{gm} / \text{cm}^2)] [Z / A]$$

Ionization energy loss

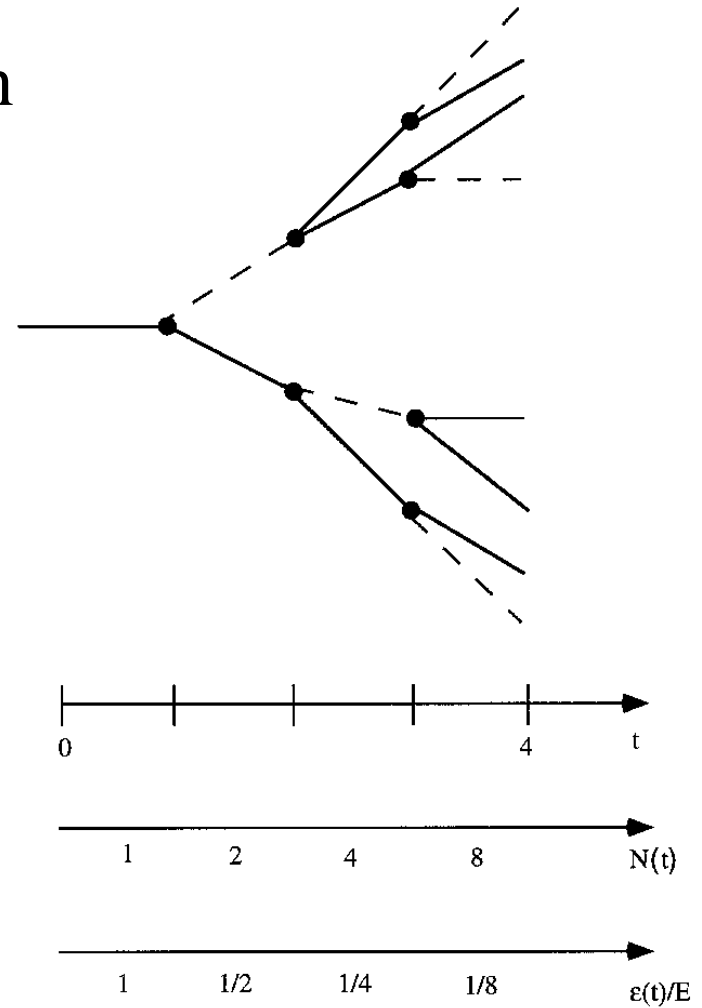
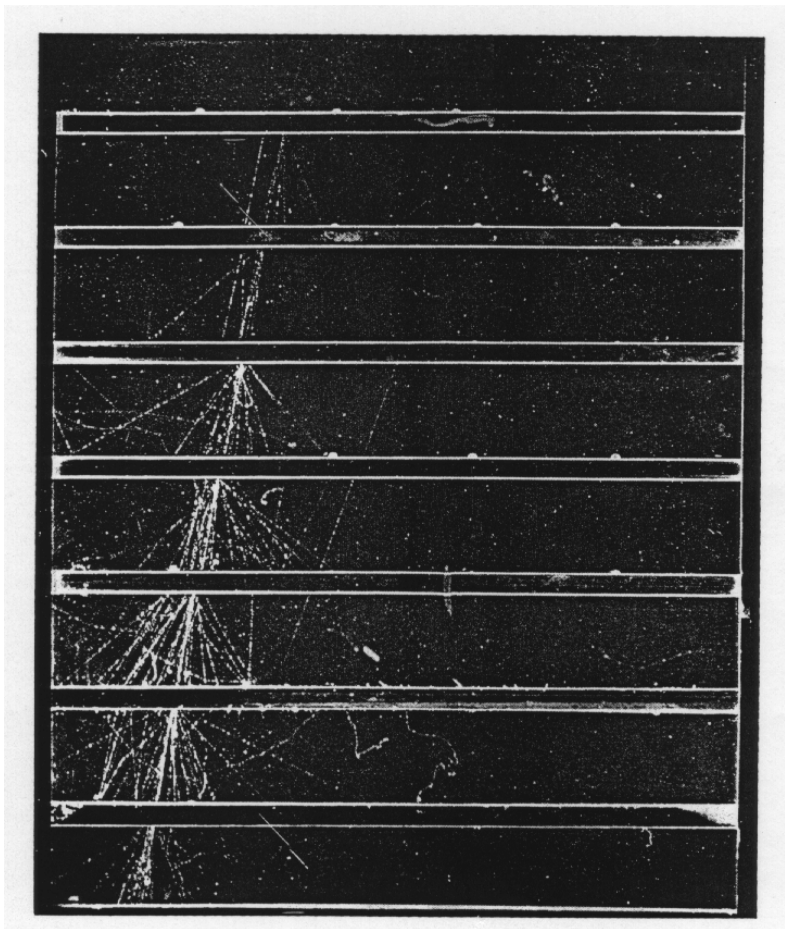
[After shower ceases to grow]



EM Cascade



Bremss + Pair \rightarrow multiplication





Simple EM Cascade Model



Geometric growth of cascade

Ignore Fluctuations:

But for initial interaction point

$$\langle L \rangle = X_0$$

$$\sigma = X_0$$

And energy sharing of daughters

- goes from 0 to full parent
- energy, = 1/2 on average

$$E_C = E / 2^{t_{max}} = \epsilon(t_{max}) = yE$$

$$t_{max} \sim \ln(y)$$

$$N_{max} \sim E / E_C = N(t_{max}) = y$$

$$L \sim X_0 \sum_{i=1}^{t_{max}} N(t)$$

$$\frac{L}{X_0} \sim \int_0^{N_{max}} N(t) dt \sim \int_0^{t_{max}} 2^t dt$$

$$\sim (E / E_C) / \ln^2 = N_{max}^{\ln 2}$$

e.g. 1 GeV e in Pb

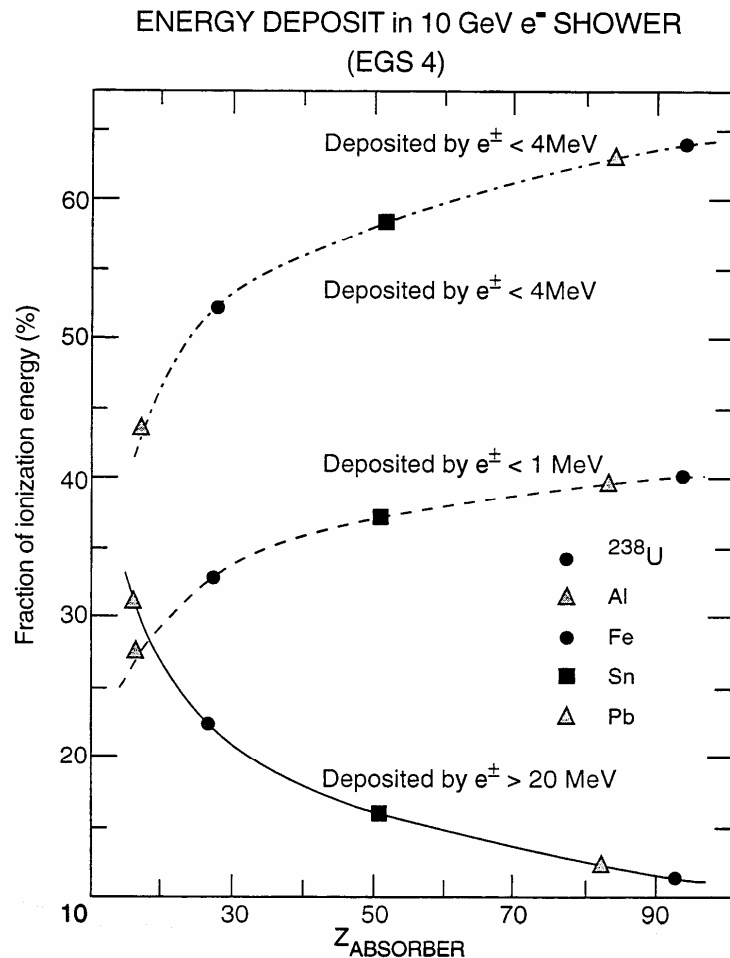
$$N_{max} \sim 140$$

L = total path length
of all tracks in the shower

**n. b. calorimetry is linear - non trivial
ears, eyes, dynamic range**



EM Showers - Energy Deposit



After shower maximum there is
No more particle multiplication
But
 $E_c \sim 7 \text{ MeV}$ in Pb
 e^- ionize
photons Compton scatter
or photoeffect ($\gamma \rightarrow e^-$)

ultimately the shower dies off
 \rightarrow energy deposit is due to soft e^-



Stochastic Term - dE/E



$$N_{\max} = E / E_c$$

$$\frac{dE}{E} \sim 1/\sqrt{E} \sim dN/N$$

E.g, 1 GeV e in Pb
 $dE/E \sim 8\%$ due to
 statistical fluctuations

Profile

$$\frac{dE}{du} = \left[u^a e^{-u} \right] / \Gamma(a+1)$$

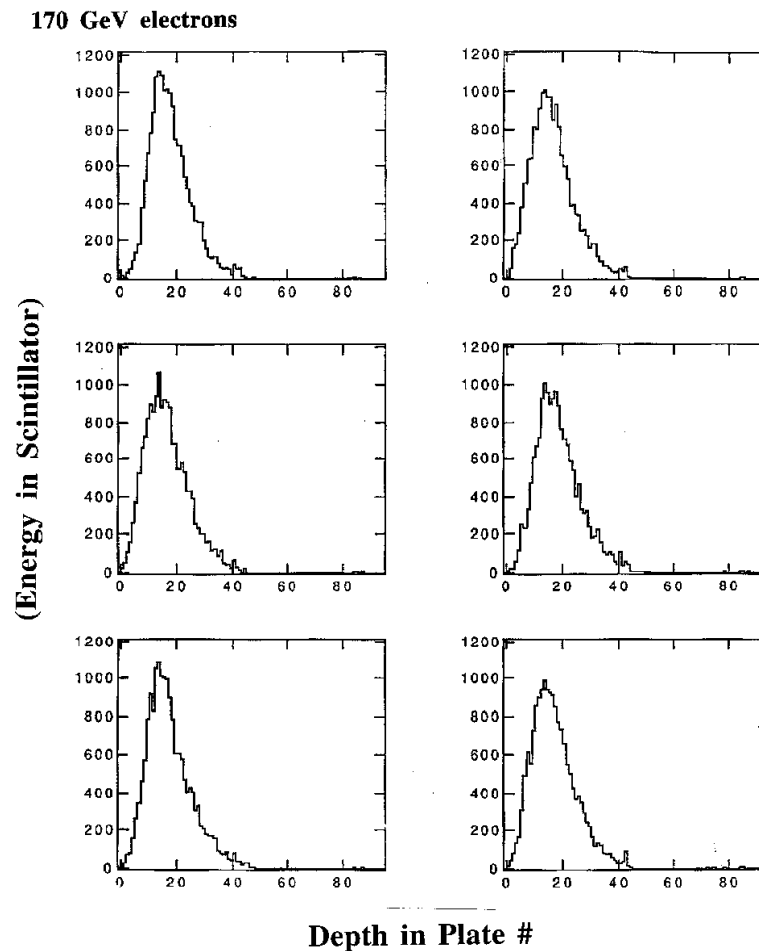
$$u = bt, \quad b \sim 1/2$$

$$t_{\max} \sim \ln y \sim (a - 1)/b$$

1 GeV e in Pb

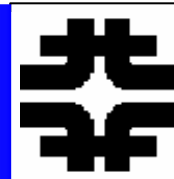
$$t_{\max} \sim 5$$

Individual showers ~ profile smeared by
 +- X_0 due to first interaction point fluctuations





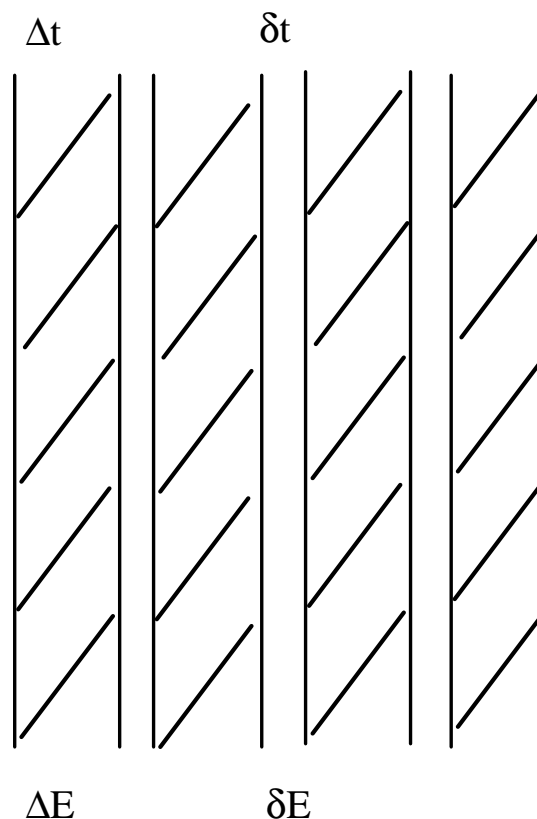
Sampling Calorimetry



Shower develops in high Z inert plates
Shower is sampled in low Z detectors
(scintillator, gas chambers, Si, noble liquids, crystals)

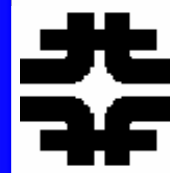
$$\left(\frac{dE}{E}\right)_{\text{samp}} = 1 / \sqrt{N_S} \equiv a_{\text{samp}} / \sqrt{E}$$
$$a_{\text{samp}} \sim \sqrt{E_C \Delta t}$$
$$\sim \sqrt{\Delta E}$$

e.g. Pb with 0.5 Xo thick samples.
 $dE/E \sim 6\% / \sqrt{E}$



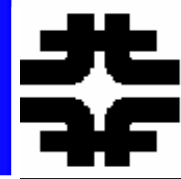


Scint-WLS Calor





Sampling - II



$$\Delta t \rightarrow \Delta t / \langle \cos \theta_{MS} \rangle$$

$$\theta_{MS} \sim (E_S / E_C) \sqrt{\Delta t} \sim 1 \quad (\text{Section 5})$$

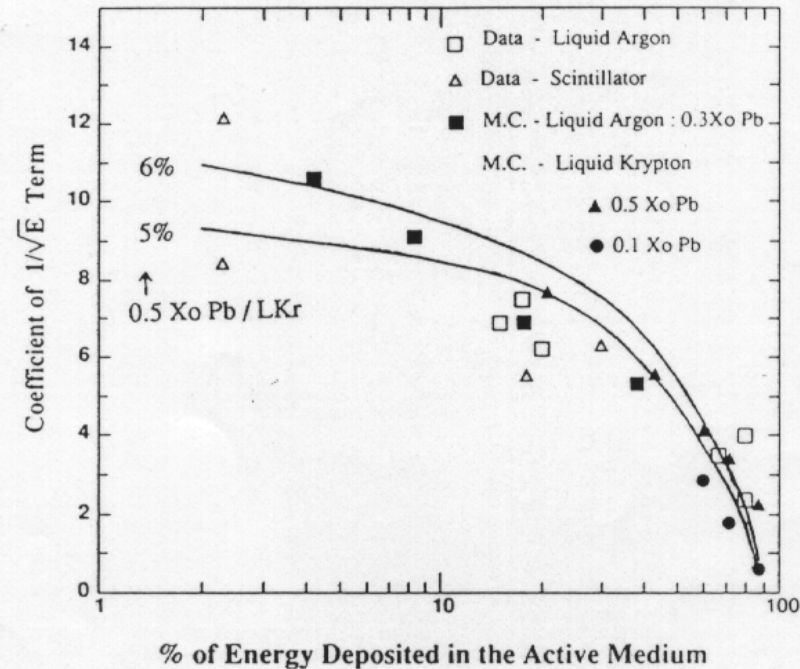
$$\sim (E_S / E_C \pi)$$

Shower is not simply 1 - d
 Energy is deposited by soft tracks
 Multiple scattering is large, $\theta_{MS} \sim 1$
 \rightarrow effective plate thickness is increased

$$a_{smp} \sim \left[(1 - W) \left(\frac{\Delta E + \delta E}{\langle \cos \theta_{MS} \rangle} \right)^{\left(\frac{1-W}{2} \right)} \right]$$

$$W = \delta E / (\delta E + \Delta E)$$

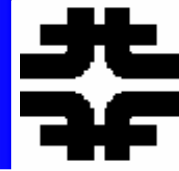
If sampling fraction becomes large
 The assumption of development solely
 In the samples breaks down



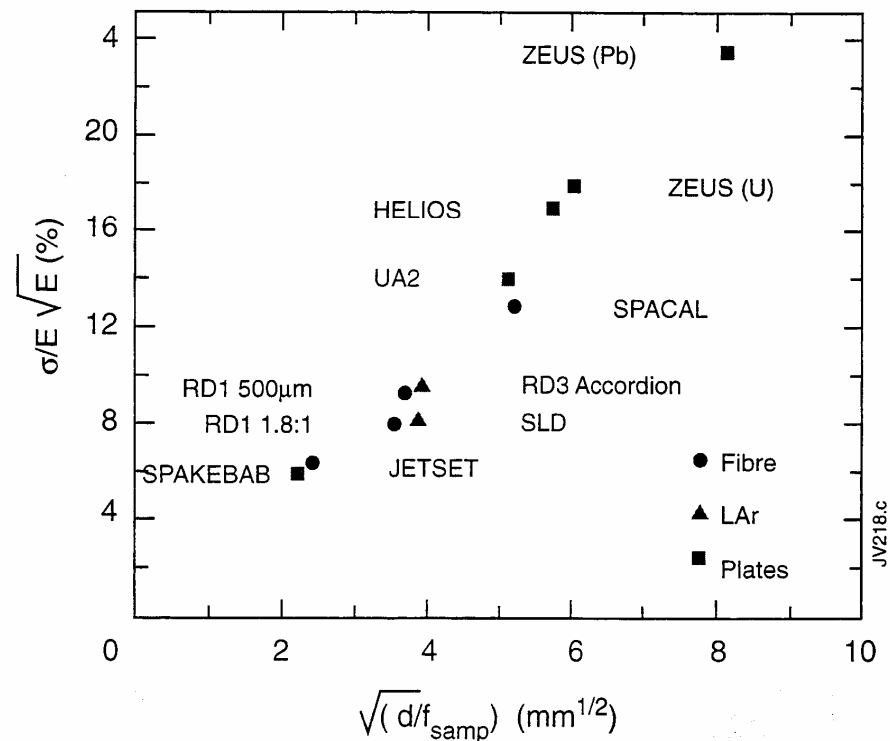
A $6\%/\sqrt{E}$ stochastic term is possible
 With fine sampling and a large
 Sampling fraction



Sampling Fraction and dE/E



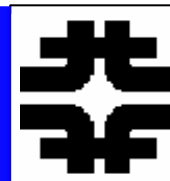
Data points on precision EM calorimeters



Scintillating Fibers can be fine grained
And have a large sampling fraction, f
Good resolution is achievable with SciFi



Nobel Liquids for Calorimeters



Ionization in noble liquids

Typical is parallel plate

Ionization chamber

e.g. D0, ATLAS,

		LAr	LKr	LXe	
Density	g/cm ³	1.39	2.45	3.06	
Radiation Length	cm	14.3	4.76	2.77	
Moliere Radius	cm	7.3	4.7	4.1	
Fano Factor		0.11	0.06	0.05	
Scintillation Properties					
Photons/MeV		-	1.9 10 ⁴	2.6.10 ⁴	
Decay Const. Fast	ns	6.5	2	2	
Slow	ns	1100	85	22	
% light in fast component		8	1	77	
λ peak nm		130	150	175	
Refractive Index @ 170nm		1.29	1.41	1.60	
Ionization Properties					
W value	eV	23.3	20.5	15.6	Charge collection time
Drift vel (10kV/cm)	cm/ μ s	0.5	0.5	0.3	Is defined by the drift velocity
Dielectric Constant		1.51	1.66	1.95	
Temperature at triple point	K	84	116	161	



Pulse Formation



$$Q = CV$$

$$U = CV^2/2 = Q^2/2C \sim QV$$

$$\begin{aligned} dU &= Q_o dQ(t) / C = Fdx \\ &= [q(t)E][\langle v_d \rangle dt] \end{aligned}$$

$$\begin{aligned} dQ(t) &= q(t) \langle v_d \rangle dt [E/V_o] = [q(t) \mu E^2 / V_o] dt \\ \frac{dQ(t)}{dt} &\equiv I(t) = q(t) \mu E^2 / V_o \end{aligned}$$

$$\mu = v_d / E$$

Parallel plate gap

U = stored energy

Field E does work on the
Charge q(t) in the gap
Which moved with drift velocity v_d

Charge Q is induced on the
electrodes. $v_d = \mu E$. $I \sim q$.



Pulse Formation - II



Line Charge (muon)

$$q(t) = q_s \left(1 - \frac{t}{\tau_d}\right), \quad t < \tau_d$$
$$= 0, \quad t > \tau_d$$
$$\tau_d = d / \langle v_d \rangle$$

$$I(t) = (q_s / \tau_d)(1 - t / \tau_d)$$
$$\int I(t) dt \equiv Q(t)$$
$$= q_s [y - y^2 / 2], \quad y = t / \tau_d$$

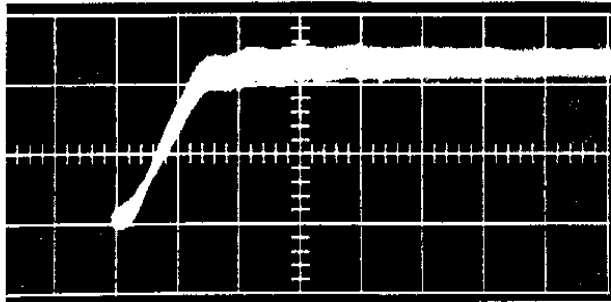
Point Ionization (α source)

$$dQ = \frac{q(t)E}{V_o} (\langle v_d \rangle dt)$$
$$q(t) = q_s \text{ for } t < \tau'_d, = 0, t > \tau'_d, \tau'_d \equiv x_o / \langle v_d \rangle$$

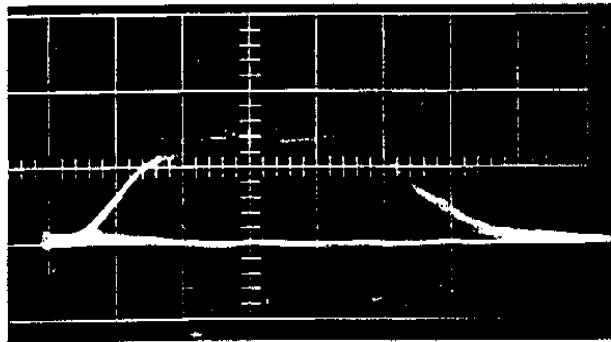
$$I(t) = \frac{q_s}{\tau_d}, \quad t < \tau'_d = 0, \quad t > \tau'_d$$
$$Q(t) = q_s t / \tau_d$$
$$\leq q_s (x_o / d)$$



Pulse Formation

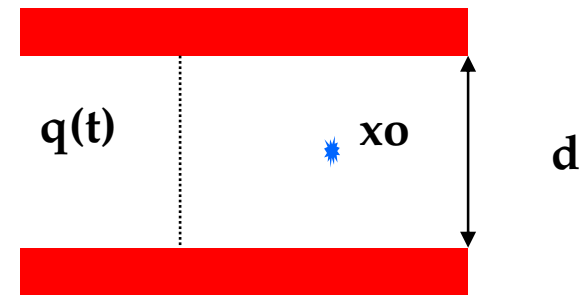


(a)



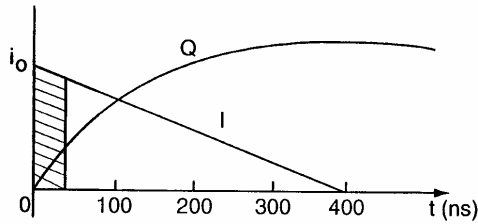
(b)

V Q I

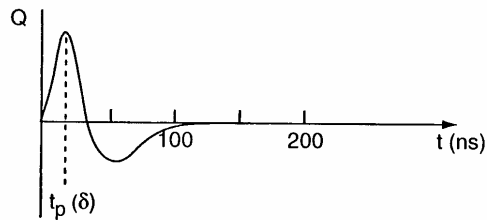




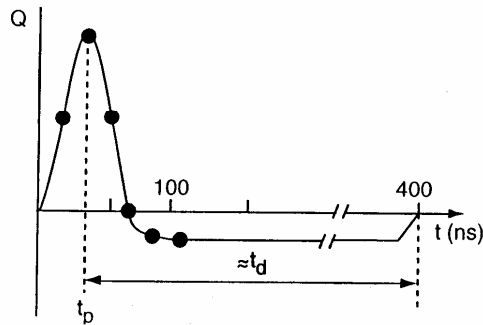
LA Pulse Shaping



$$I \sim$$
$$Q \sim t^2$$



Bipolar pulse shaping
Risetime due to source/cable
Capacity

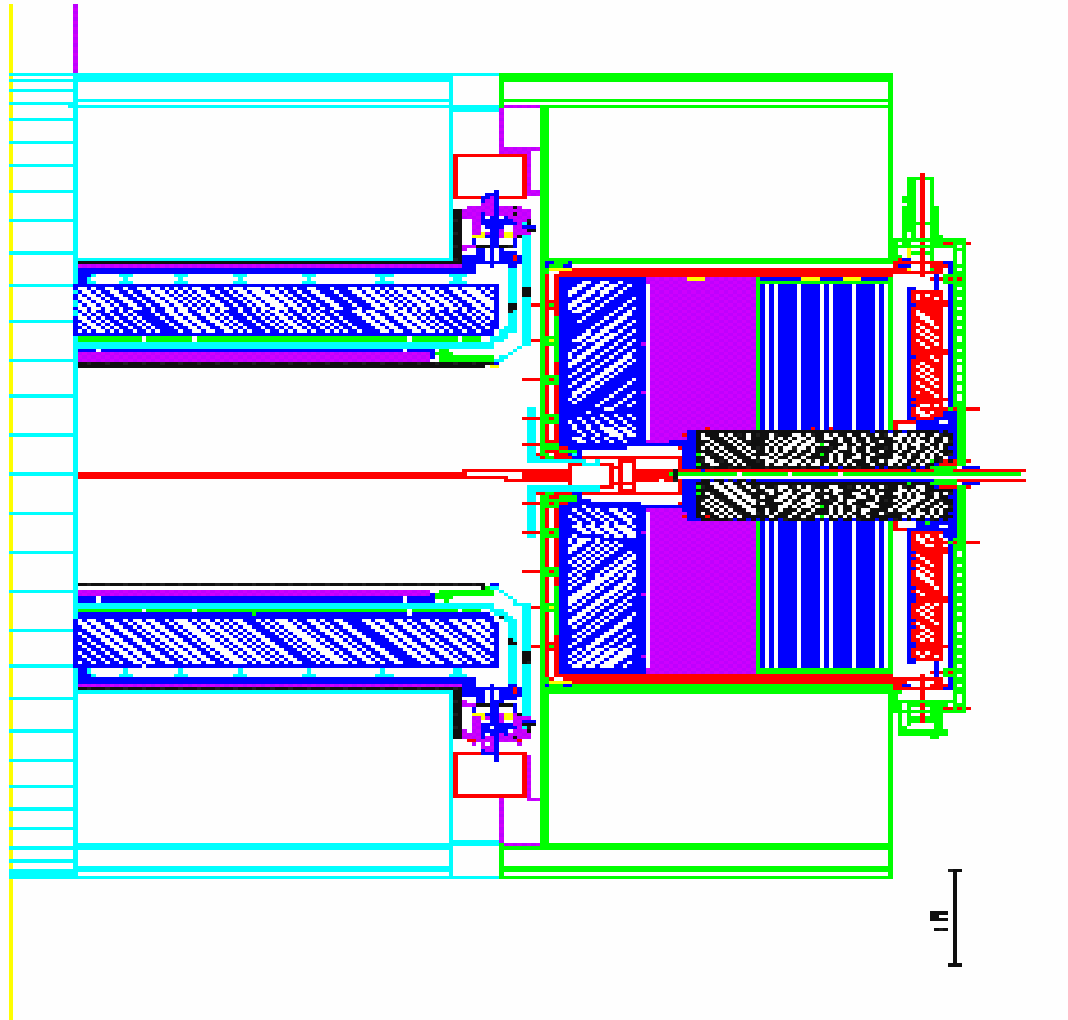


Fast rise time pulse shaped
Followed by long drift time

If $d \sim 1$ mm, then $\tau \sim 200$ nsec

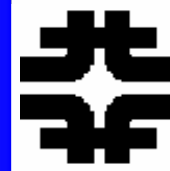


ATLAS - LA





Energy Resolution - LA



ATLAS

dE/E is $\sim 1.2\%$ at 100 GeV

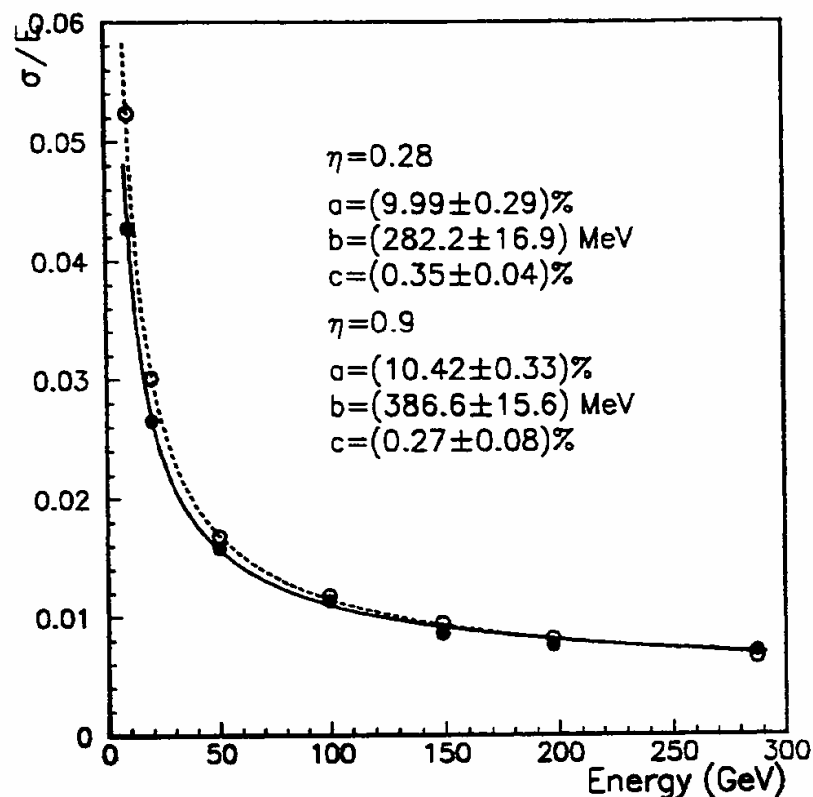
Constant term, $dE/E = b$, due to
Non-uniformity of the medium

Controlled here to $\sim 0.3\%$

An issue with large volume

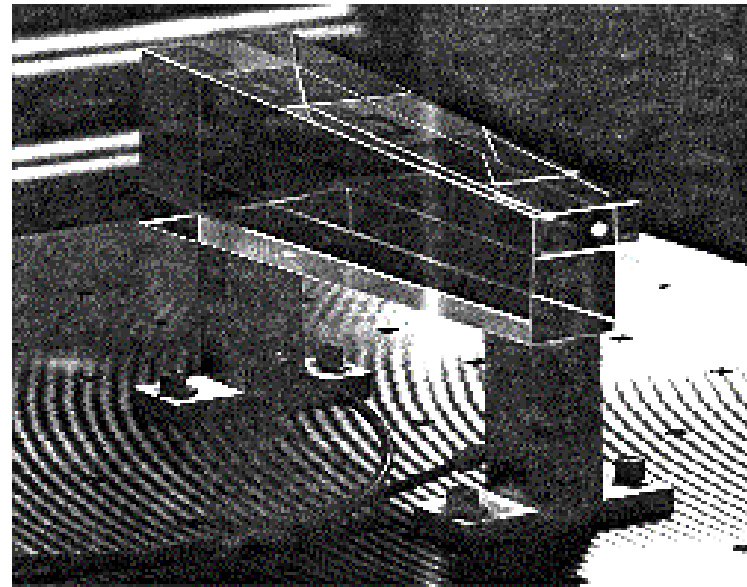
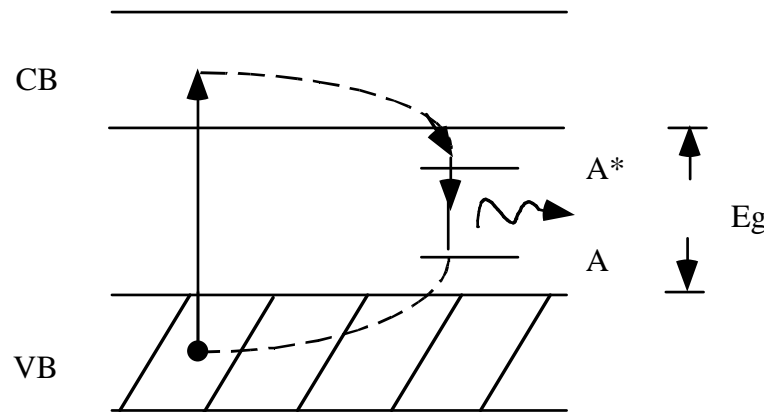
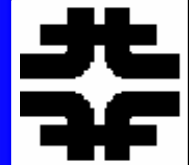
Detectors, controlling uniformity

○ *Barrel 2 meter prototype*
✓ **Energy resolution**





Xtals - Fully Active



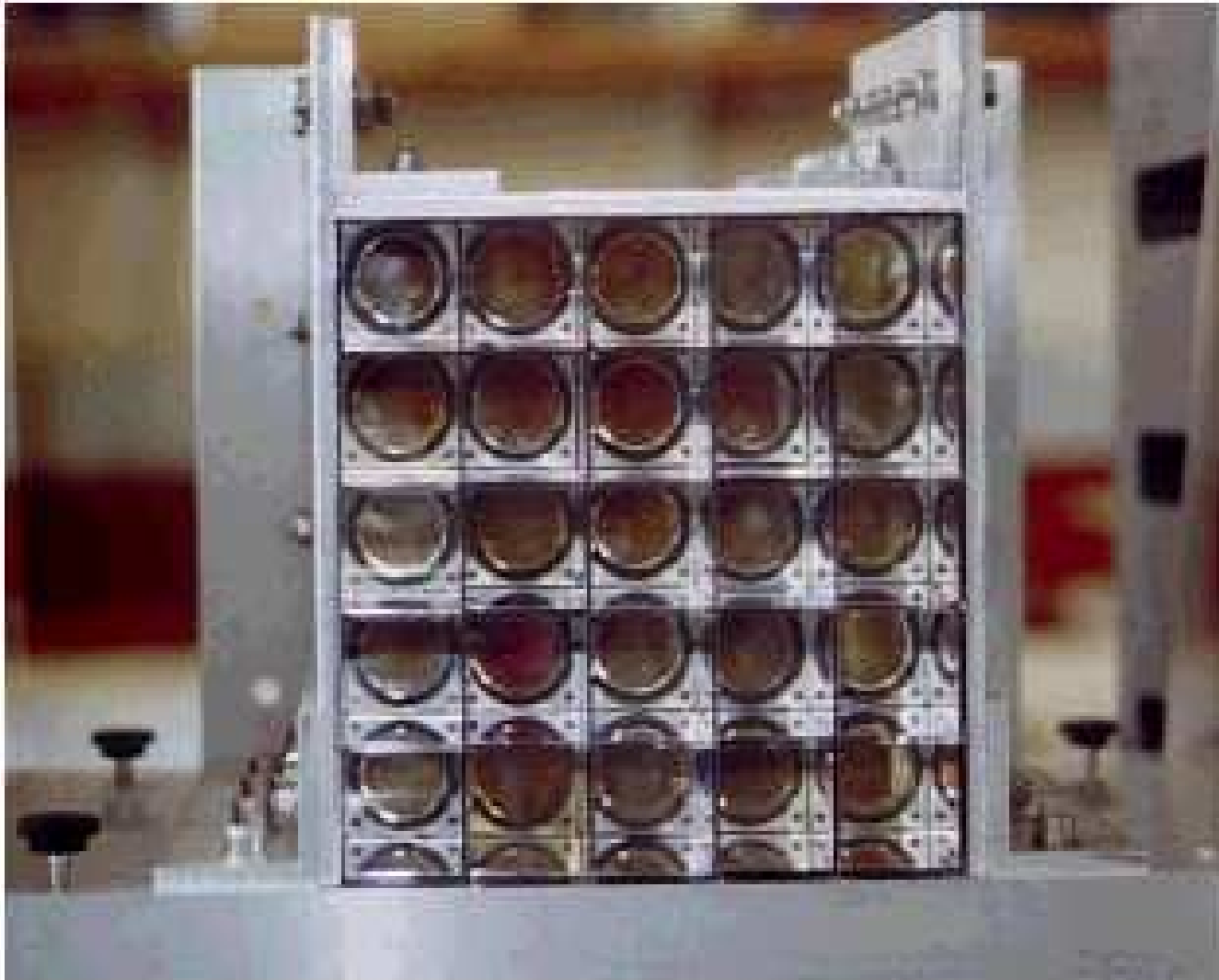
Xtal is transparent to its emissions

Uses activators, e.g, Thallium in NaU

Trap on activator quickly
For fast light output.

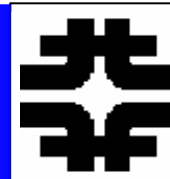


PbWO4 Array - Test Beam





Energy Resolution - Xtals



e.g. PbWO₄ – CMS

fully active devices have no sampling fluctuations. However, there is noise and photon statistics, and collection non-uniformity.

$dE/E \sim 0.7\%$ at 100 GeV even though stochastic coefficient is only $\sim 2.3\%$

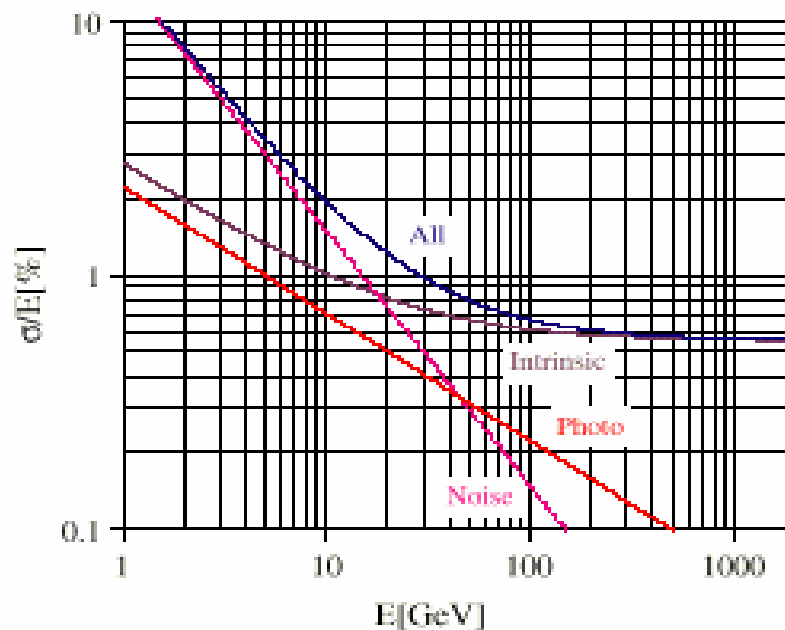
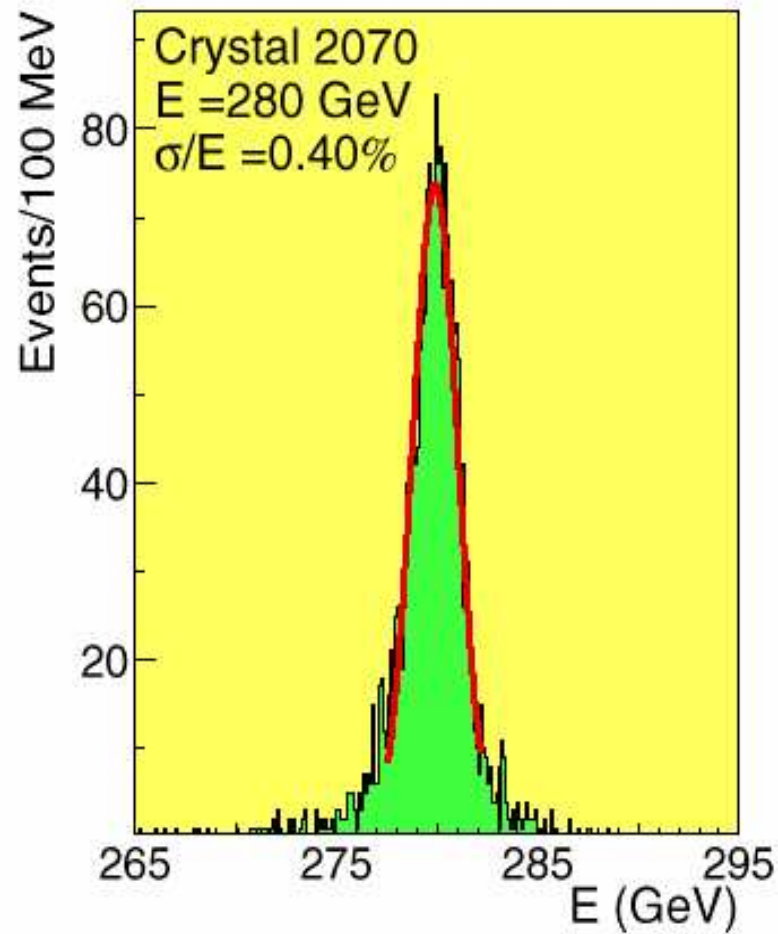
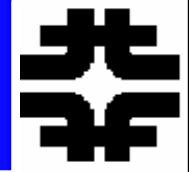


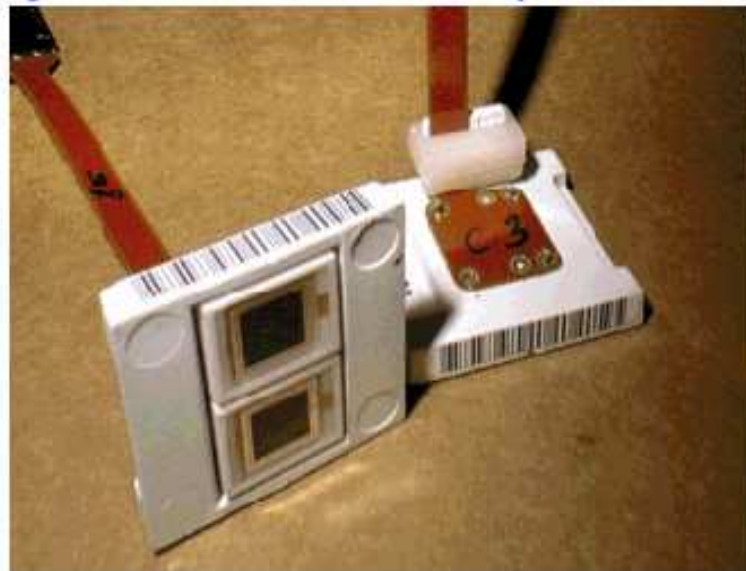
Fig. 1.3: Different contributions to the energy resolution of the PbWO₄ calorimeter.



ECAL

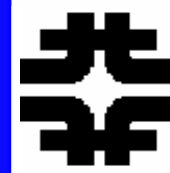


Two APDs 5 x 5 mm surface mounted in a supporting structure (capsule) glued at the rear of the crystal





Xtals and Calorimetry

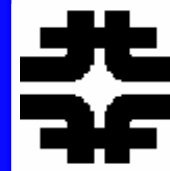


Dense – compact – fast – good photon yield – stable

Crystal		NaI(Tl)	CsI(Tl)	CsI	BaF ₂	BGO	CeF ₃	PbWO ₄
Density	g.cm ⁻²	3.67	4.51	4.51	4.89	7.13	6.16	8.28
Rad. length	cm	2.59	1.85	1.85	2.06	1.12	1.68	0.89
Molière radius	cm	4.5	3.8	3.8	3.4	2.4	2.6	2.2
Int. length	cm	41.4	36.5	36.5	29.9	22.0	25.9	22.4
Decay Time	ns	250	1000	35	630	300	10-30	<20>
				6	0.9			
Peak emission	nm	410	565	420	300	480	310-340	425
				310	220			
Rel. Light Yield	%	100	45	5.6	21	9	10	0.7
				2.3	2.7			
d(LY)/dT	%/°C	~ 0	0.3	- 0.6	- 2	- 1.6	0.15	-1.9
					~ 0			
Refractive Index		1.85	1.80	1.80	1.56	2.20	1.68	2.16



Transverse Size - Moliere



Physics

$$\langle p_T \rangle \sim m_e$$

$$\langle \theta \rangle \sim m_e / \epsilon(t)$$

$$\langle \theta \rangle_{SM} \sim m_e / E_C$$

Multiple Scattering

$$\langle p_T \rangle_{MS} \sim E_S \sqrt{t}, \sqrt{t} \equiv 1$$

$$\langle \theta \rangle_{SM}^{MS} \sim E_S / E_C$$

$$r_M \sim E_S X_o / E_C = \langle \theta \rangle_{SM}^{MS} X_o$$

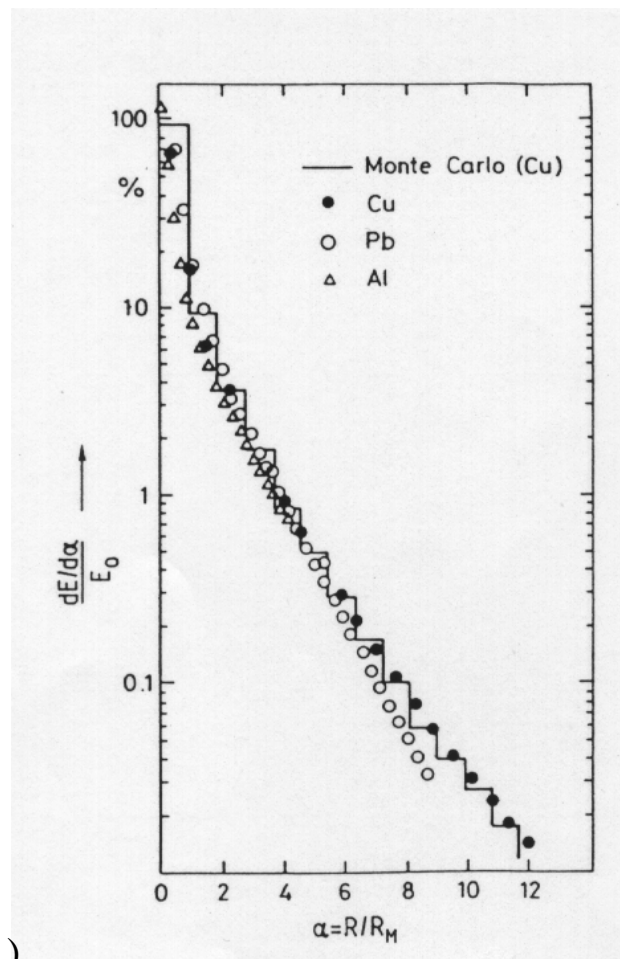
$$r_M \sim [7(gm/cm^2)] (A/Z)$$

In crystals

A fraction of the Moliere radius - (2-2cm)

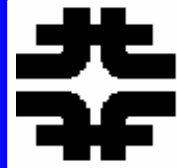
Find θ position using energy centroid to

EM shower is well localized transversely





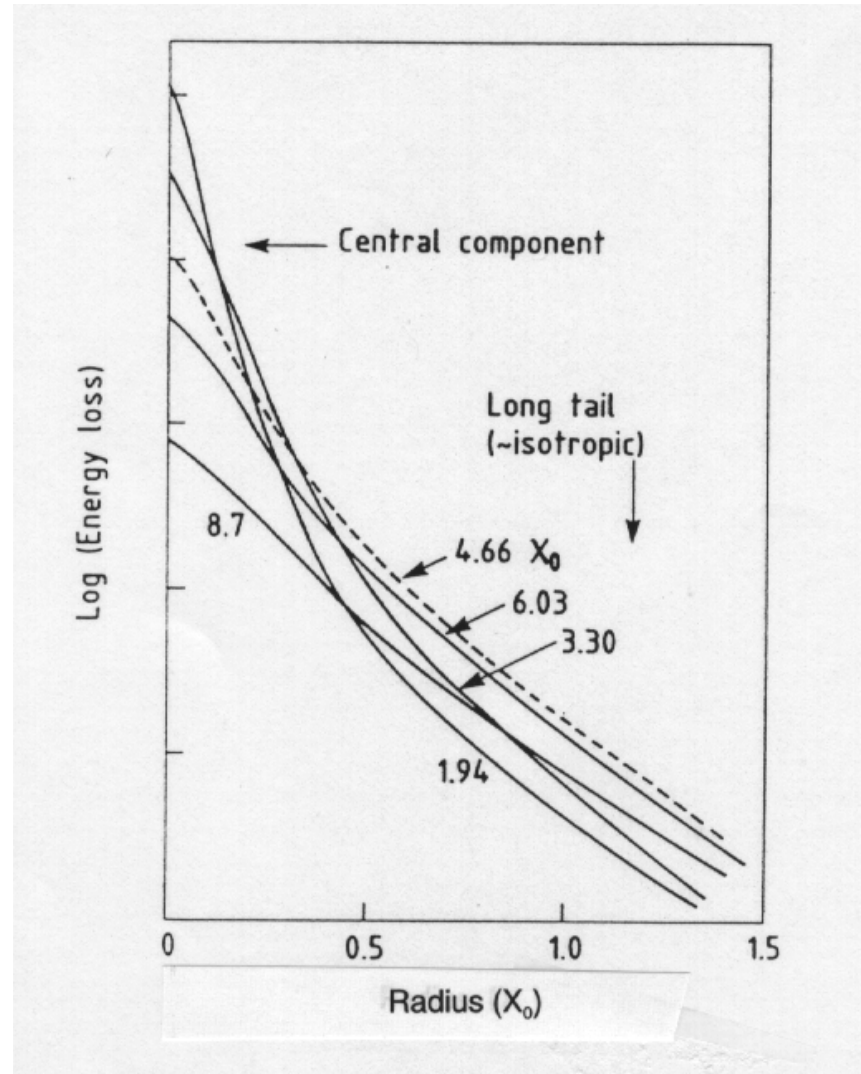
Transverse Size and Depth



n.b logarithmic plot

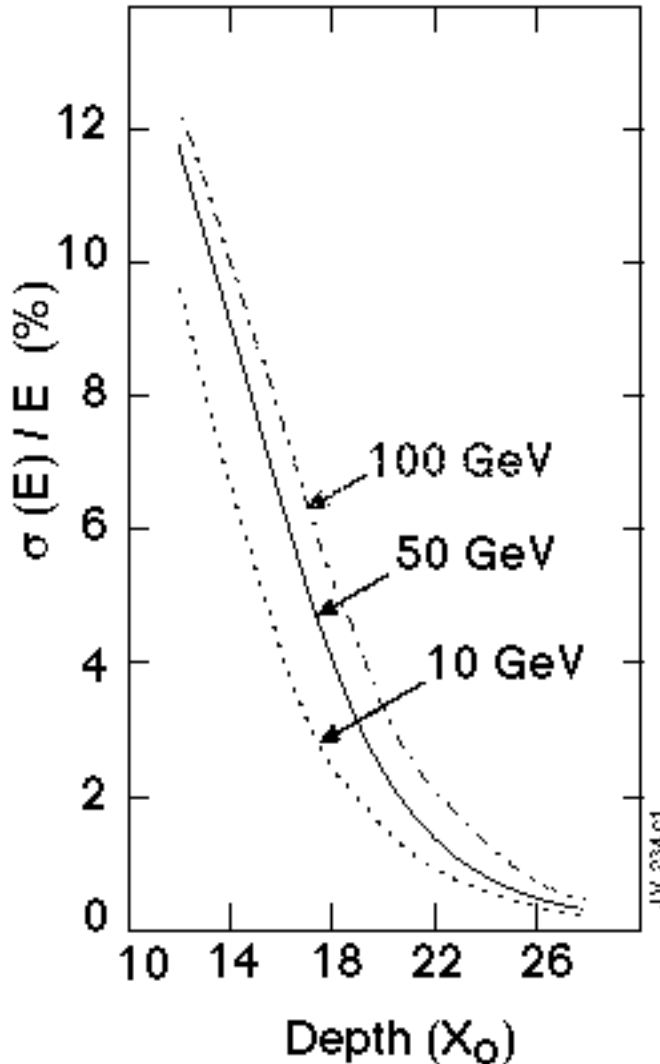
shower easily contained in $1 X_0$
 ~ 0.56 cm in Pb

the shower widens as the depth increases since $\langle \theta(t) \rangle \sim E_s / \epsilon(t)$





Leakage Energy and Depth

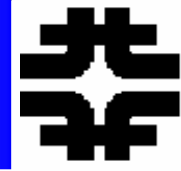


Any EM calorimeter is of finite length
Recall $t_{\max} \sim y$
→ fluctuations hurt because energy lost
in leakage fluctuates

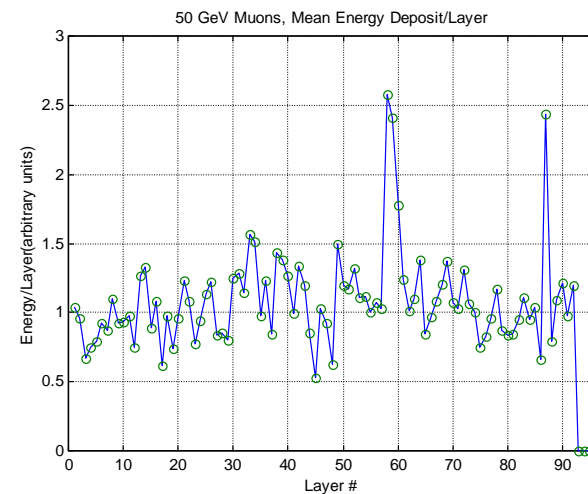
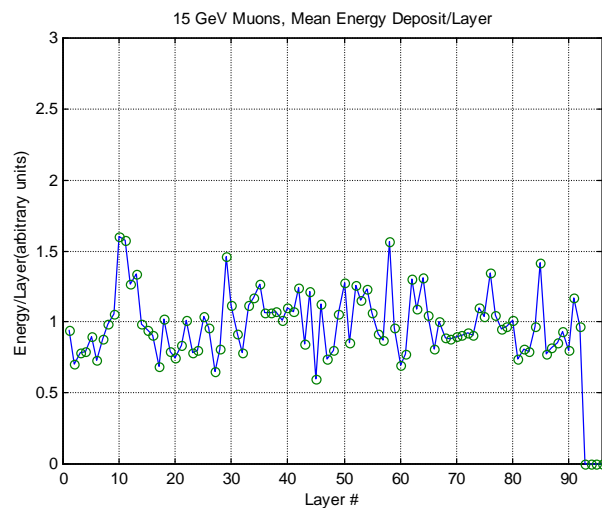
gets worse with E
@ 20 X_0 total depth → 2% @ 50 GeV
this dE/E would dominate all other
error sources for CMS → deeper crystals



Muon Calibration



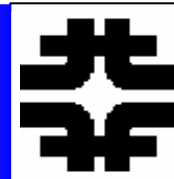
Calibrate the EM calorimeter in a test beam
With e of variable energy.



Use muons from cosmics or $\pi \rightarrow \mu\nu$ from beam
Puts a M.I.P. in each sample
e.g. 96 individually read out samples.
n.b. 15, 50 GeV muons give $\sim dE/dx$
recall the relativistic rise in
ionization energy is a small effect



Hadronic Calorimetry



- **Basic Parameters**
- **Hadronic Cascade**
- **Profiles**
- **Individual Cascades and Neutral Clusters**
- **Sampling Fluctuations**
- **Non-Compensation**
- **Transverse Size**
- **Energy Leakage**
- **Calibration**
- **Radiation Damage**
- **Neutrons**
- **Standard Model and Detectors**
- **Intrinsic Limitations – Jets and Missing Energy**



Basic Parameters



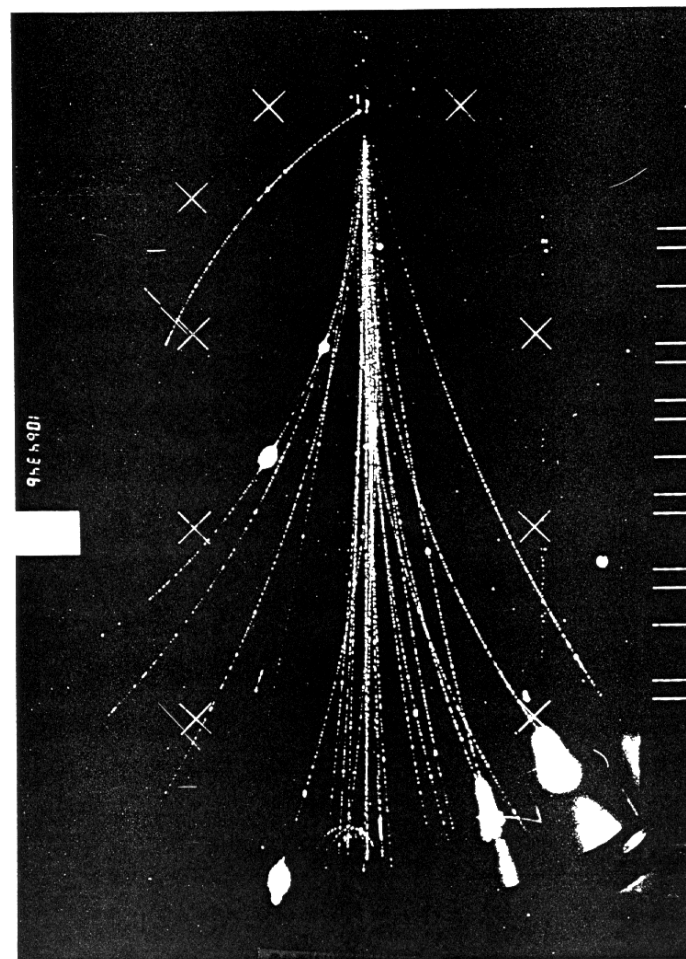
200 GeV π p Interaction

$$\pi^+, \pi^-, \pi^0$$

$$\langle p_T \rangle_{EM} \sim m_e$$

$$\langle p_T \rangle_h \sim 0.4 \text{ GeV}$$

Note large multiplicity
And small angle production
→ limited P_T





Basic Parameters - II



Threshold for π multiplication
 $\pi p \rightarrow \pi \pi p$

$$E_{TH} \sim 2m_{\pi} = 0.28 \text{ GeV}$$

$$N \sim \langle N \rangle \sim \ln E$$

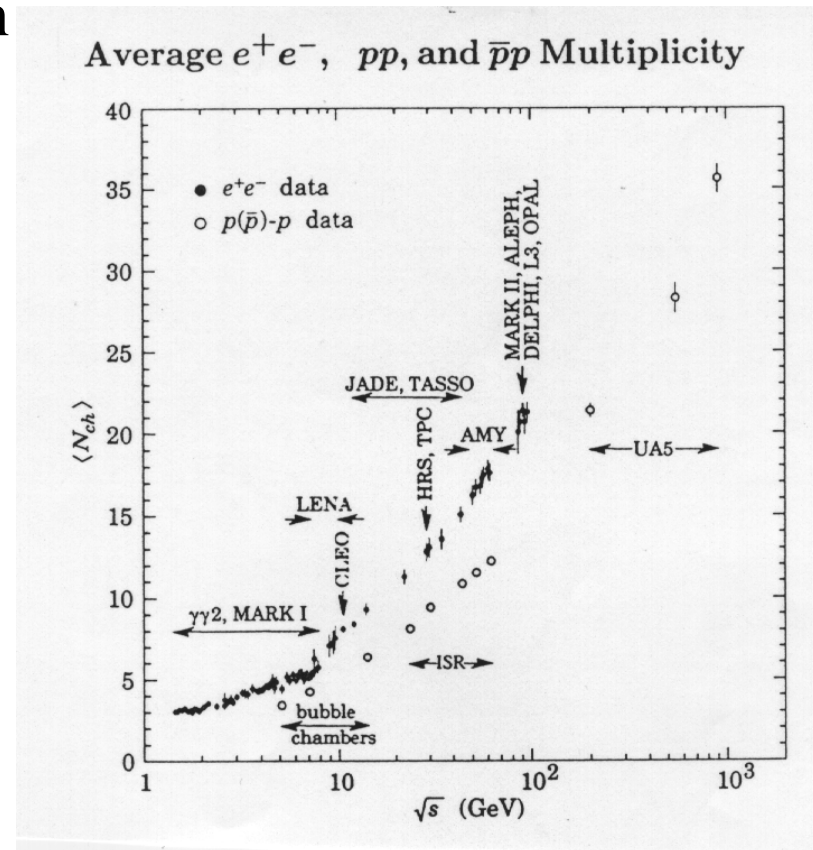
$$X_o / \lambda_l \ll 1$$

$$f_o = 1/3$$

Basis of EM/HAD separation

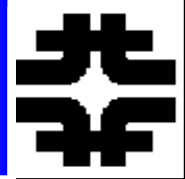
Neutral fraction

Multiplicity of secondary pions
Depends only on log of energy





Hadronic Cascade



Simple Model, $\langle N \rangle = 3$

$$\epsilon(v) = E / N^v, N = \langle N \rangle$$

$$N_{(v)}^o \sim N f_o [N(1 - f_o)]^v$$

$$N_{(v)}^\pm \sim [N(1 - f_o)]^{v+1}$$

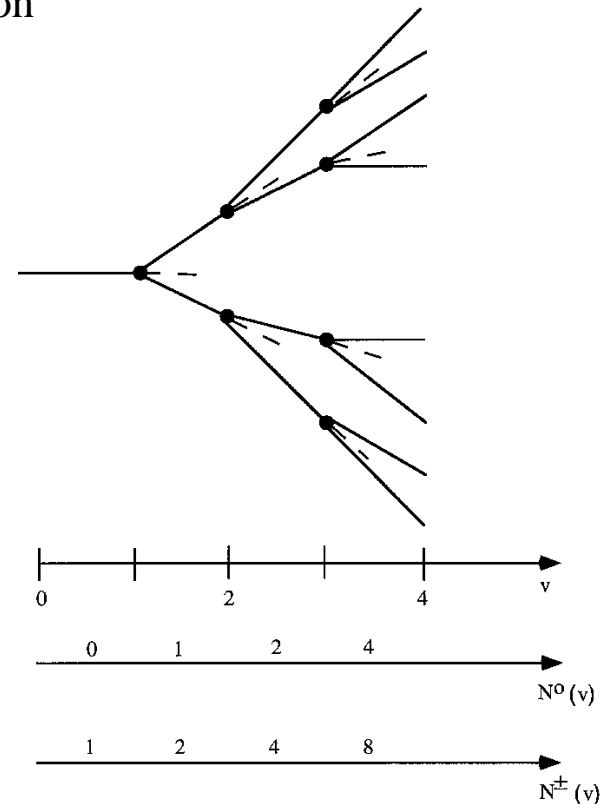
Ignore fluctuations in multiplicity,
Energy sharing, and interaction
Points

$$E_o \sim \sum_v \epsilon(v) N_{(v)}^o$$

$$E_o \sim E f_o \sum_v [1 - f_o]^v, \text{ total neutral energy}$$

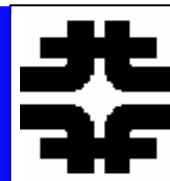
$$"f_o" \sim f_o \sum_o^{v_{\max}} (1 - f_o)^v \rightarrow 1$$

Neutrals are quickly absorbed.
Charged pions transport energy of shower





Hadronic Cascade - II



Simplified model for a hadronic cascade developed
by a 250 GeV incident pion.

Generation v	$\epsilon(v)$ GeV	$N^+(v)$	$N^0(v)$	$E_0(v)$ (GeV)
0	250	1	0	0
1	28	6	3	84
2	3.1	36	18	56
3	0.35	216	108	38
				178 GeV

$$f_0 = 1/3, "f_0" = 0.71$$

Ignore energy deposited by charged pions

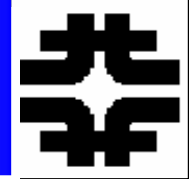
Total path length $\sim [\sum N^{+-}] \lambda$

Energy lost in ionization =
Path length * $dE/dx \sim 49.6$ GeV
Ionization fraction ~ 0.2

Ignore binding
energy and nuclear
fragments

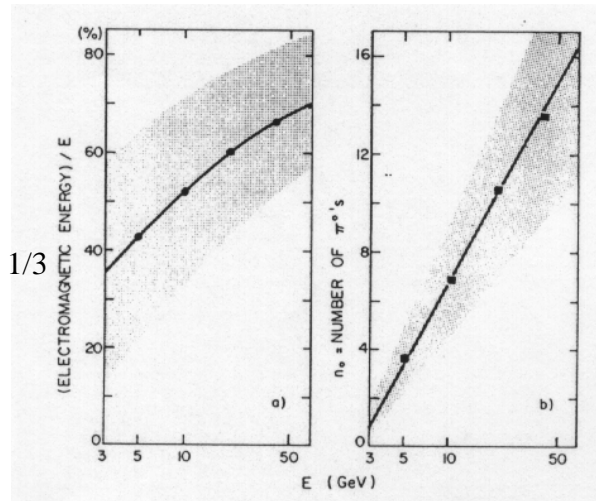


Hadronic Cascade - III



Monte Carlo Models

$$f_0 = \pi^0 / (\pi^+ \pi^0 \pi^-) \sim 1/3$$

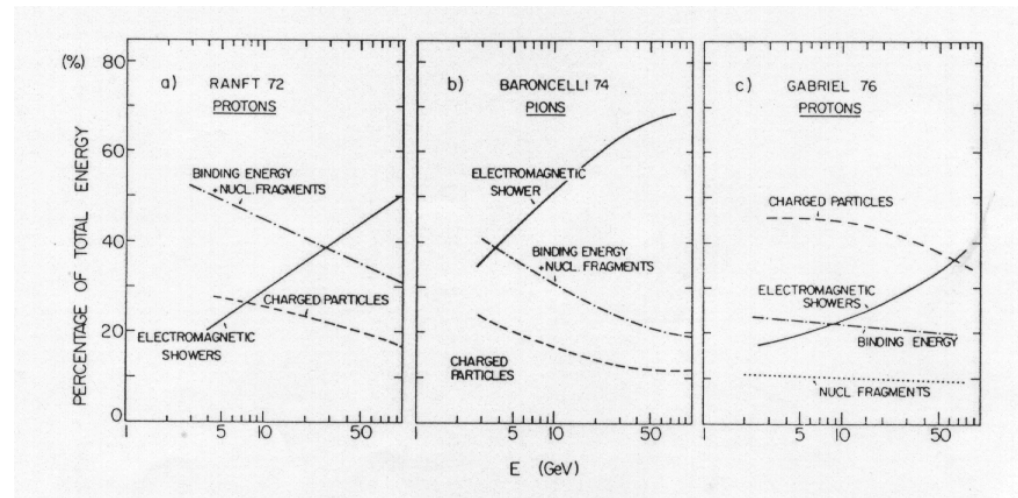


In EM cascade, $P_T \sim \text{Me}$ and nuclei are inert

In hadron cascade, $P_T \sim 400 \text{ MeV}$

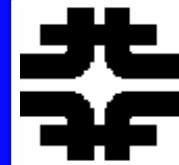
And nuclei are disrupted

$B \sim 8 \text{ MeV/nucleon}$

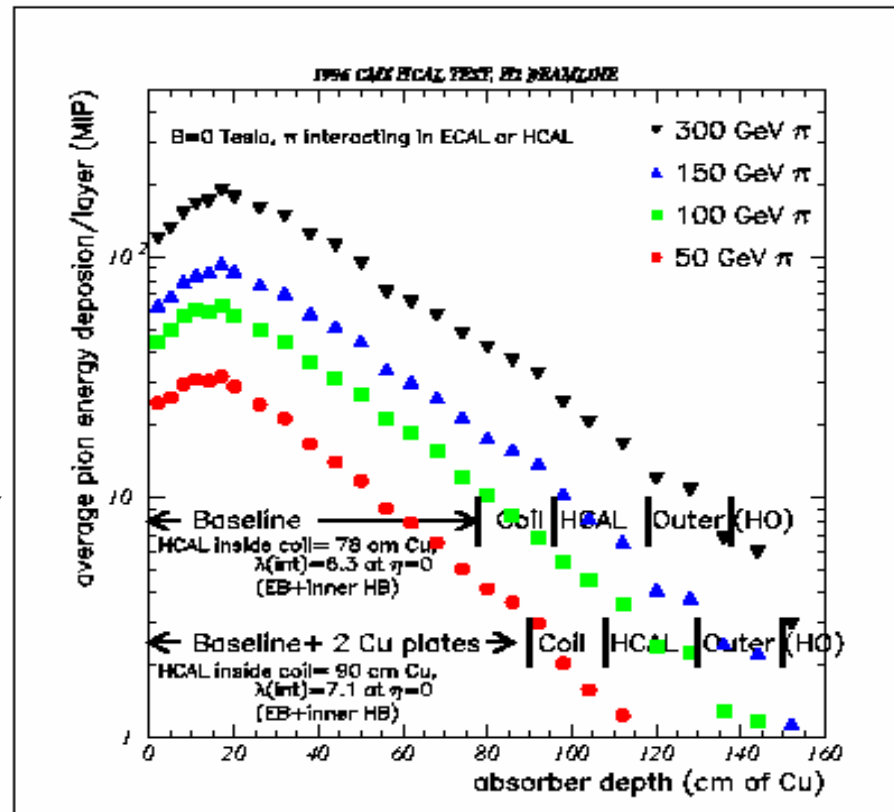




Hadron Showers, Longitudinal



as $E \rightarrow, v_{\max} \rightarrow$
 $v_{\max} [\ln(\langle N \rangle)] = \ln(E/E_{\text{TH}})$
 ex. $E = 250 \text{ GeV}, \langle N \rangle = 8$
 $v_{\max} \sim 3.3$
 Fewer generations than EM
 And lower cascade multiplicity



Falloff with length scale λ
 $\sim 15 \text{ cm in Cu}$

Fig. 26. Average 50, 100, 150 and 300 GeV pion shower profiles as a function of calorimeter absorber depth.



Profiles and Cascades

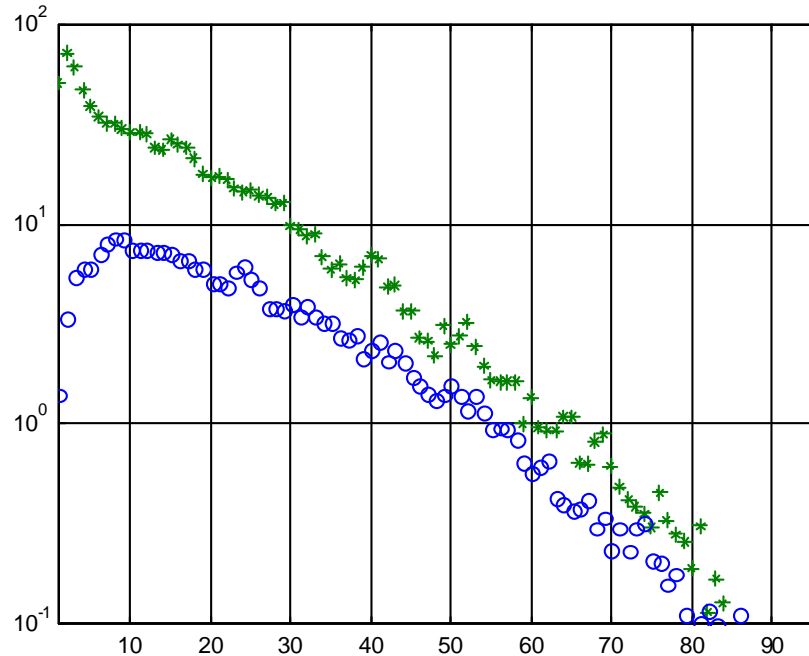


$$\left(\frac{dE}{E}\right) = \left[\frac{u^a e^{-u}}{\Gamma(a+1)} f_o du + \frac{\omega^c e^{-\omega}}{\Gamma(c+1)} (1-f_o) d\omega \right]$$

$$\omega = dv, d \sim 1 \quad (\text{Eq. 11.7})$$

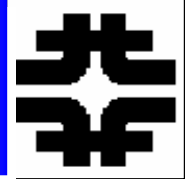
Profile with an EM (X_0)
and a hadronic (λ) component

Profile in calorimeter and
Profile with interaction point
Subtracted. \rightarrow see EM in first
Interaction of cascade, later
Generations washed out by
Fluctuations

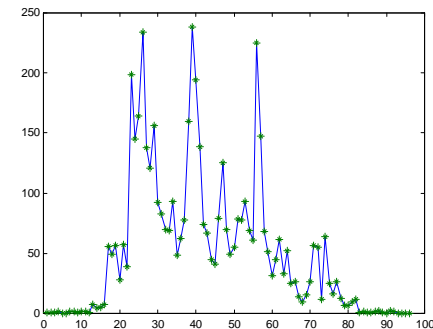
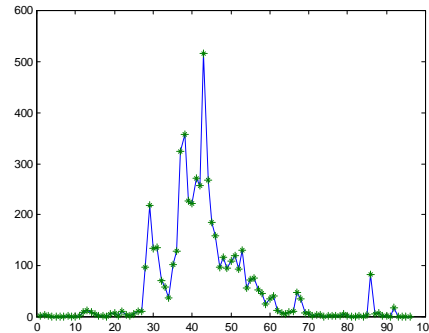
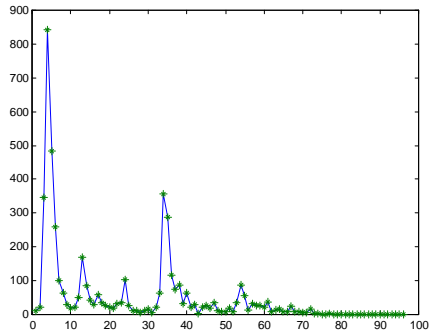
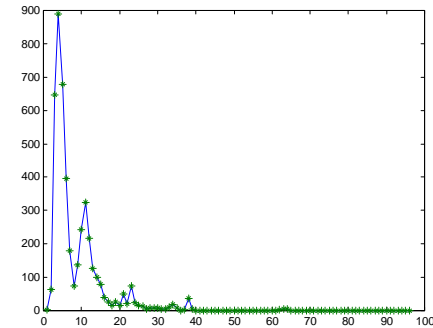
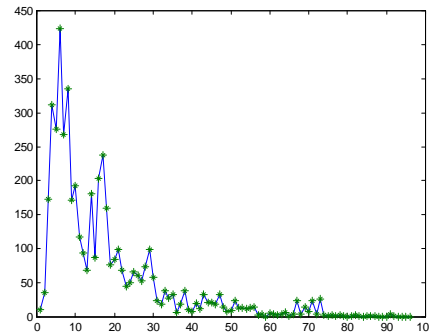
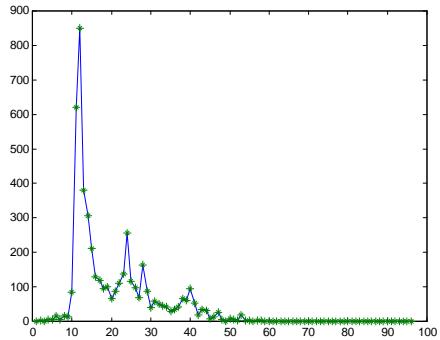




Individual Cascades, Clusters



Pb calorimeter with $X_0/\lambda \sim 30$
EM shower contained in ~ 6 samples



96 layers of sampling
each read out by a phototube

large fluctuations are seen
w.r.t. the smooth profile

hadron shower must be understood
event by event because the fluctuations
are large in a hadron shower



Energy Resolution



$$dE/E = a/\sqrt{E} \oplus b \equiv \sqrt{a^2/E + b^2}$$

$$a_h/a_e \sim \sqrt{E_{TH}/E_C} \quad (\text{Section 11})$$

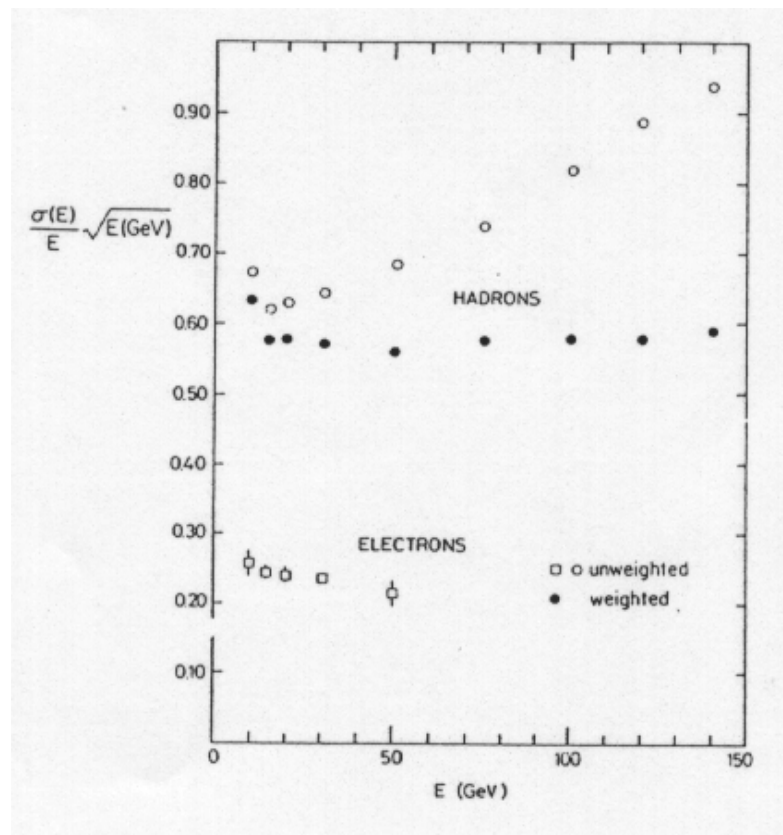
~ 6

$E_{TH} \sim 280 \text{ MeV}$

$E_C \sim 7 \text{ MeV}$

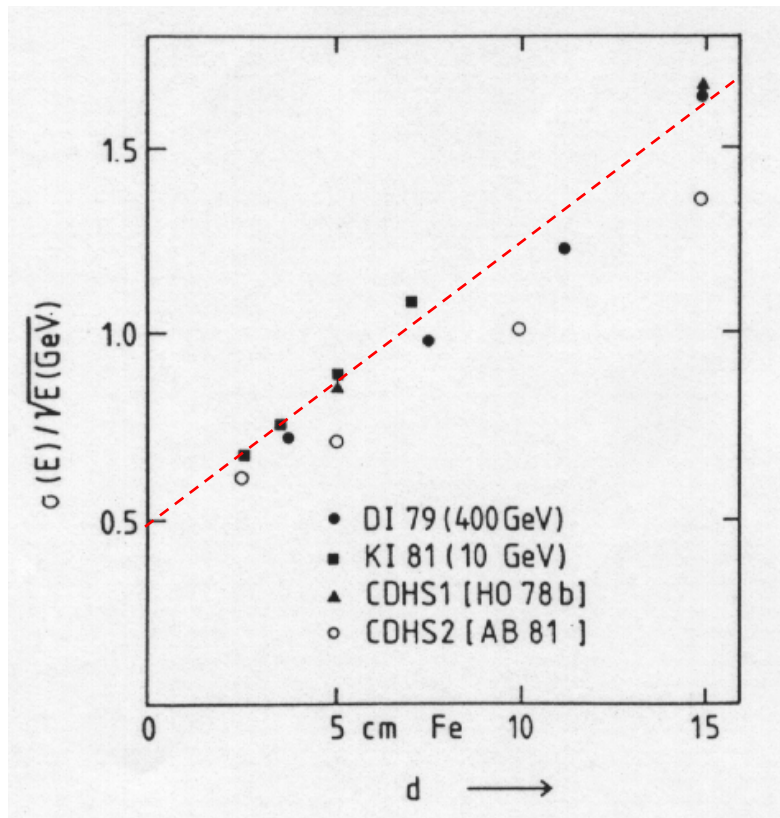
→ expect $\sim 50\%$ stochastic coefficient

in addition, there are fluctuations between ionization/binding/photons and interaction multiplicity/neutral fraction





Sampling Fluctuations



The stochastic coefficient scales roughly as sqrt of sample thickness as expected, but with a non-zero intercept. Sampling fluctuations are not the full story.



dE/E and HCAL



80% stochastic coefficient +
4% constant term

Is the device inhomogeneous?

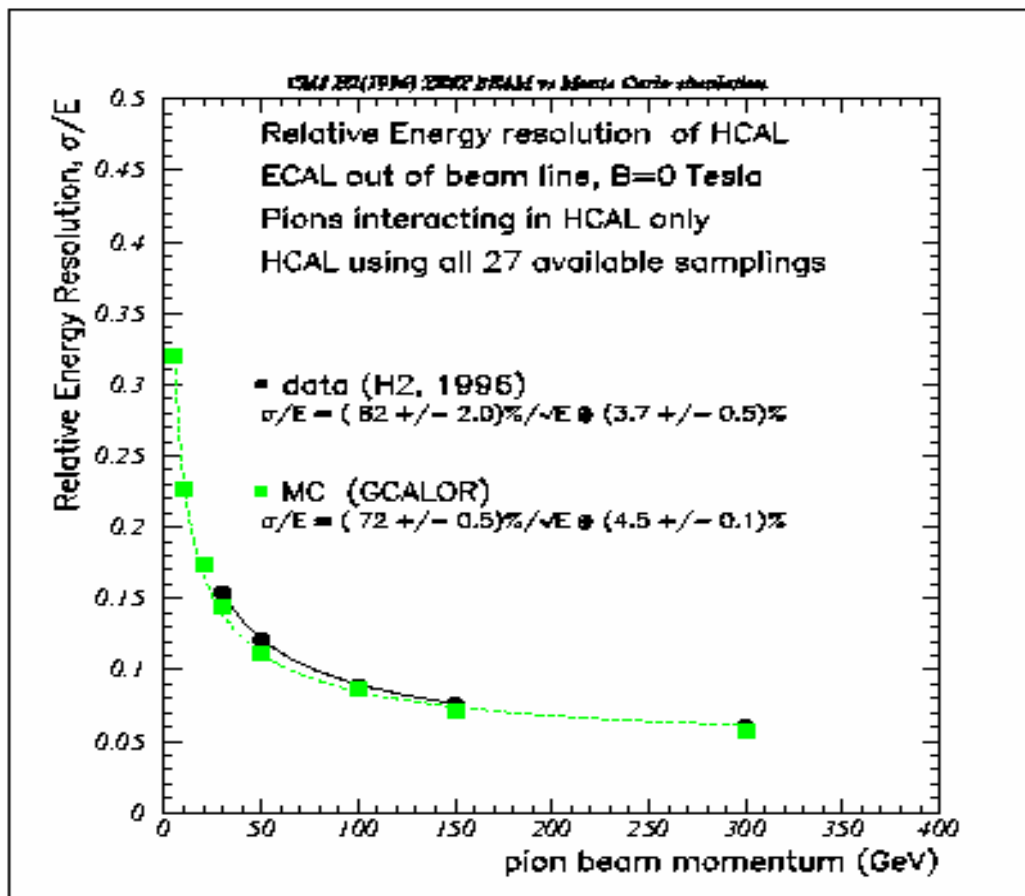


Fig. 32. Relative resolution of the calorimeter for pions and comparison with MC simulation.



Sampling Uniformity and dE/E



Relation of constant term to the r.m.s. of the sampling medium (scintillator tiles)

→ constant term $< 3\%$
since uniformity $< 7\%$
was achieved

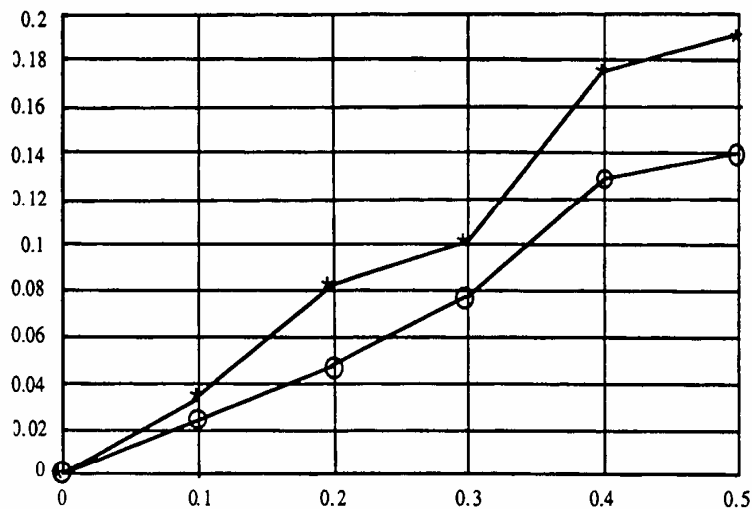


Fig. 6. 6: Induced constant term in the fractional energy error in the HCAL (y axis) as a function of tile manufacturing quality (fractional rms of light yield, x axis). The star symbols correspond to global calibration case and the open circles correspond to the local calibration case.

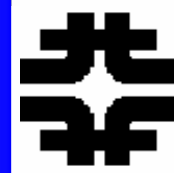


HCAL : HE and HB





CMS HB Calorimeter



Sampling calorimeter: brass (passive) & scintillator (active)

Coverage: $|\eta| < 1.3$

Depth: $5.8 \lambda_{\text{int}}$ (at $\eta=0$)

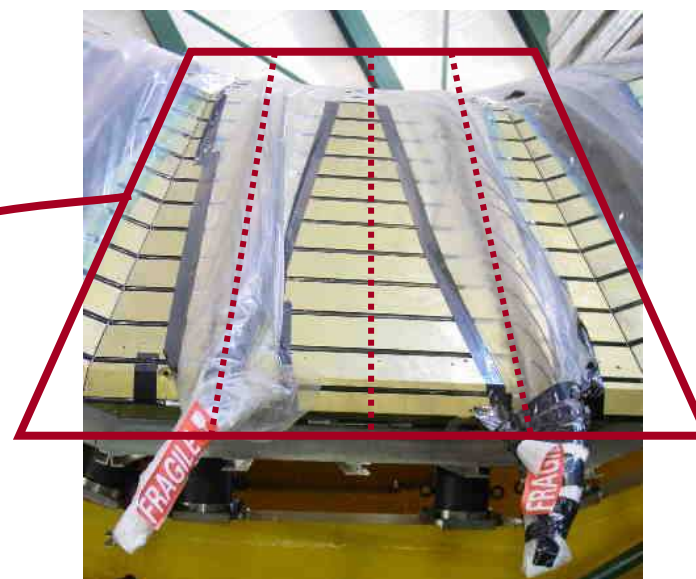
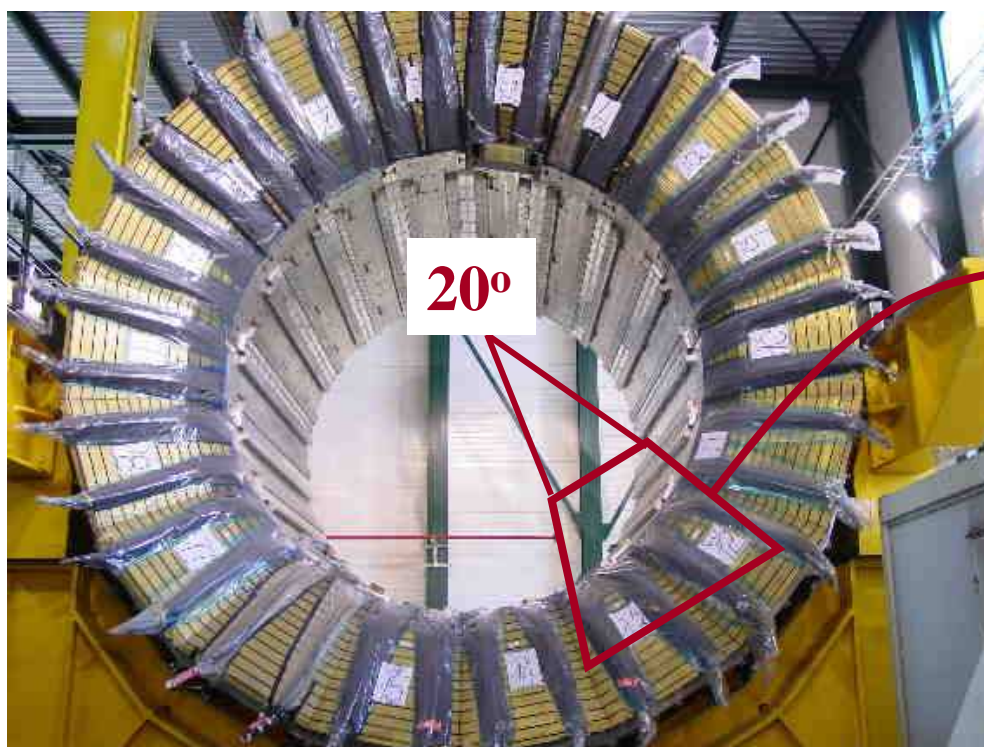
π resolution: $\sim 120 \% / \sqrt{E}$

Completed & assembled

segmentation: $\phi \times \eta =$
 0.087×0.087

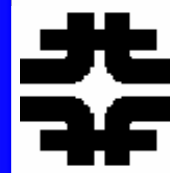
17 layers longitudinally,

$\phi \times \eta = 4 \times 16$ towers





CMS HE Calorimeter



Sampling calorimeter: brass (passive) & scintillator (active)

Coverage: $1.3 < |\eta| < 3$

Depth: $10 \lambda_{\text{int}} \sqrt{E}$

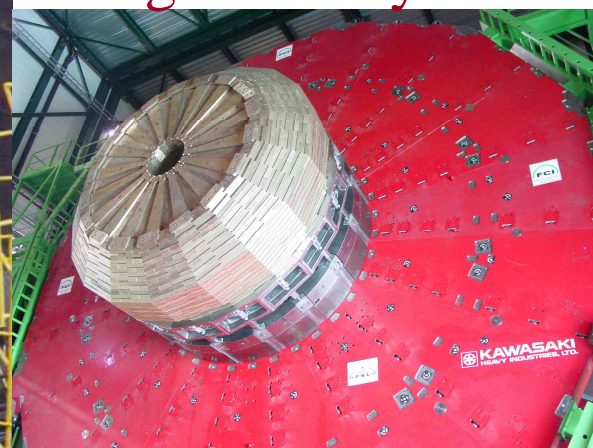
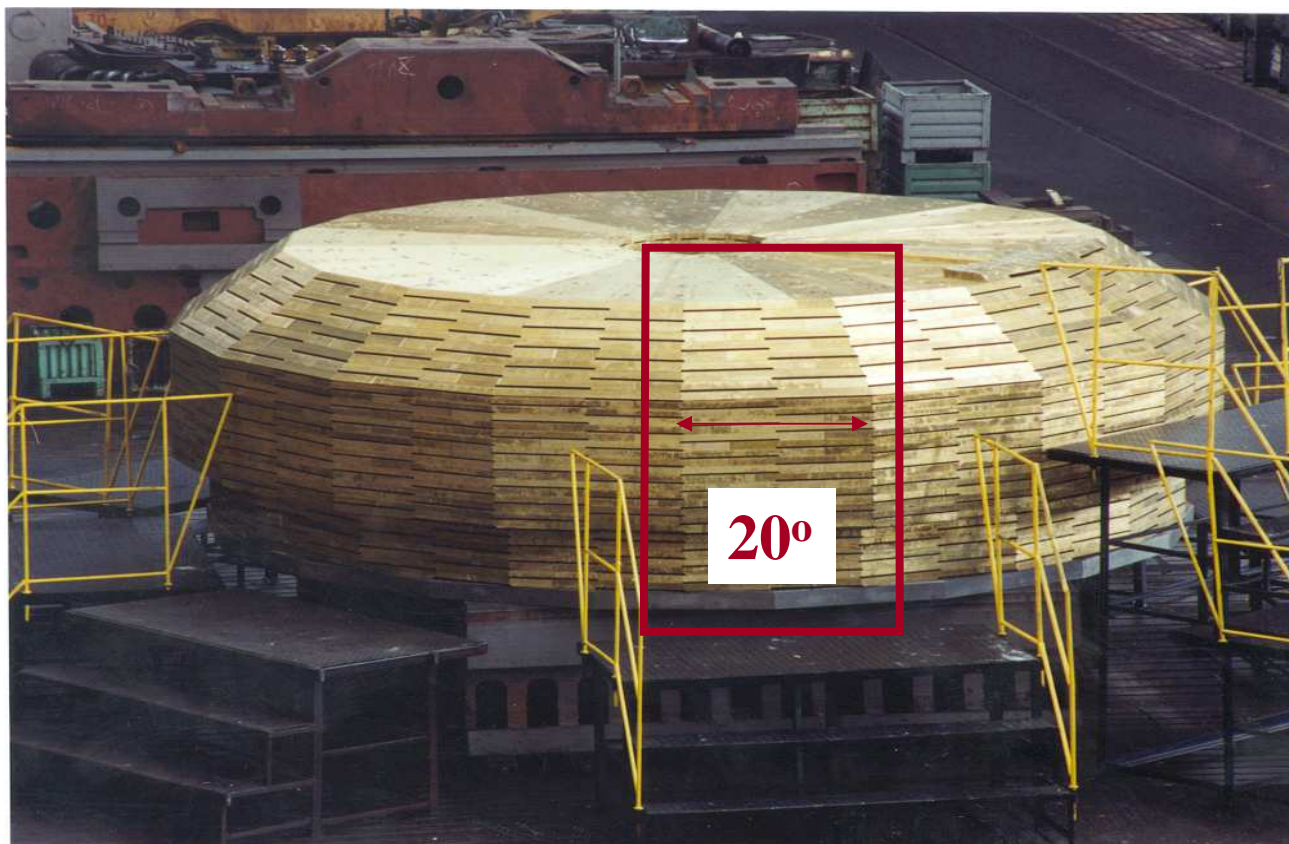
π resolution: $\sim 120\% / \sqrt{E}$

segmentation: $\phi \times \eta =$

0.087×0.087

19 layers

longitudinally



Completed, assembled,
HE-1 installed

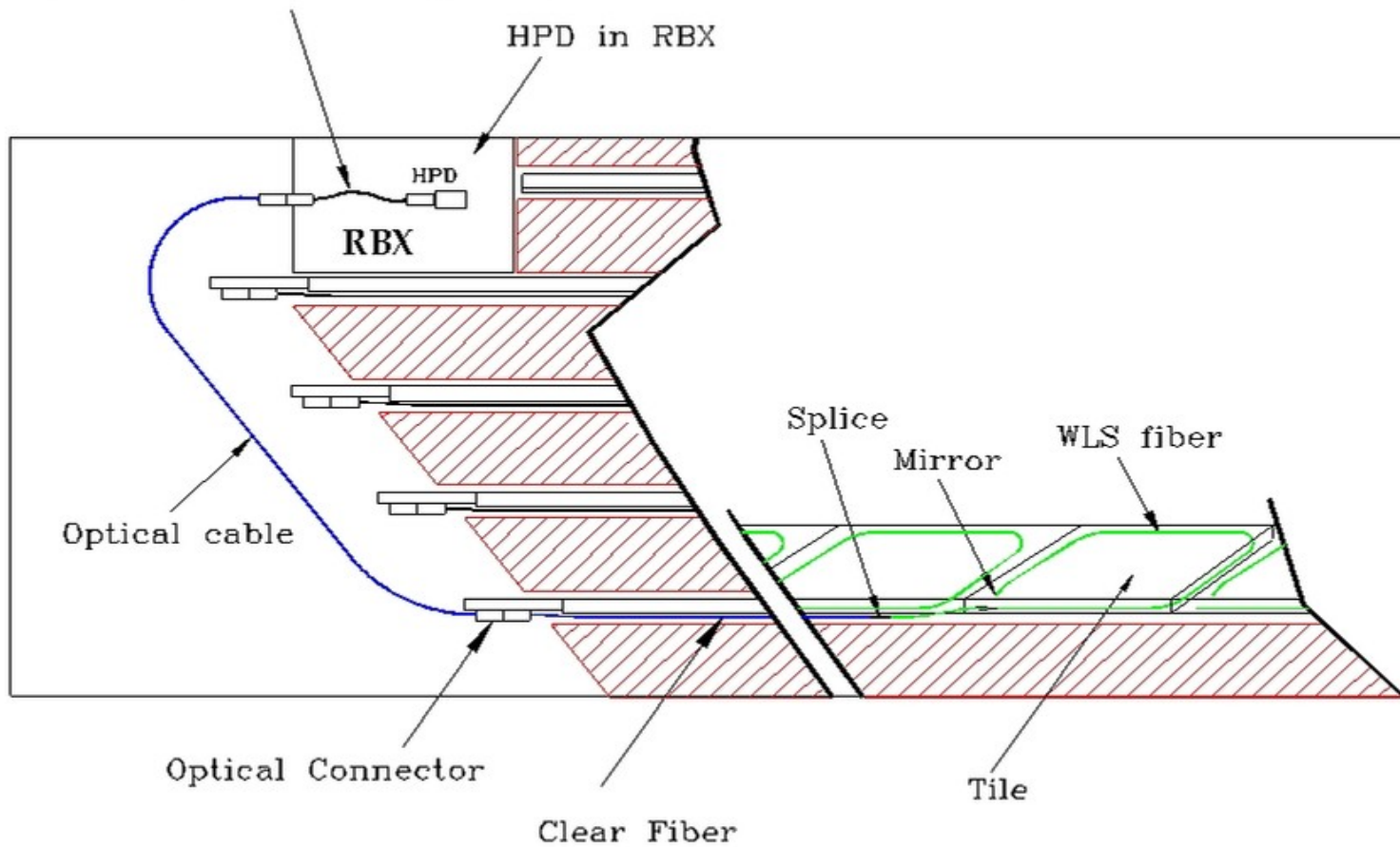


Optical Design for CMS HCALs



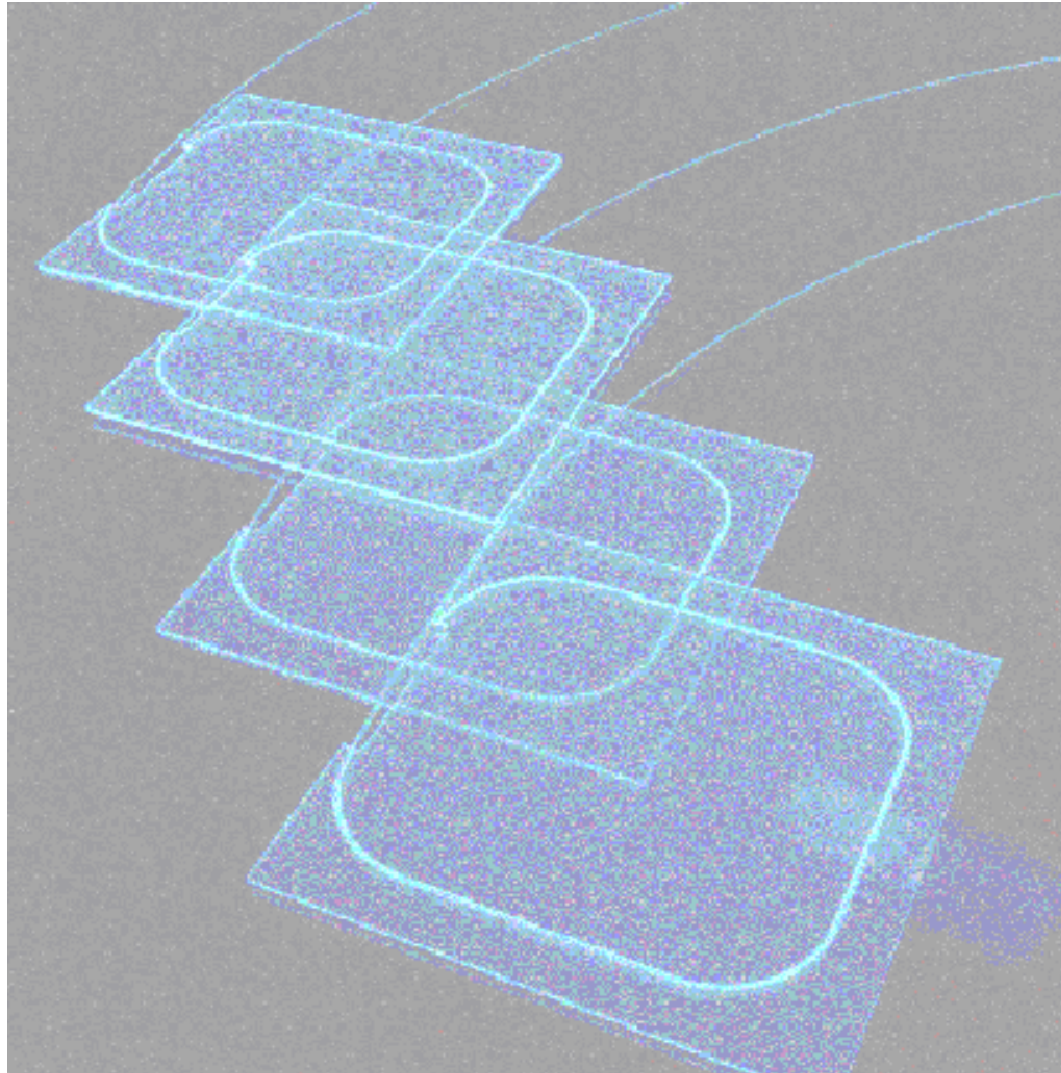
Common Technology for HB, HE, HO

Layer to Tower Decoding Fiber



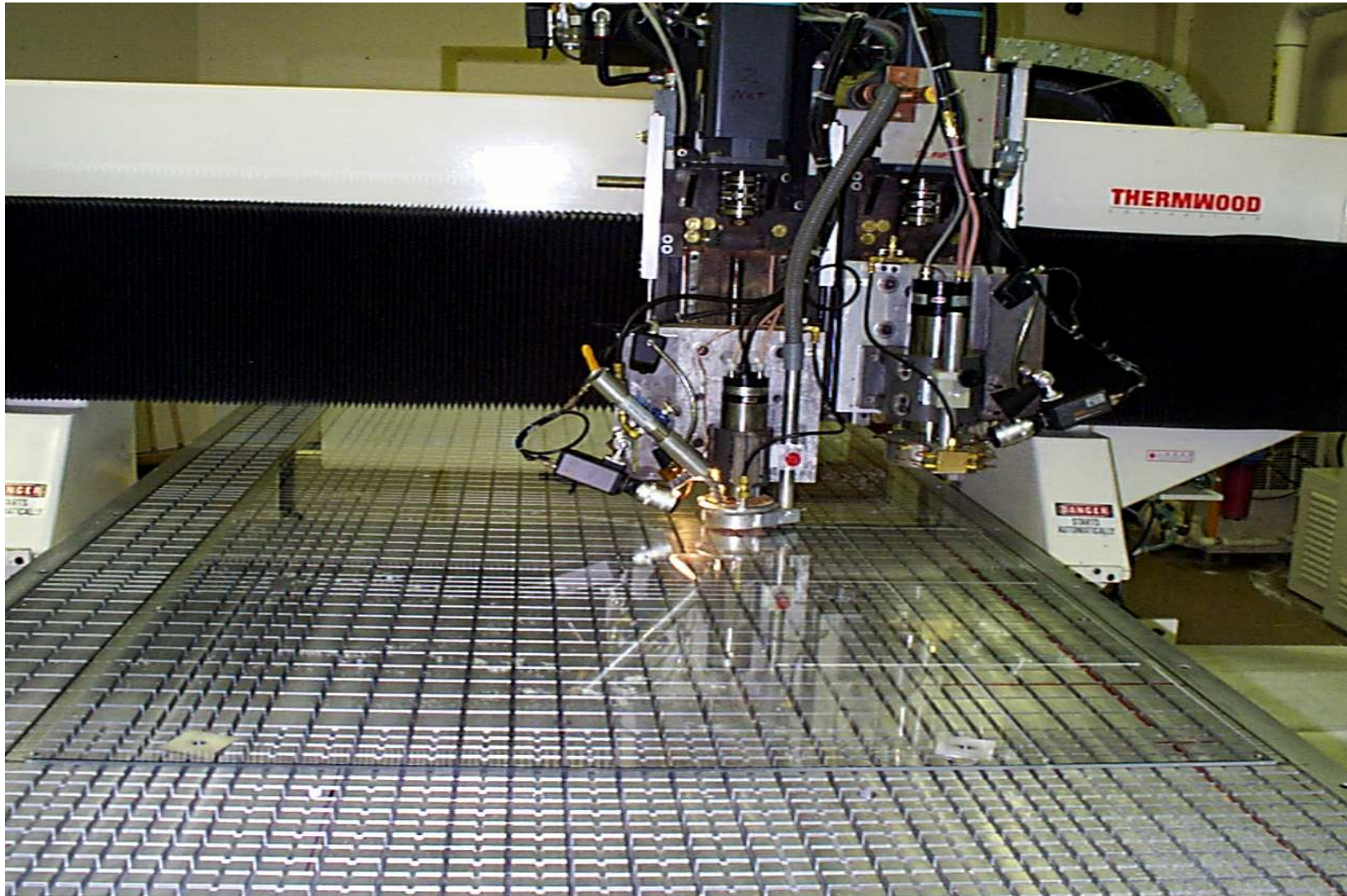
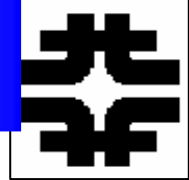


Tile/WLS Fiber Calorimetry





HCAL - Tiles in Lab5





PPP1 and PPP2 at CERN





HCAL - PPP1, Scintillator



- absorber done in industry to FNAL design
- scintillator done in Lab5
- wedge assembled at CERN





Non-Compensation



$$E \sim [e f_o + h(1 - f_o)] E_{IN}$$

$$\left(\frac{dE}{E} \right)_{df_o} \sim |e/h - 1| df_o$$

$$df_o \sim \sqrt{\langle N^o \rangle} / \langle N \rangle \sim 0.17$$

$$\left(\frac{dE}{E} \right)_{df_o} \sim |e/h - 1| \left[\sqrt{\langle N^o \rangle} / \langle N \rangle \right]$$

$$\left(\frac{dE}{E} \right)_{df_o} \sim 1 / \sqrt{\ln(E)} \rightarrow 0 \text{ as } E \rightarrow \infty$$

What if the medium responds differently to EM shower (e) and the hadron cascade (h) ? Recall ionization, binding and nuclear fragments

Typically a medium responds to EM More efficiently than HAD because of Time delay in fragments and loss of Neutron energy to the sampling.

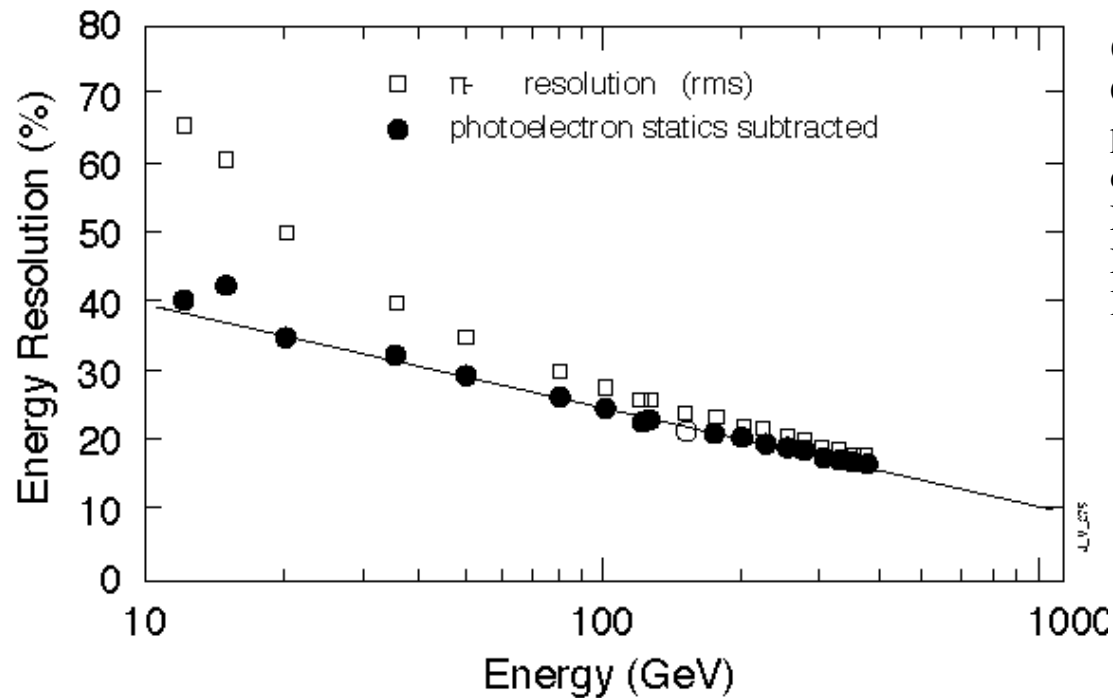
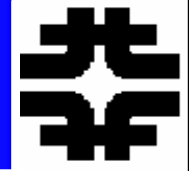
Fluctuations in the neutral fraction Induce a “constant term” in the Energy resolution dE/E

If e/h = 1.2, then a 6.8 % constant Term is induced.

n.b. not “constant” at high energies, as “fo” → 1, “dfo” → 0 and dE/E → 0



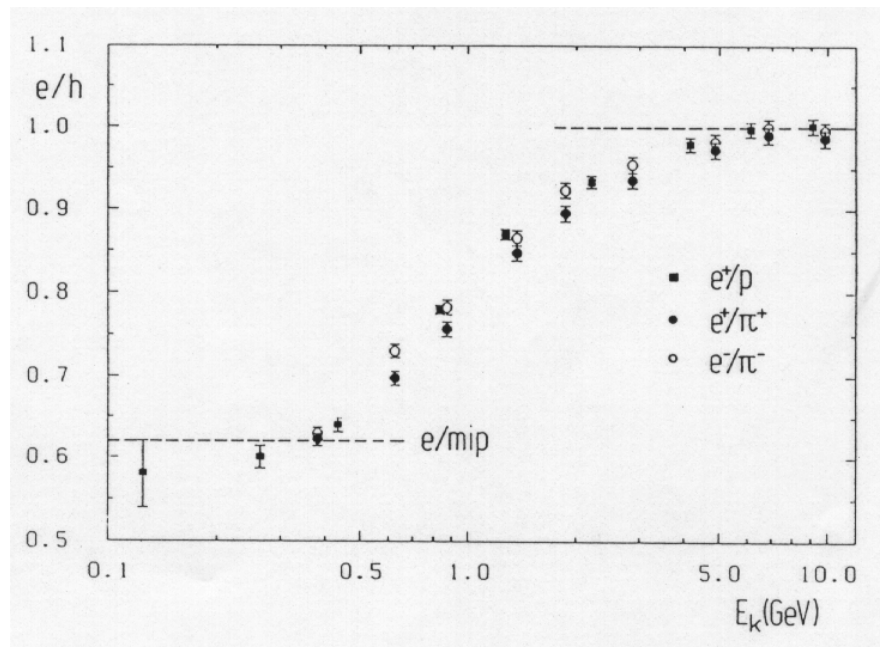
Quartz Samples and dE/E



Quartz calorimeter responds to Cerenkov light of fast e in the EM part of the shower. $h \sim 0$.
 $dE/E \sim "df_0"/"f_0"$
Expect resolution determined by Neutral fluctuations. Note the $\ln(E)$ behavior.



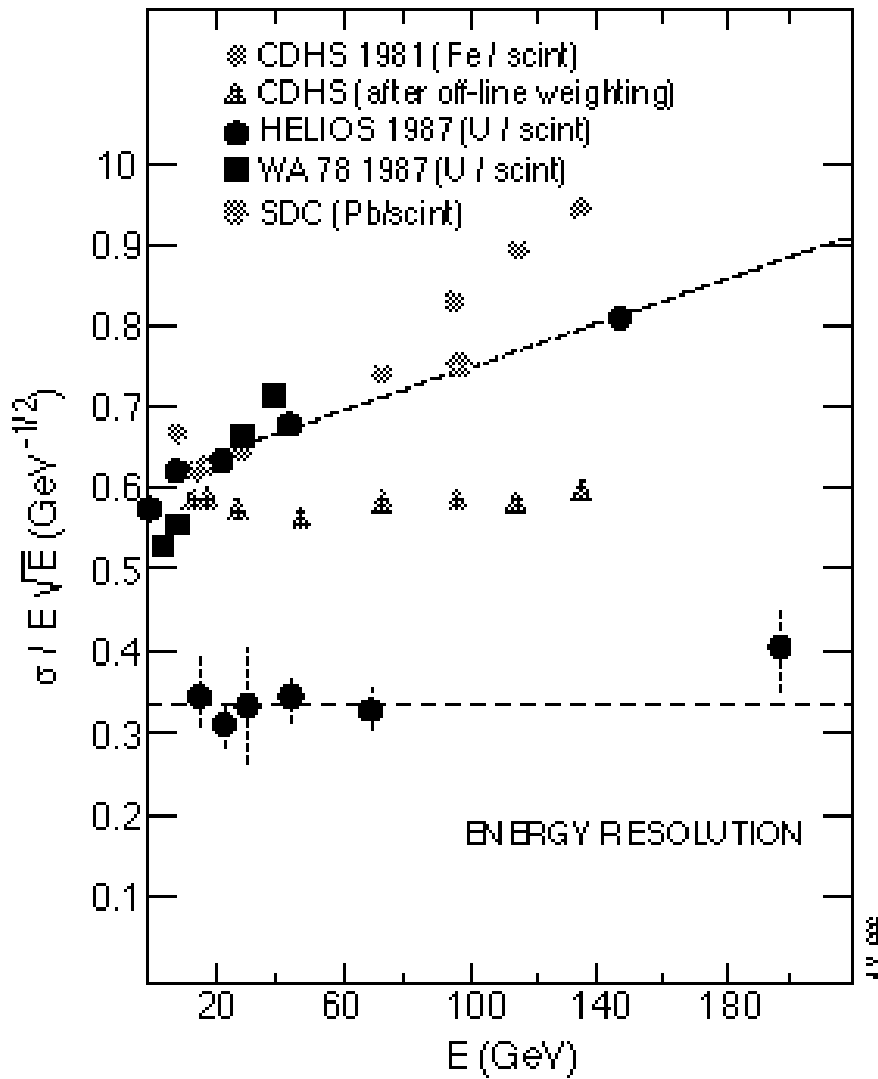
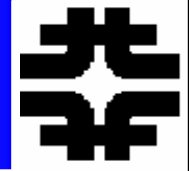
Non-Compensation - II



At low energy, e/h decreases.
As $E \rightarrow E_{TH} \sim 280$ MeV from above, e/h falls even for devices designed to have $e/h \sim 1$ for $E > 5$ GeV. Intrinsic physics



dE/E and e/h



U/scint can be made compensating

Fe/scint is typically not compensating



Fe HCAL and e/h

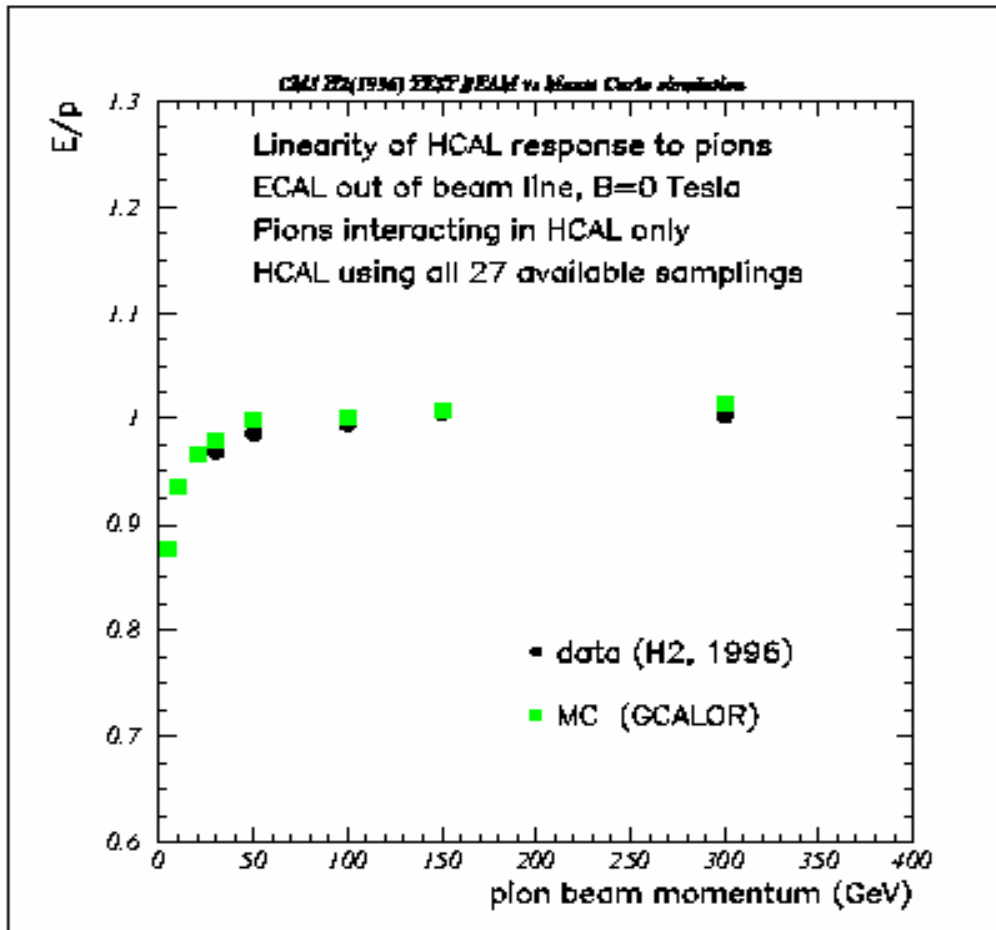
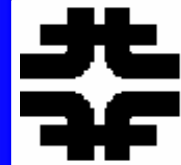


Fig. 31. Linearity of energy response of pions and comparison with MC simulation.

Non - linearity due to non-compensation

$$\pi = e''fo'' + h(1-''fo'')$$

$$e = e$$

$$\pi/e = 1 + (1-''fo'')(h/e-1)$$

if e/h=1 then $\pi/e = 1$

if "fo"-->1 then $\pi/e --> 1$

if e/h>1 then $\pi/e < 1$

if "fo" = fo = 1/3 and e/h = 1.4, then $\pi/e = 0.81$



Evading “Mixed Media”



If you identify energy as hadronic, you can correct for non-linearity due to different ECAL and HCAL materials but not non-compensation.

$$R = \text{response} = eE_e + hE_h$$

combined setup

$$E = E_E + E_H$$

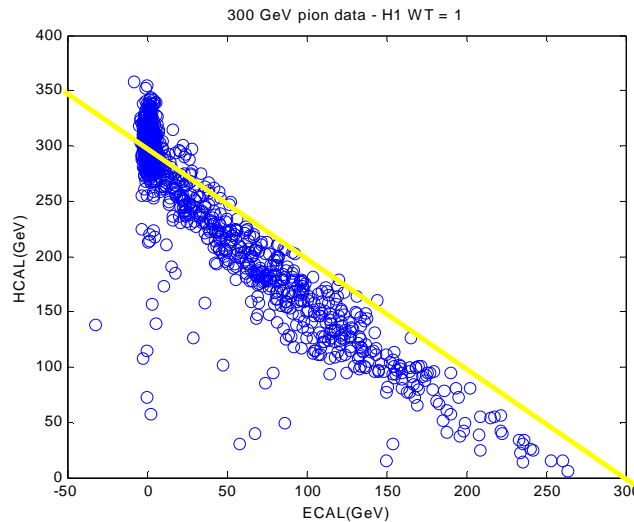
$$E = 1/e_E(e/\pi)_E R_E + 1/e_H(e/\pi)_H R_H$$

ECAL/HCAL calib to electrons – e_E, e_H

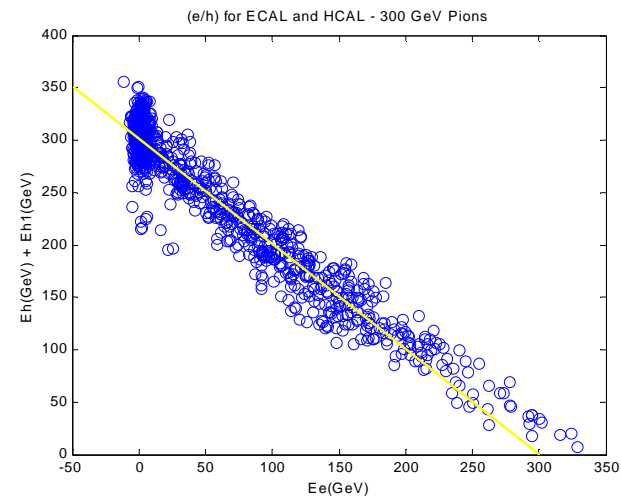
$$(e/h) = (e/\pi)(1 - F_o) / [1 - F_o(e/\pi)]$$

Works over a large energy range. Still dfo and $e/h > 1$ cause dE.

EH



EE





Fe HCAL and e/h



Fe calorimeter
 Fit to non-linearity
 using a parametrized
 “fo(E)”.
 Find that e/h ~ 1.4 for Fe

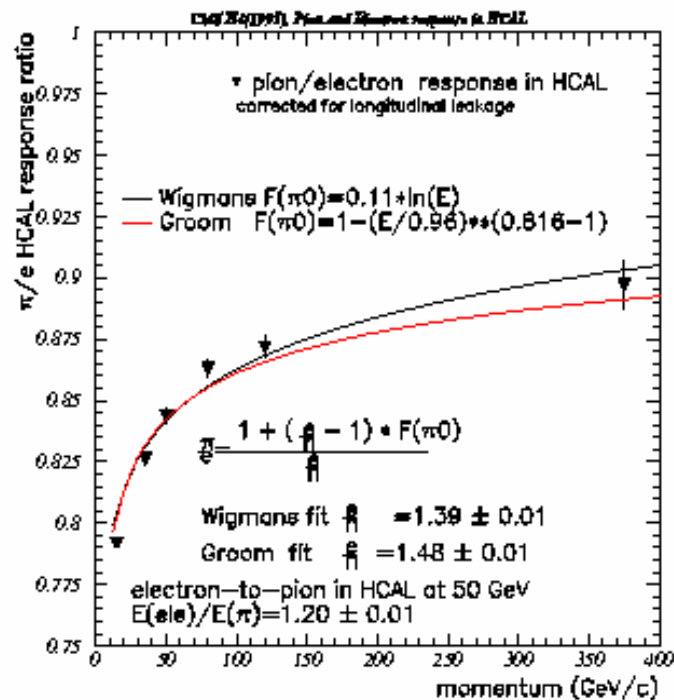
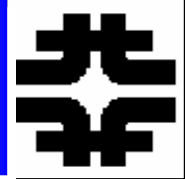


Fig. 25. H4(1995) data: the pion/electron ratio of response of the copper sampling prototype HCAL as a function of beam momentum. The calorimeter consists of the Inner HCAL (ten 3 cm Cu samplings followed by nine 6 cm Cu samplings), the magnetic coil mltic (8 cm Cu+29 cm Al) and the HCAL Outer (two 8 cm Cu and two 10 cm Cu samplings). The scintillator is 4 mm thick SCSN-81. The pion response of HCAL has been corrected for longitudinal leakage. We have assumed a linear electron response of HCAL, $E(ele)/E(\pi)$ at 50 GeV = 1.20 ± 0.01 . The extracted values of e/h correspond to the two different parameterizations of the average fraction of π^0 's produced in pion induced showers.



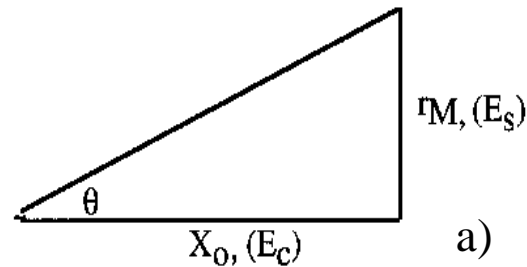
Transverse Size



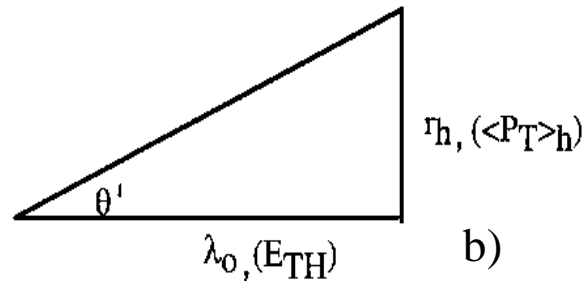
$$\langle \theta \rangle \sim \langle p_T \rangle_h / \mathcal{E}(v)$$

$$\langle \theta \rangle_{SM} \sim \langle p_T \rangle_h / E_{TH}$$

$$r_h \sim \lambda_l \langle p_T \rangle_h / E_{TH}$$
$$\sim \lambda_l \left[\frac{\langle p_T \rangle_h}{2m_\pi} \right] \sim \lambda_l$$



EM



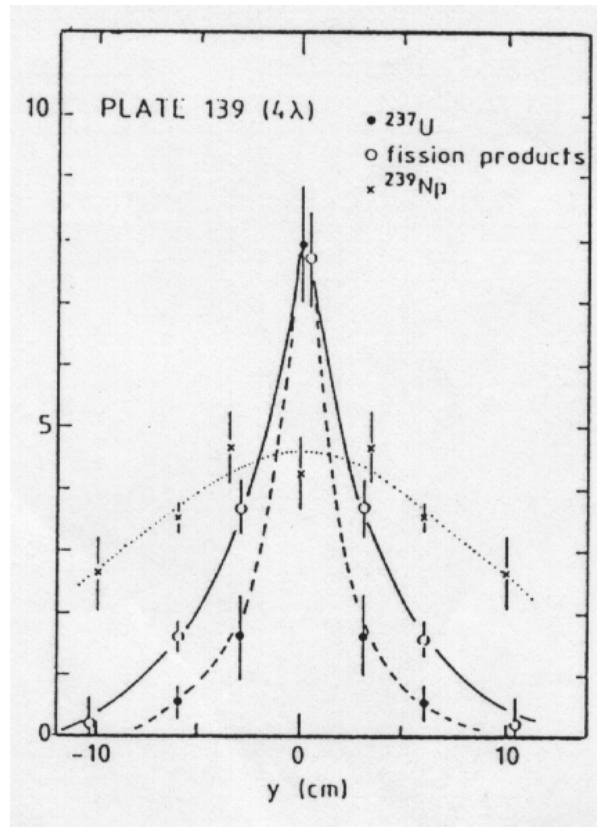
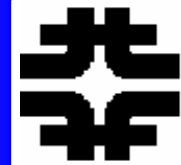
Hadronic

Expect that a hadron shower
Has a transverse size $\sim \lambda$

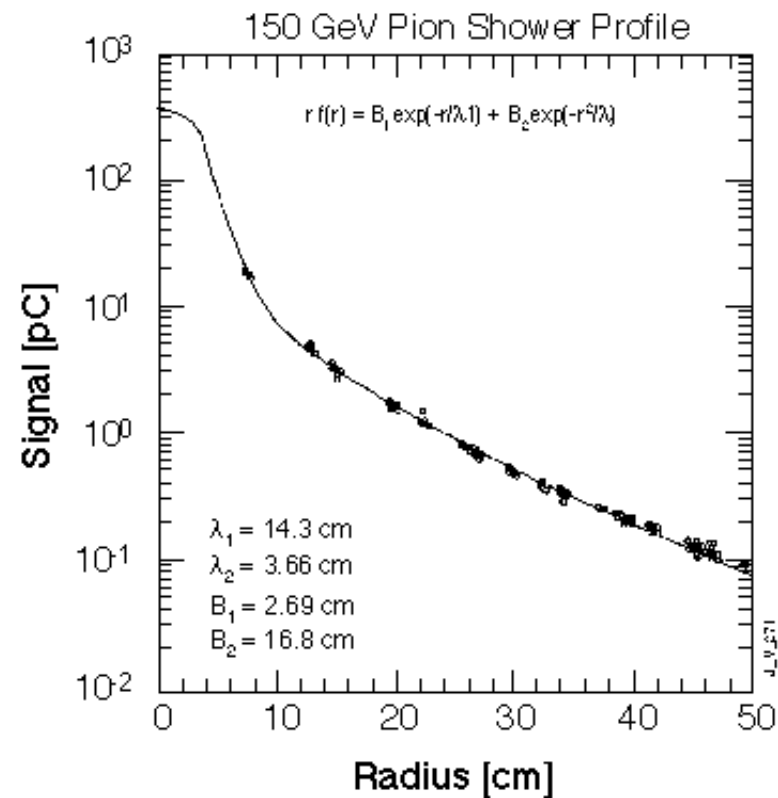
$r_M \sim 2$ cm for crystals
 $\lambda \sim 15$ cm for Cu
EM showers are transversely
smaller than hadronic showers



Transverse Size - II



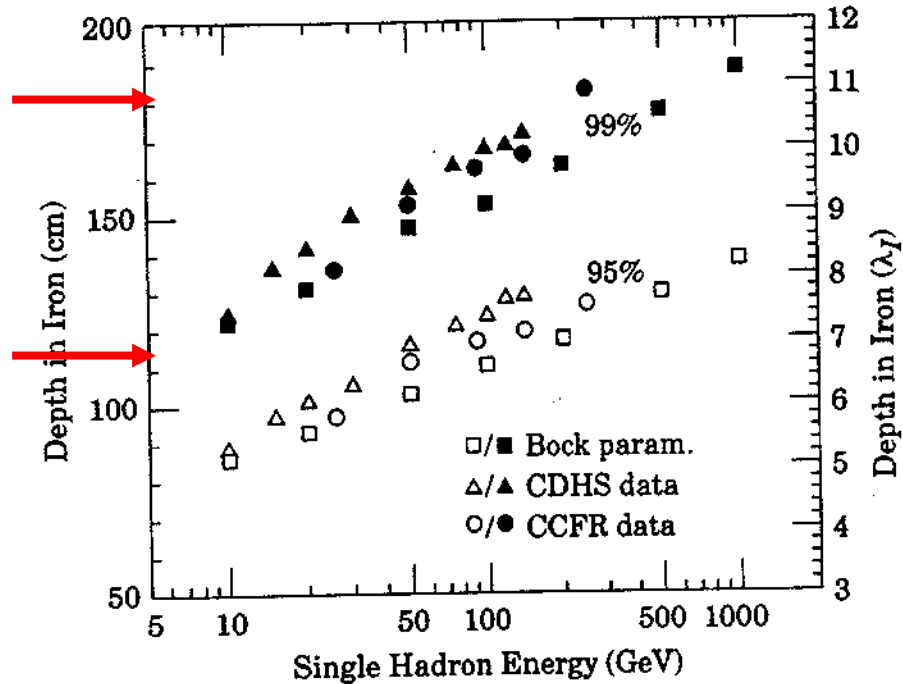
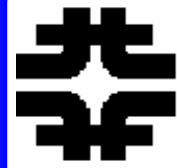
Transverse distribution has
A EM “core” and a hadronic
“tail” – 2 components



n.b. there are 2 distance scales,
one $\sim r_M$ and the other $\sim \lambda$.
Data is integrated over all
depths in the shower



Energy Leakage

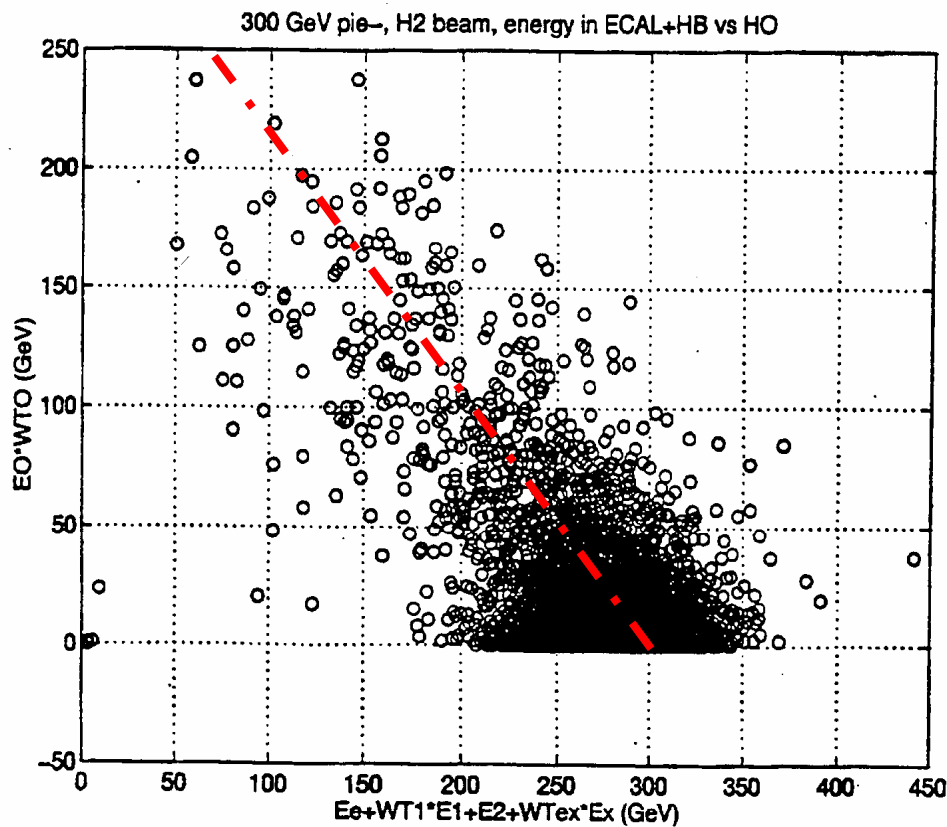
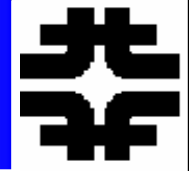


For 95 % containment, the
Fluctuation in the leakage is
➤ 5 %.

With 7λ total depth, single pions are
➤ 95 % contained for energies < 100 GeV
As the LHC is a 7 TeV + 7 TeV machine,
That is a bit thin.



CMS - Leakage and "Catcher"



CMS outer calorimetry
300 GeV pions
"exit weighting" to
oversample late developing showers

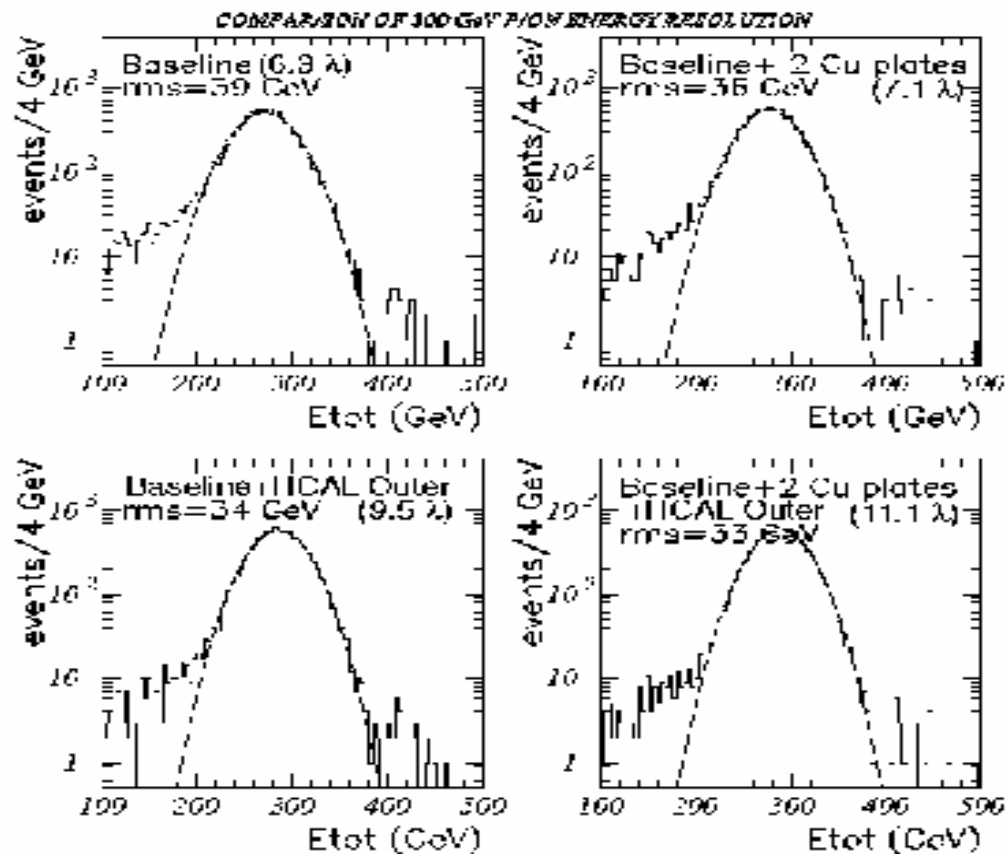
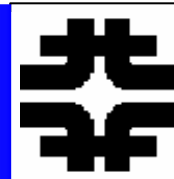
4 λ

Figure. 7: Scatter plot of energy inside the solenoid vs. the energy outside the solenoid in the HO layers for single 300 GeV pions.

7 λ



dE/E and Energy Leakage

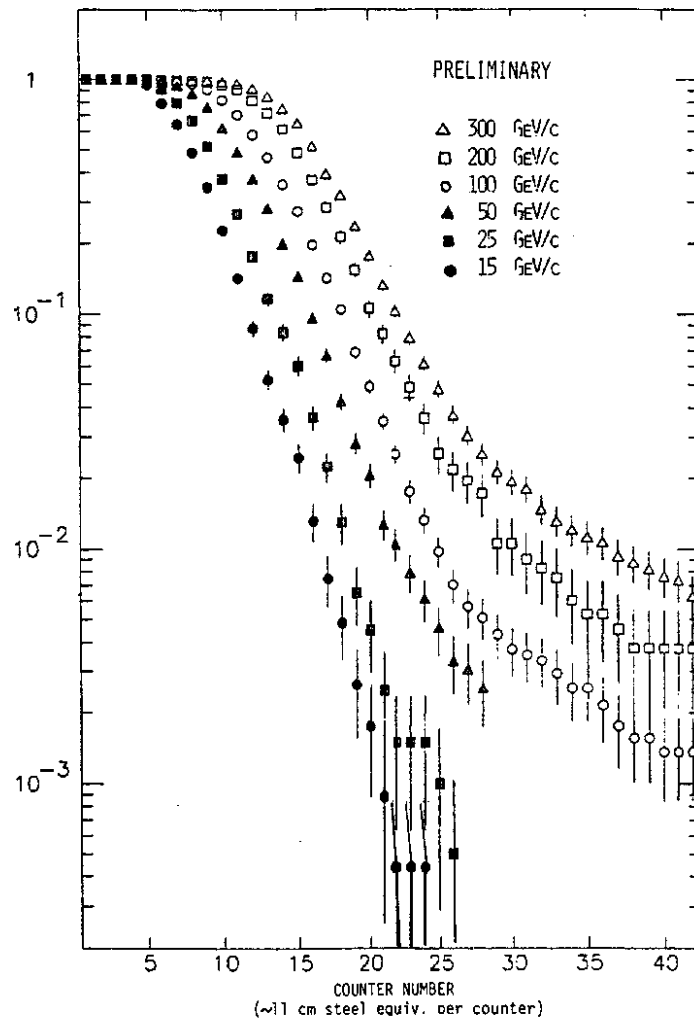
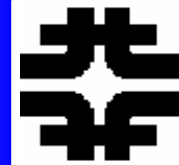


Leakage “tails” are reduced
By adding in the outer calorimeter
With suitable relative weights.

Fig. 27. Comparison of energy resolution (rms) for 300 GeV pions for different HCAL sampling configurations: Baseline Inner HCAL, Baseline Inner HCAL + 2 plates, Baseline Inner HCAL + HO, and Baseline Inner HCAL + 2 plates + HO.



Intrinsic Neutrino “Leakage”



“punch through” displays a length scale
 $\sim \lambda$ except for very deep into high
energy showers.

There is a component that does not fall off
rapidly in depth and which has a fraction
which rises rapidly with energy.

1 % at 300 GeV

due to $\pi \rightarrow \mu \nu$ decays of cascade pions

n.b. earth’s atmosphere -

We live at the bottom of a very diffuse

$\sim 10 \lambda$ calorimeter – the atmosphere.

Cosmic ray muons supply the background

dose of ~ 0.2 rad/yr natural background



Muons and Single Samples

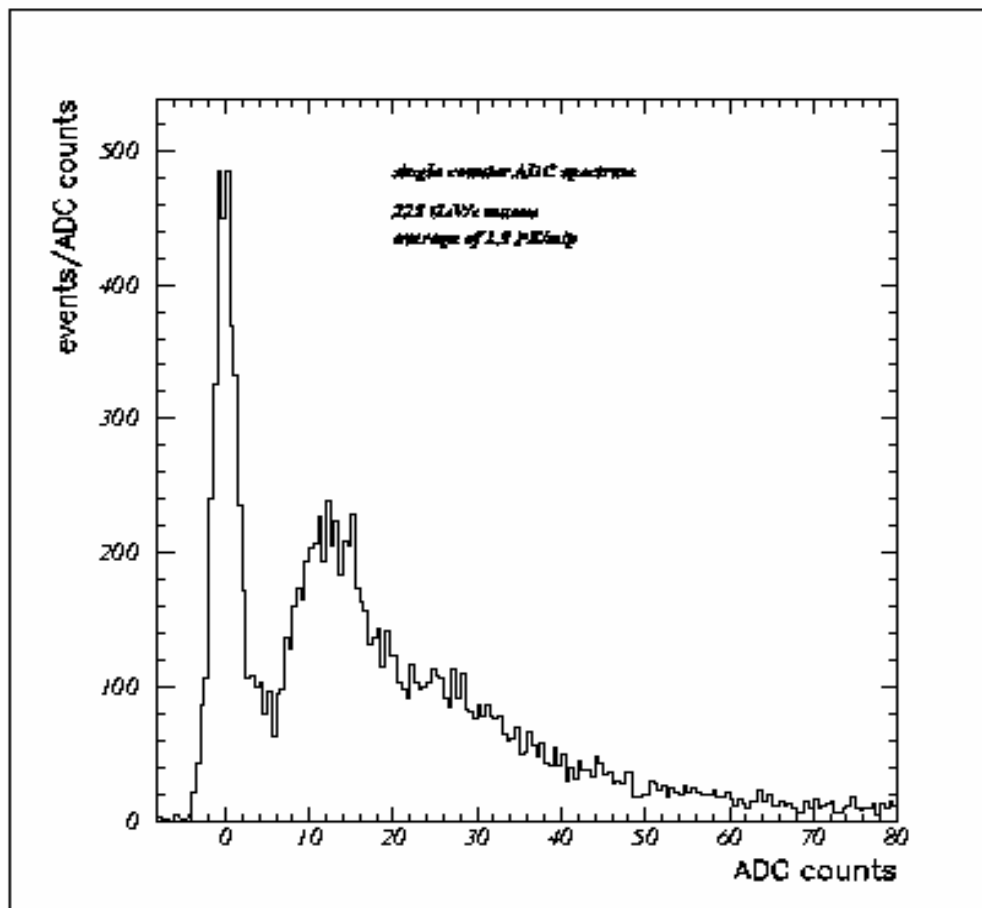


Fig. 3. E2(1995) Test Beam results: ADC spectrum of 225 GeV/c muons in a single counter. Based on the observed inefficiency of the counter, we estimate the average number of photoelectrons per minimum ionizing particle to be 1.3 PE/mip.

Single scint tile test
1.3 p.e./MIP

$$\exp[-\langle N \rangle] = 1 - \epsilon$$

$\langle N \rangle = 3$ is 95 % efficient



Muons in Sampling Calorimeters

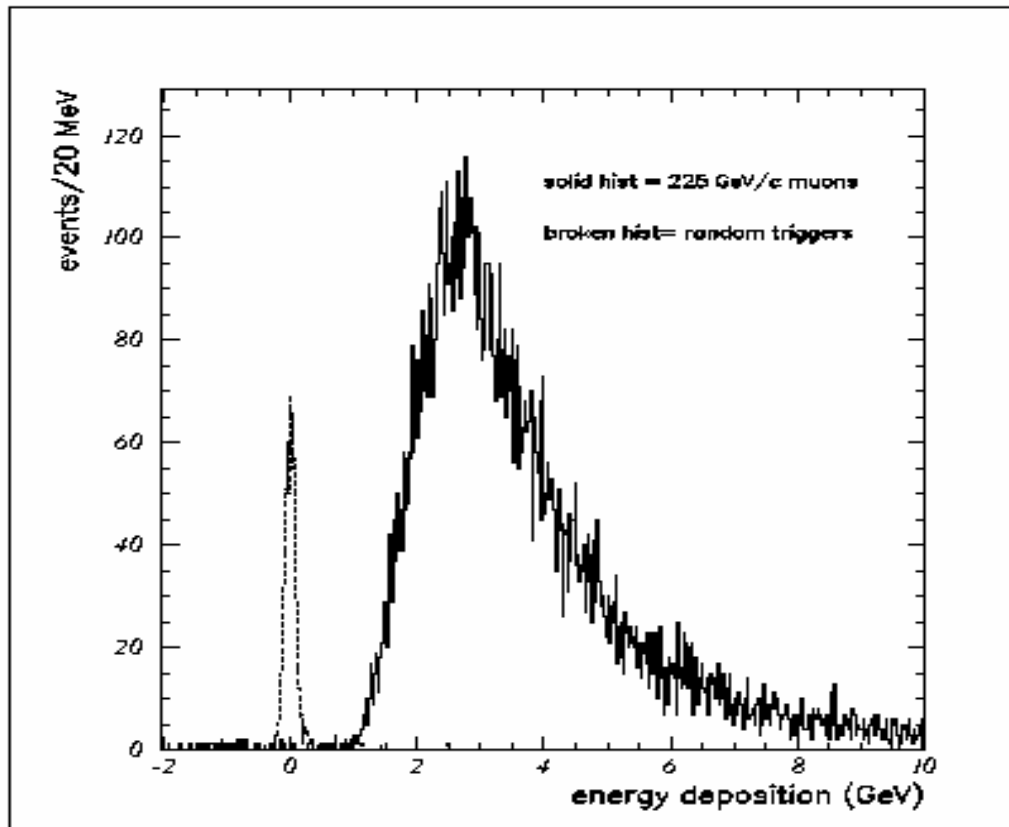
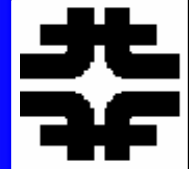
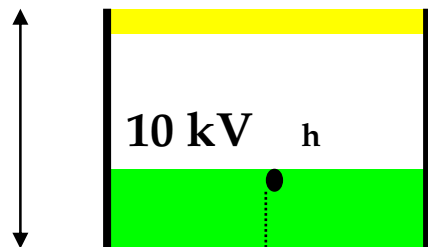
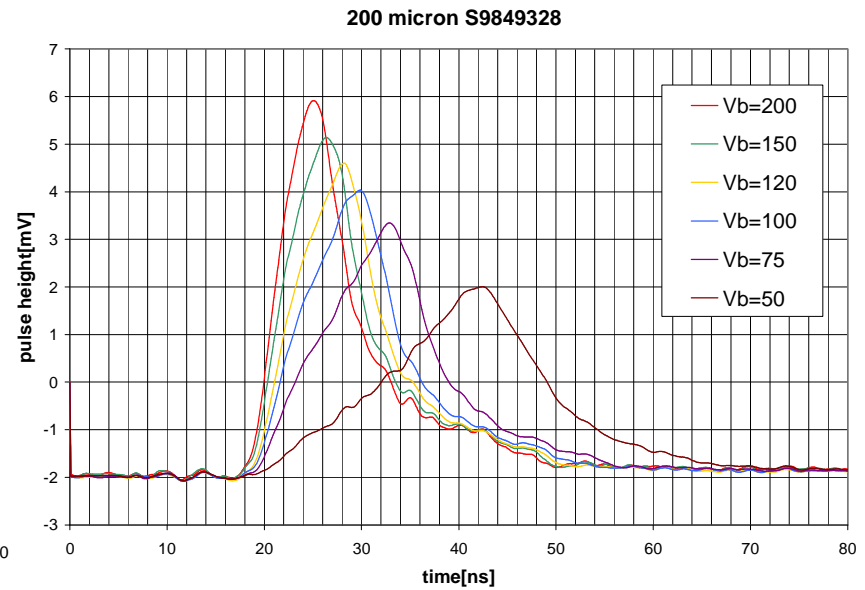
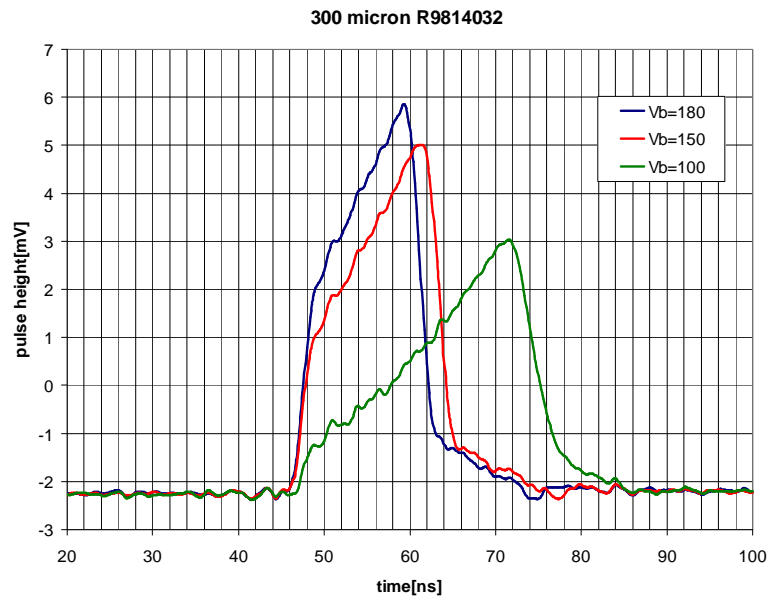
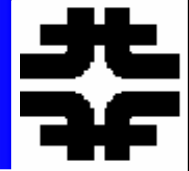


Fig. 8. H2(1995) Test Beam results: Energy deposited by 225 GeV/c muons in HCAL. Broken line shows the energy reconstructed in the HCAL for random triggers (pedestal events). The pedestal peak has RMS width of 80 MeV equivalent energy.

Muon calibration for the full HCAL in depth
 $\langle E_\mu \rangle \sim 3 \text{ GeV}$



Pulse Formation - Bias



Photocathode

Si Diode

E field

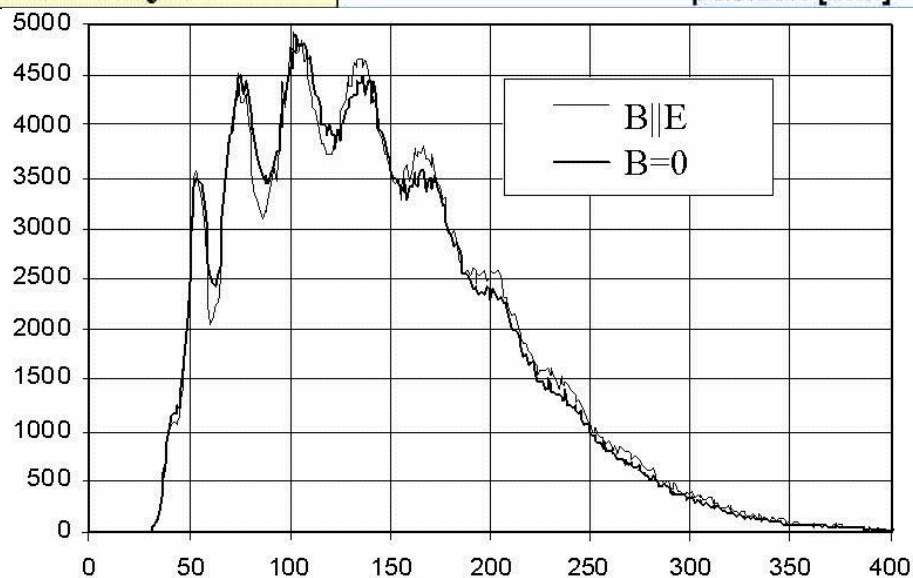
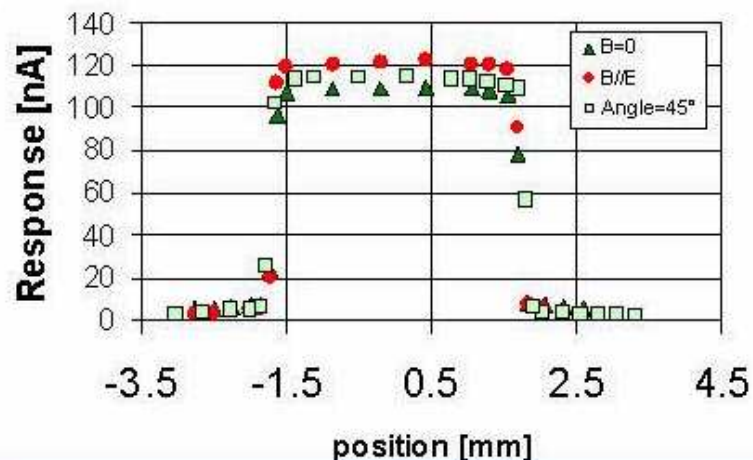


Backscatter in B Field



Backscatter focus yields 10% more signal with magnetic field on

Off-angle gain is reduced by longer path length through surface layer

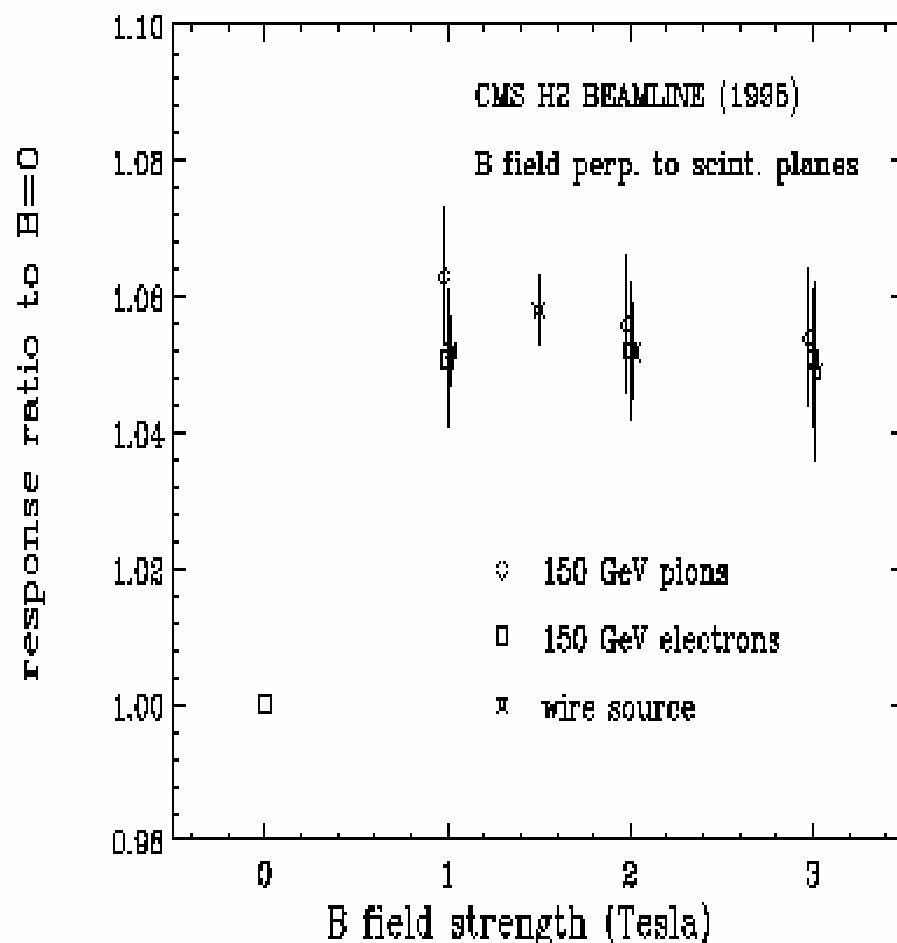




Scintillator and B Fields



Pion, electron, and gamma source response vs B field



Scintillators get brighter in B fields

For B perpendicular to sampling plates,
 π , e, μ , γ all show ~ 6 % increase

The effect saturates for $B > 2$ T



HCAL and e/π in B Fields

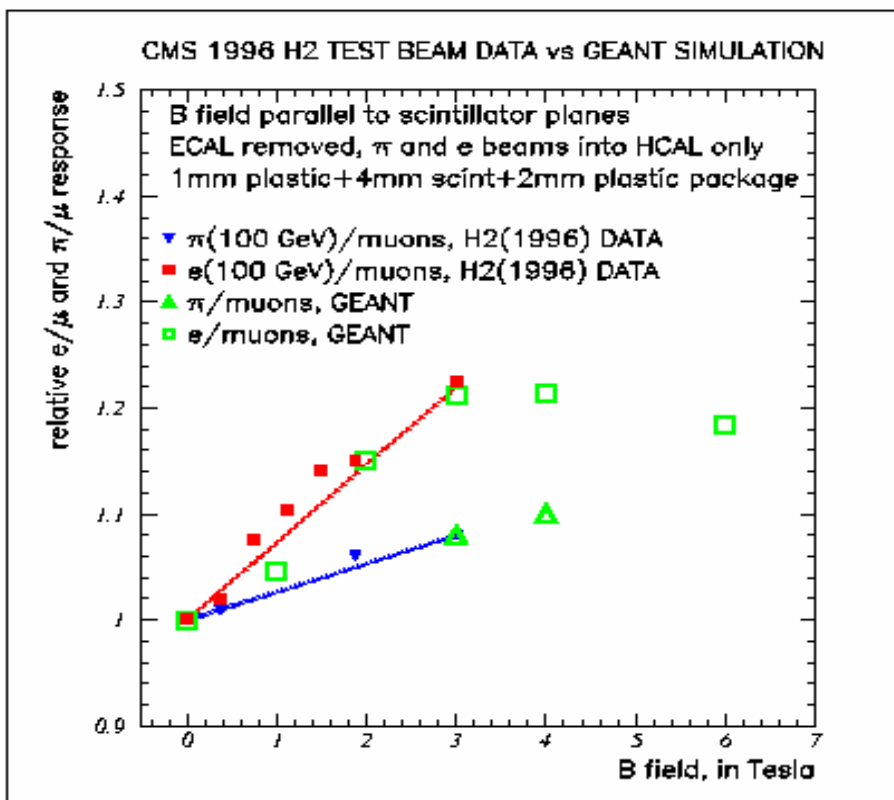


Fig. 7. Effect of B field on the average energy response of the tile/fiber calorimeter to pions, electrons (H2 data) (divided by the muon response) and comparison with GEANT predictions. B field lines were parallel to the scintillator plates (Barrel configuration). The overall scintillator brightening B field effect cancels when the ratio of electrons to muons is taken (upper curve), thus illustrating the increase from curving low energy electrons in the shower. The ratio of hadrons to muons (lower curve) shows a smaller increase thus indicating that the effect is a function of the electromagnetic fraction in the shower.

For B parallel to the sampling plates, π , e , μ , γ all show different effects. μ , γ show only the 6 % brightening e show $\sim 20\%$ increased response, while 100 GeV π show $\sim 10\%$ increase – after correcting for brightening

π are $< e$ since “fo” < 1 .

Recall shower energy deposited by soft e in the EM clusters. For $E_c \sim 7 \text{ MeV}$, the radius of curvature is $\sim 7.7 \text{ mm}$



HCAL - Path Length/Loopers

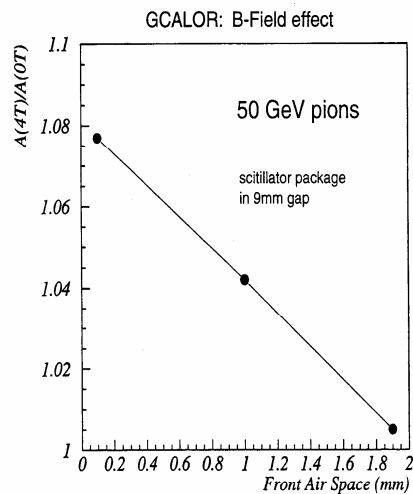
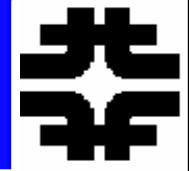
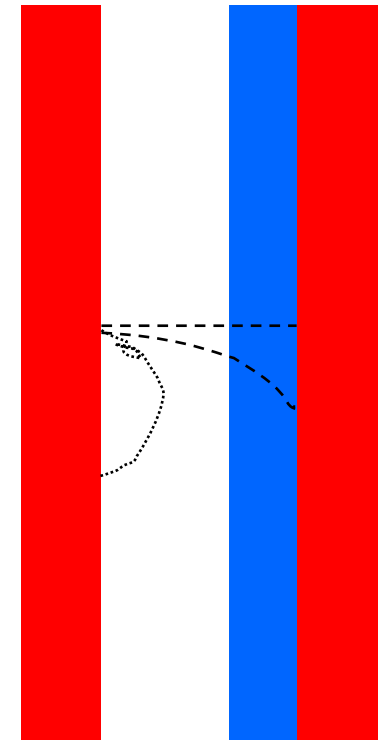


Fig. 1.35: Monte Carlo study on response of HB to 50 GeV pions in 4 Tesla field relative to response in 0 Tesla field with different air space between upstream absorber and scintillator package placed in 9mm gap between absorbers. The scintillator package consists of a 2mm plastic front cover plate, a 4mm scintillator and a 1mm plastic back cover plate.



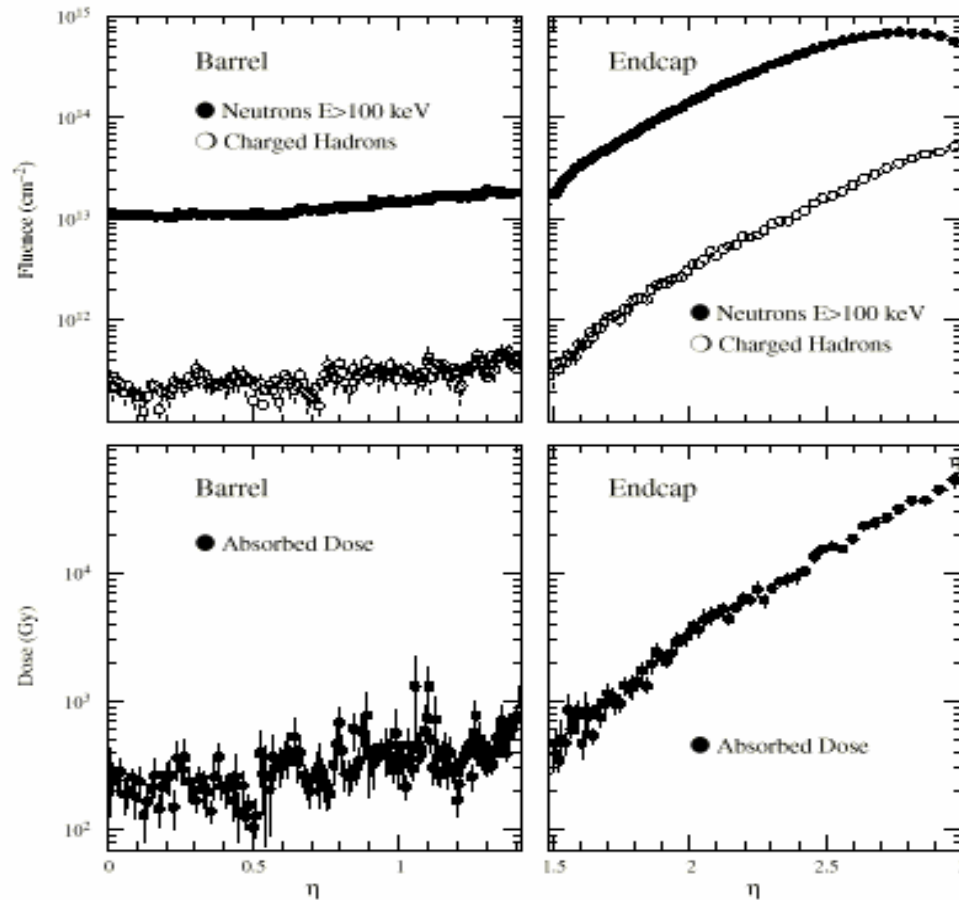
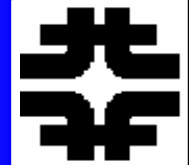
Can tune the effect out by playing “loopers” off against path length – but there are open spaces in the calorimeter which is inefficient

Increased path length gives increased light. This competes with “loopers” if there is a gap between the plate and the scint

n.b. mm scale



LHC - Radiation Fields



dose < 10 Mrad over the lifetime of the LHC

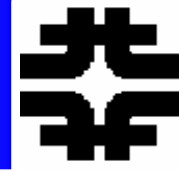
note the large n background inherent in pp machines

dose $\sim \exp(3\eta)$

Fig. A.7: Neutron ($E > 100$ keV) and charged hadron fluence and absorbed dose immediately behind the crystals as a function of pseudorapidity. The values are obtained in an aluminium-air mixture. Values correspond to an integrated luminosity of 5×10^5 pb⁻¹.



LHC - HCAL Dose



HCAL dose is monotonic, falling
From max in ECAL with length
Scale $\sim \lambda$. The dose is due to soft
pions, $P_T \sim 0.4$ GeV, $\eta \sim 3$, $P \sim 4$ GeV

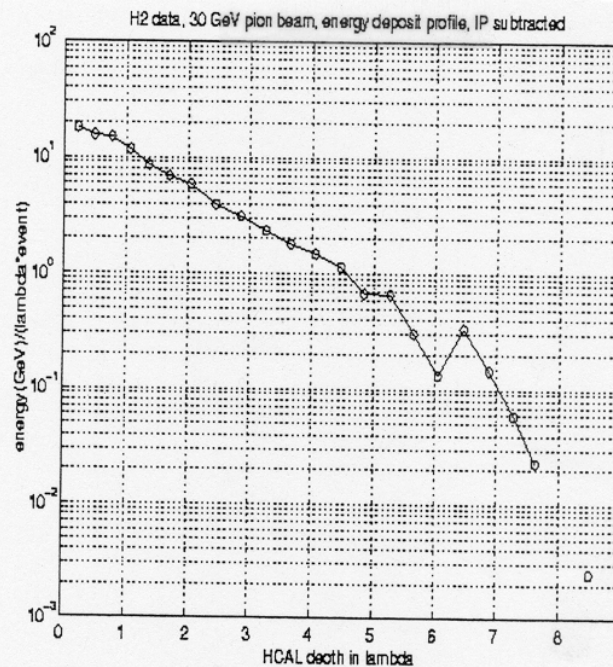
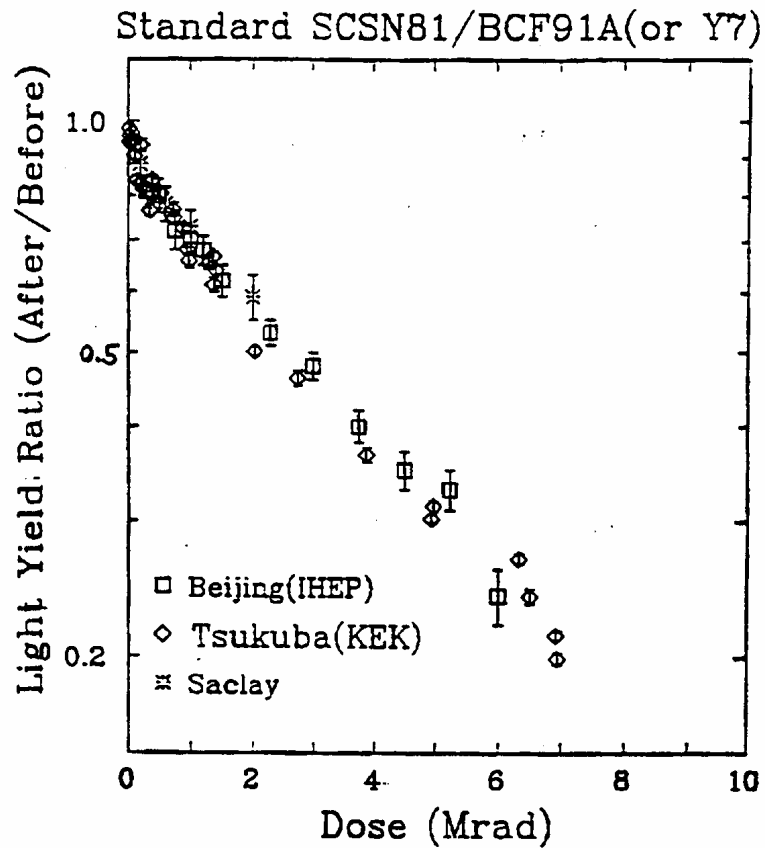


Fig. 1.9: Energy deposit as a function of depth for 30 GeV pions from the H2 test beam.



Scintillator - Dose/Damage



Scintillator under irradiation forms
Color centers which reduce the
Collected light output (transmission loss).

$$LY \sim \exp[-D/Do], Do \sim 4 \text{ Mrad}$$



HCAL - Raddam and z Sampling

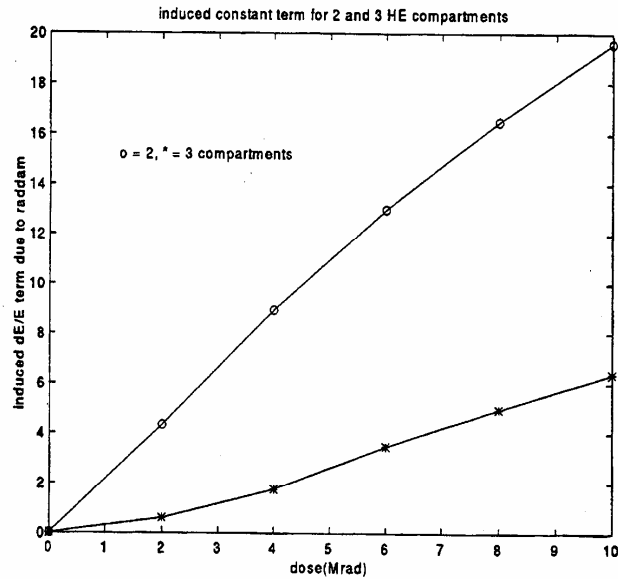
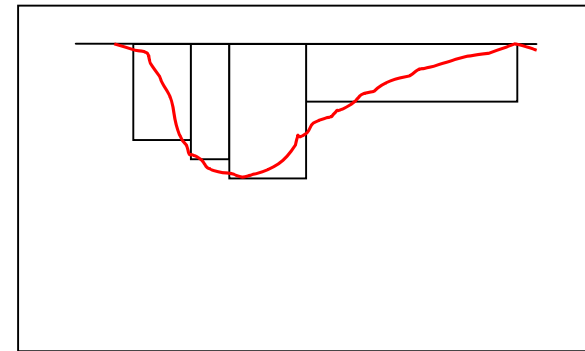


Fig. 1.10: Induced constant term in the energy resolution as a function of dose for 2 and 3 longitudinal compartments.

Solve Radiation Damage with Longitudinal Segmentation

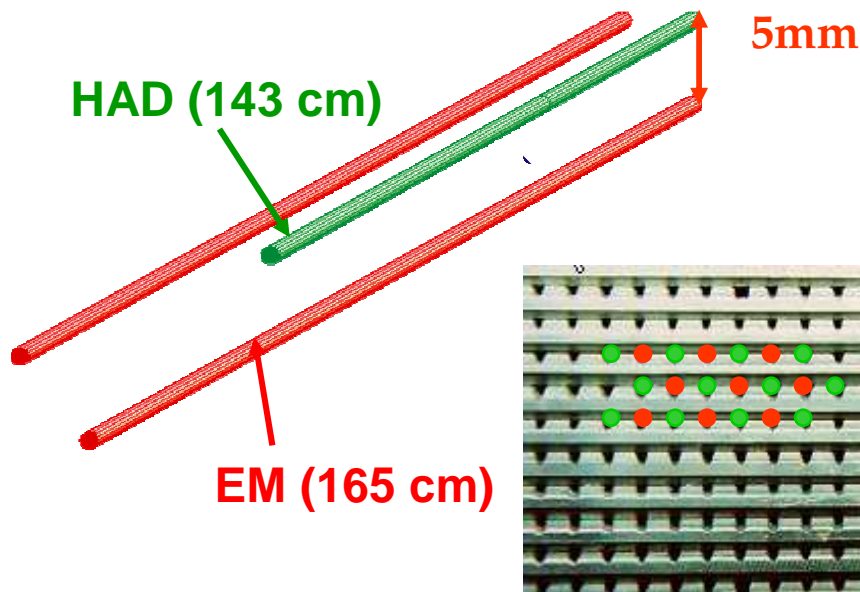
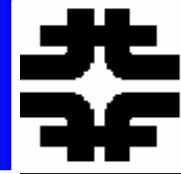
Independent calibration and readout of Each distinct segment.



For HCAL, at 5 Mrad maximum, dE/E goes from 10% \rightarrow 2% with 2 \rightarrow 3 compartments



HF detector



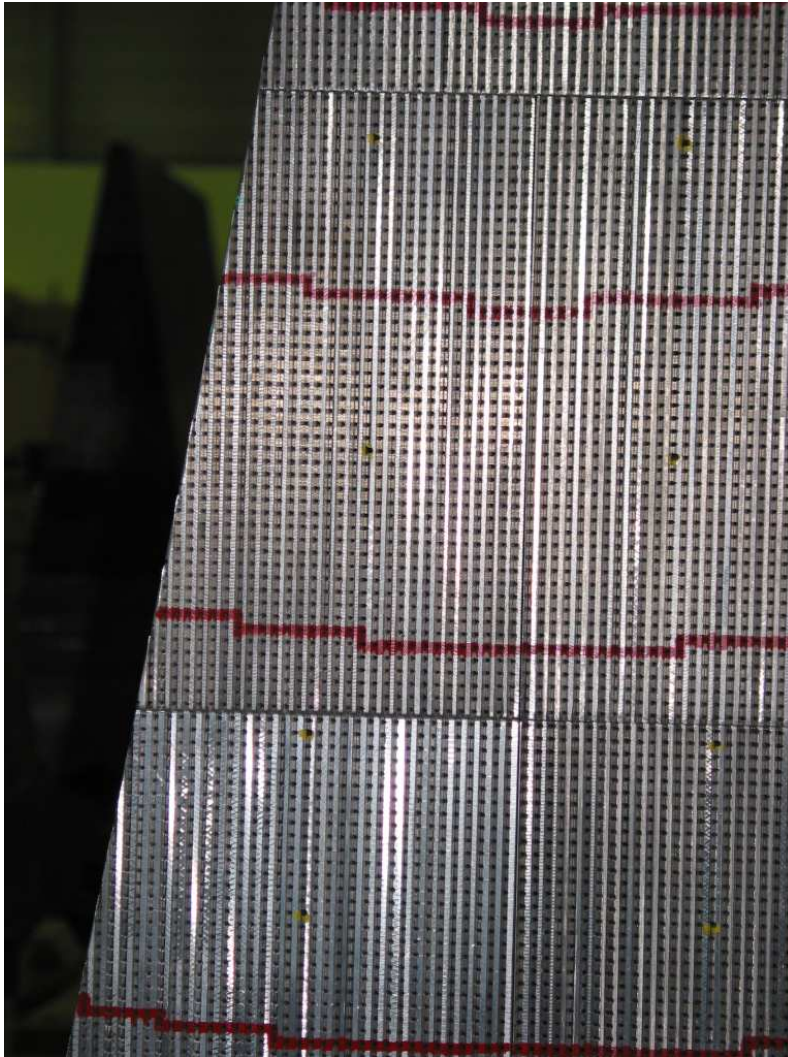
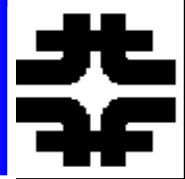
To cope with high radiation levels (>1 Grad accumulated in 10 years) the active part is Quartz fibers: the energy measured through the Cerenkov light generated by shower particles.

Iron calorimeter
 Covers $5 > \eta > 3$
 Total of 1728 towers, i.e.
 2 x 432 towers for EM and HAD
 $\eta \times \phi$ segmentation (0.175 x 0.175)

ETA	RADIUS		
2.866	1300.0	1 *	14 *
2.918	1234.2		
2.976	1162.0	2 *	15 *
3.064	1065.4		
3.152	975.0	3	16
3.240	893.3		
3.327	818.0	4	17
3.503	686.0		
3.677	576.0	5	18
3.853	483.0		
4.027	406.0	6	19
4.204	340.0		
4.377	286.0	7	20
4.552	240.0		
4.730	201.0	8	21
4.903	169.0		
5.205	125.0	9	22
		10	23
		11	24
		12	25
		13	26

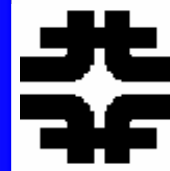


Fibers in the HF absorber



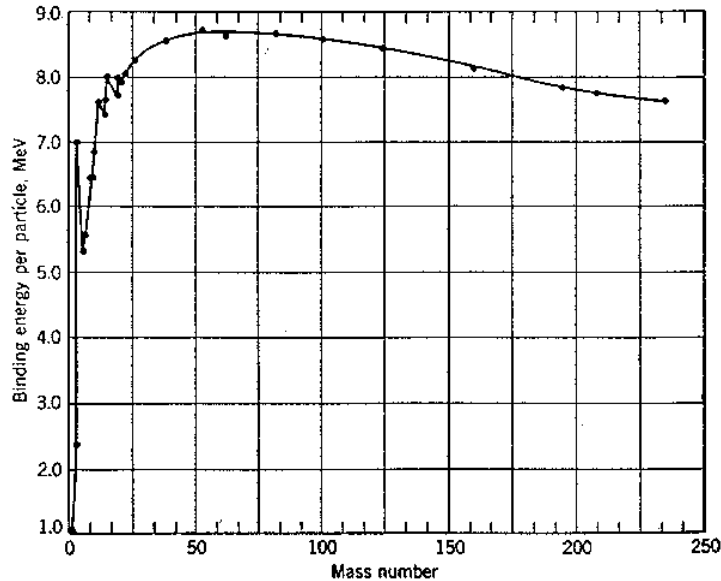


HF Fiber stuffing at CERN





Neutrons



Recall hadrons disrupt the medium

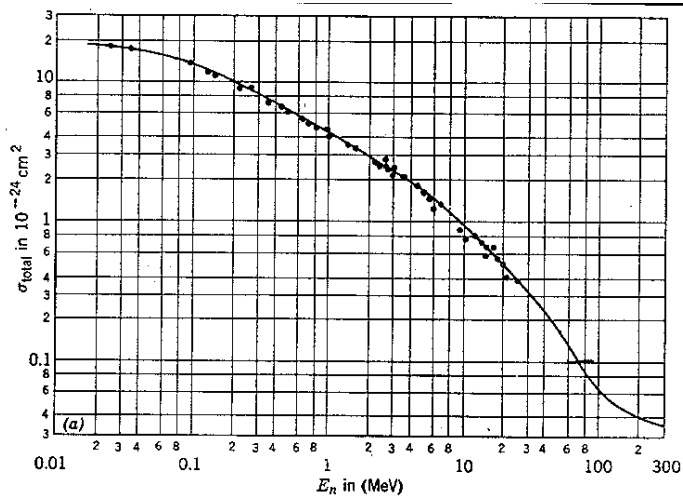
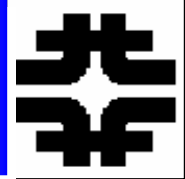
For 100 GeV pion, there are ~ 500 n near hadron shower maximum with $T_n \sim 1$ MeV [$B \sim 8$ MeV/nucleon], slow down and escape \rightarrow sea of soft n at the LHC

$$N_n \sim [5 E(\text{GeV})]$$

$$\langle T_n \rangle \sim 1 \text{ MeV}$$



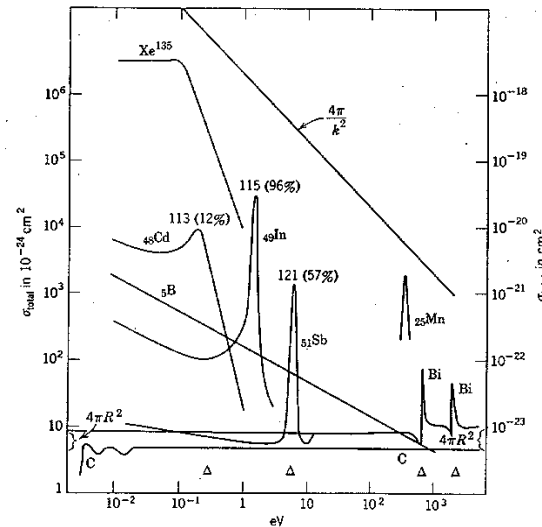
Neutron Detection



$$\left(\frac{A-1}{A+1}\right)^2 \leq \frac{T}{T_n} \leq 1$$

Recall billiards: off cushion - $T/T_n \sim 1$
 Off cue - $T/T_n \rightarrow 0$

n.b. scintillator sampling “eats” the n



S wave unitarity

Geometric cross section

exothermic reactions to detect thermal n



Standard Model



The Basic Constituents of the “Standard Model”

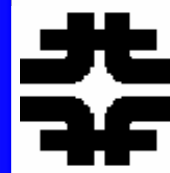
MATTER (SPIN 1/2)+	Generations			CHARGE Q *	
	$\begin{pmatrix} e \\ \nu_e \end{pmatrix}$	$\begin{pmatrix} \mu \\ \nu_\mu \end{pmatrix}$	$\begin{pmatrix} \tau \\ \nu_\tau \end{pmatrix}$	$\begin{pmatrix} 1 \\ 0 \end{pmatrix}$	LEPTONS
$\begin{pmatrix} u \\ d \end{pmatrix}$	$\begin{pmatrix} c \\ s \end{pmatrix}$	$\begin{pmatrix} t \\ b \end{pmatrix}$	$\begin{pmatrix} 2/3 \\ -1/3 \end{pmatrix}$	QUARKS	
INTERACTIONS (SPIN 1)	QUANTA	FORCE	COUPLING	# QUANTA	SYMBOL
	Gluons	Strong	$\alpha_s = g_s^2$	8	g
	Photons	EM	$\alpha = e^2$	1	γ
Weak Bosons	Weak	$\alpha = g_w^2$	3	$W^- Z^0 W^+$	

* Units are electron charge $|e|$.

+ Units are \hbar .



SM - Detection, ID



Detection/Identification Methods

SIGNATURE	DETECTOR	PARTICLE
Jet of Hadrons λ_o	Calorimeter	$u, c, t \rightarrow Wb$ d, s, b g
“Missing” Energy	Calorimeter	ν_c, ν_μ, ν_τ
Electromagnetic Shower, x_o	Calorimeter	$e, \gamma, W \rightarrow e\nu$
Only Ionization Interactions, dE/dx	Muon Absorber	$\mu, \tau \rightarrow \mu\nu\bar{\nu}$ $Z \rightarrow \mu\mu$
Decay with $c\tau \geq 100\mu m$	Si Tracking	c, b, τ



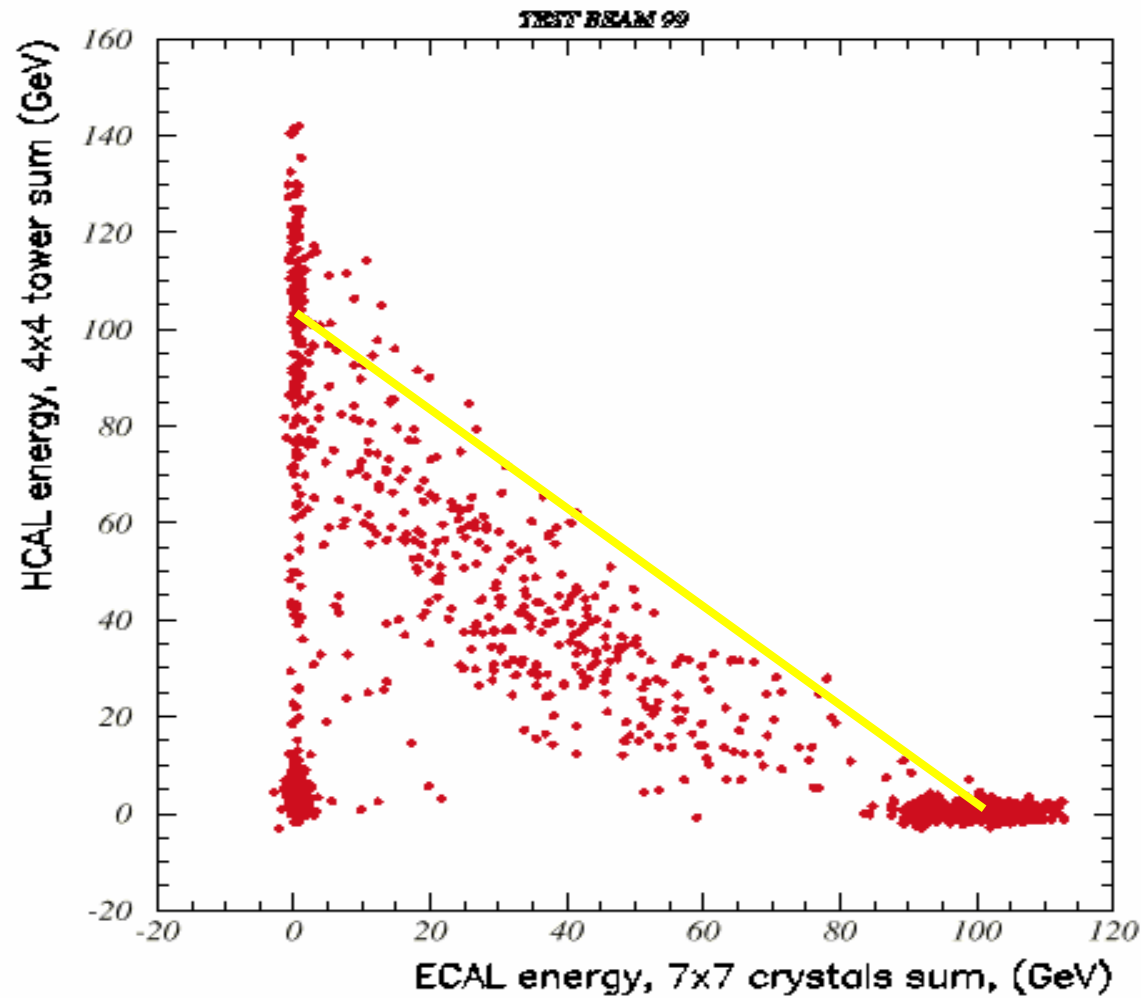
Detector Subsystems



Particle type	Tracking	ECAL	HCAL	Muon
γ				
e				
μ				
Jet				
Et miss				



HCAL + ECAL and Particle ID



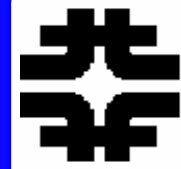
e, μ, π

in

"ECAL" +
HCAL



Jets and Calorimetry

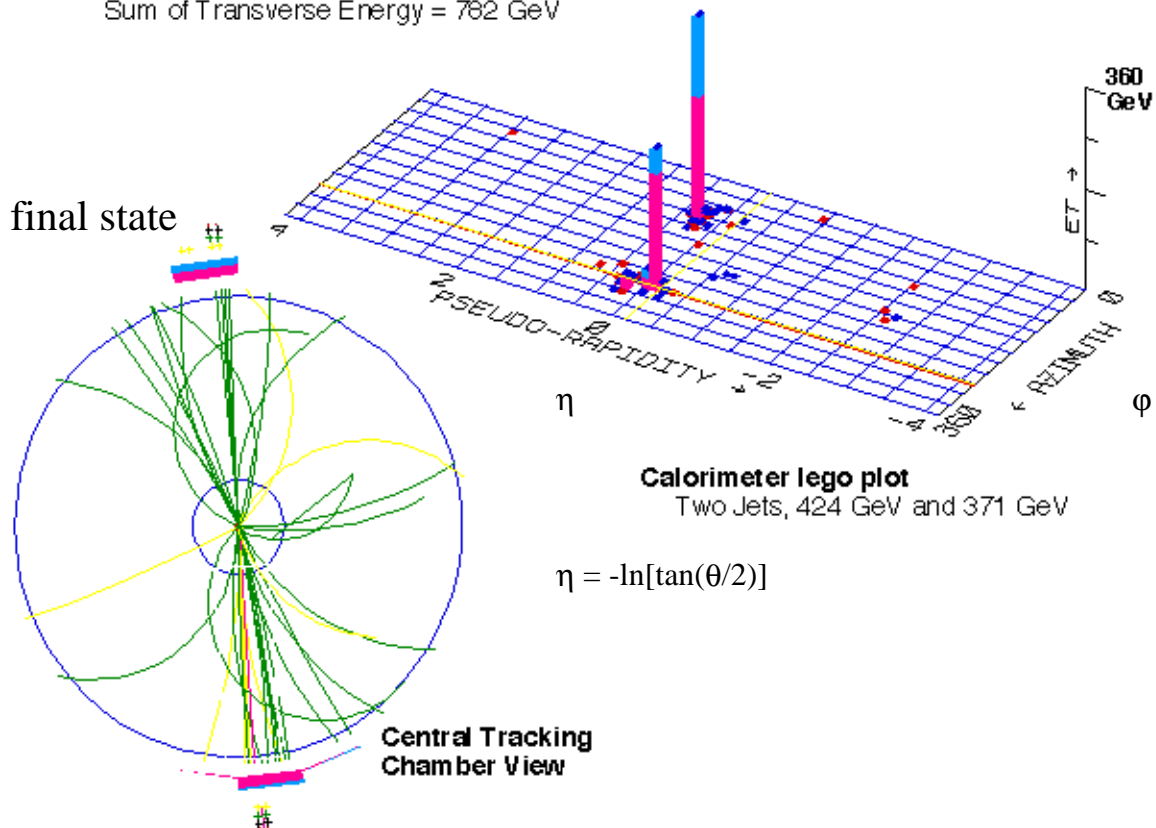


CDF: Highest Transverse Energy Event from the 1988-89 Collider Run

Sum of Transverse Energy = 782 GeV

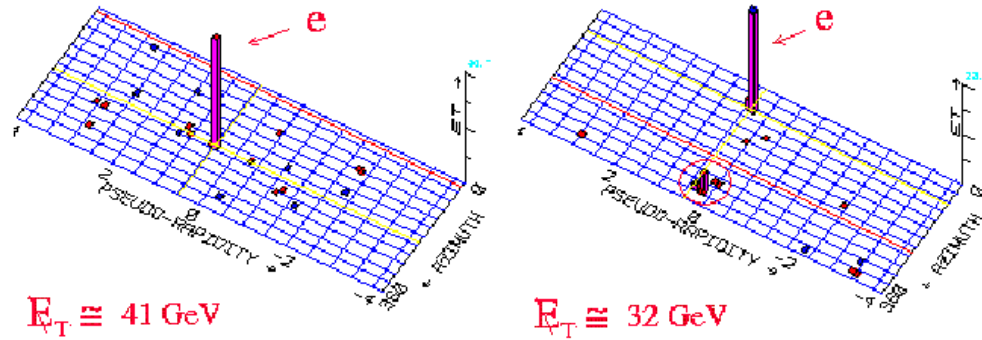
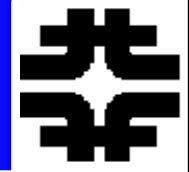
Jets

If quarks have $P_t \sim 0$, then final state
Is (2 body) “back to back”





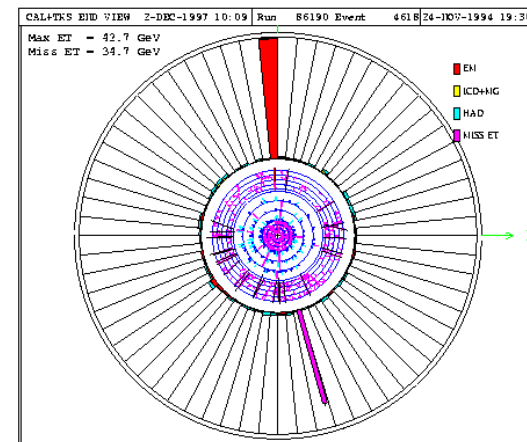
W --> e + ν and Calorimetry



$W \rightarrow e \nu$

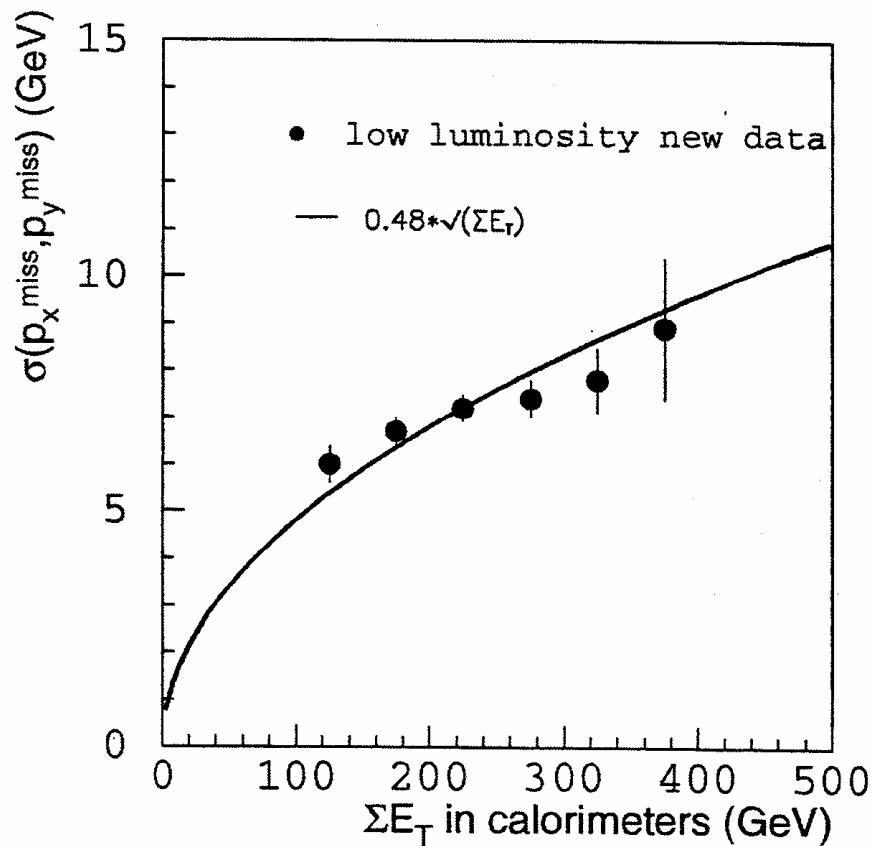
$M_W \sim 2 Pt \sim 80 \text{ GeV}$

EM Calor (e) + HCAL (missing Et)





Calorimeters and Neutrinos



Missing E_T is a global variable

$$dE/E \sim a/\sqrt{\Sigma(E_T)}$$

summed over all E_T in the event



Intrinsic Limitations



Transverse size set by shower extent, either X_0 or λ -> limit to tower size.

Longitudinal depth set by containment to $\sim 10 \lambda$. Limit on depth set by jet leakage.

Speed needs to be fast enough to identify bunch crossing (25 ns/LHC ; 12.5 ns/SLHC)

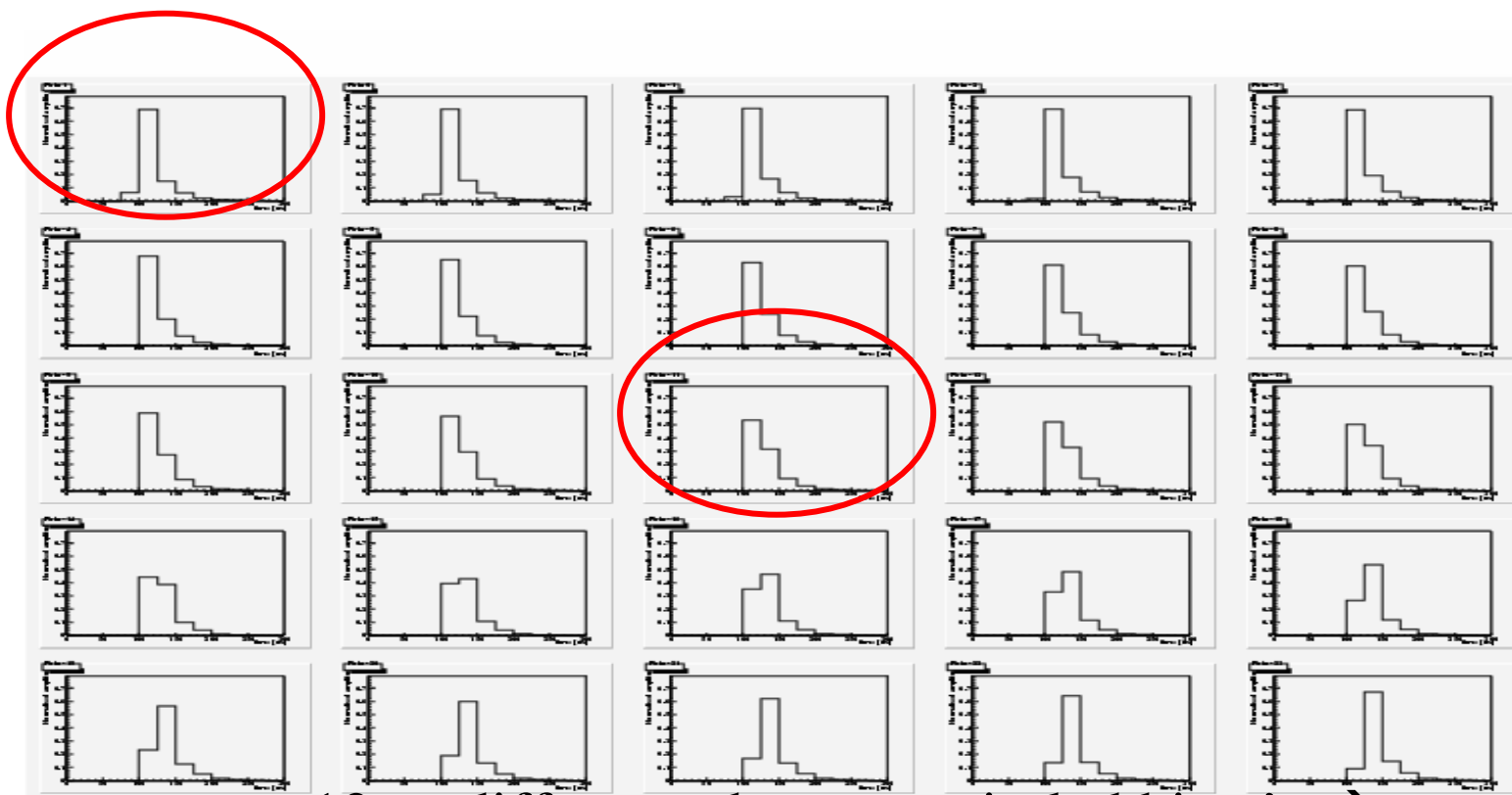
Jet resolution limited by FSR at LHC, not calorimeter energy resolution.



CMS HB Pulse Shape



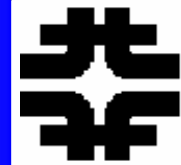
100 GeV electrons. 25ns bins. Each histo is average pulse shape, phased +1ns to LHC clock



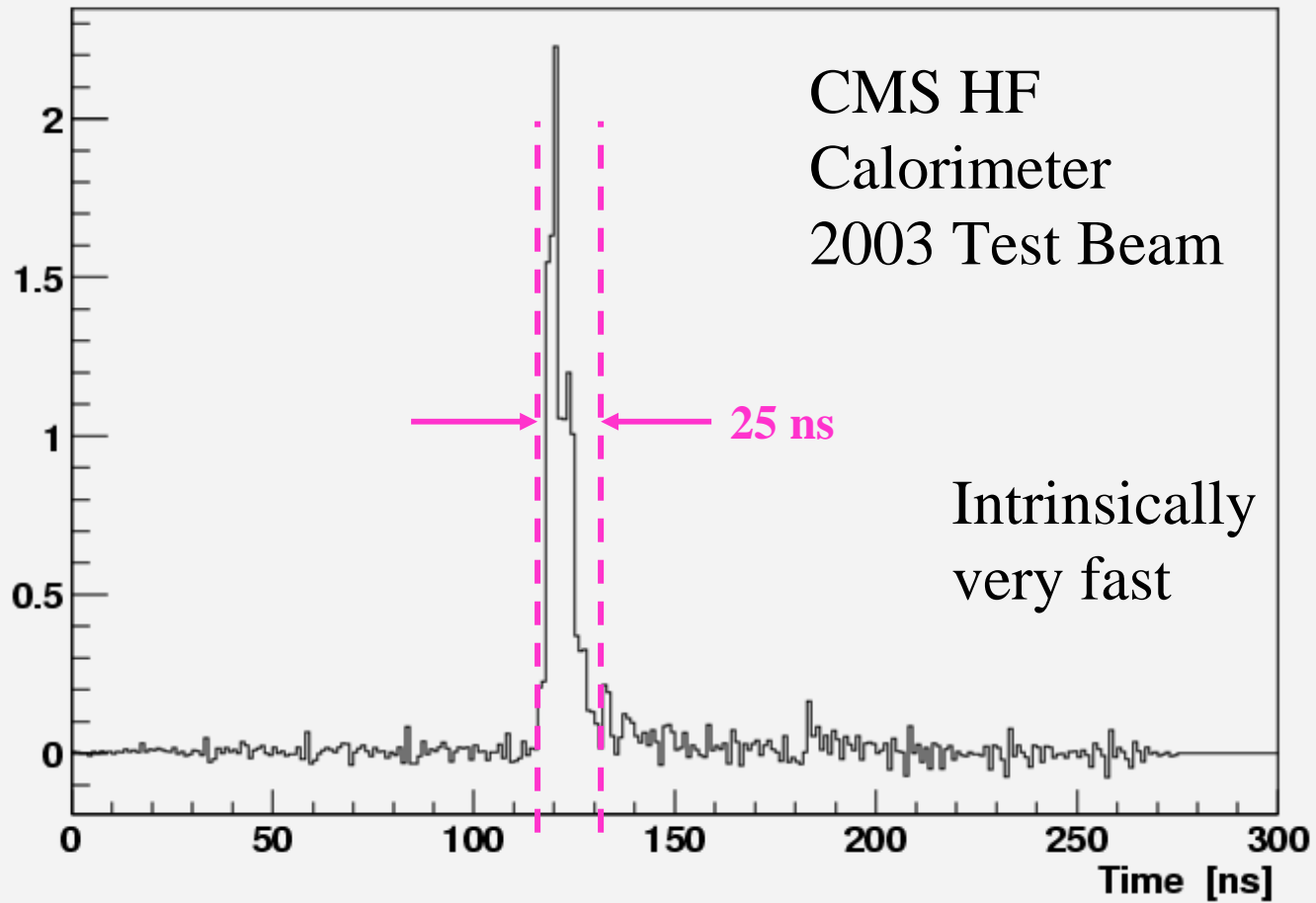
12 ns difference between circled histo's → no problem with bunch ID



HF Cerenkov Calorimeter Pulse Shape

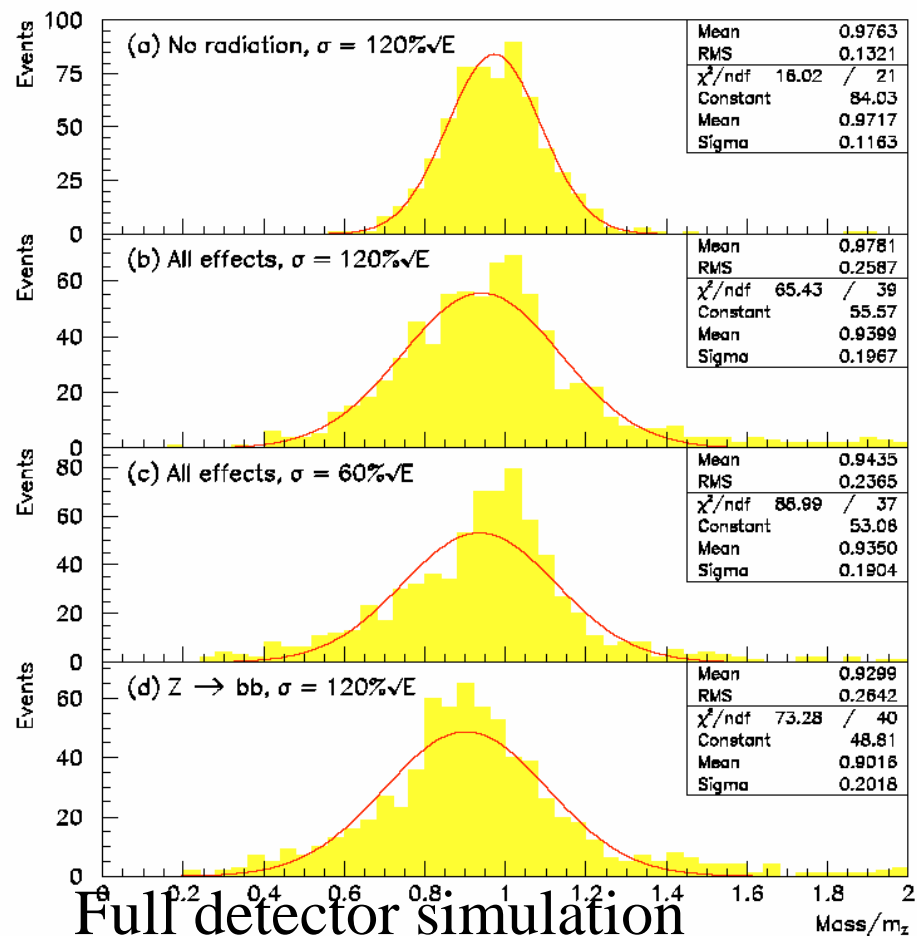
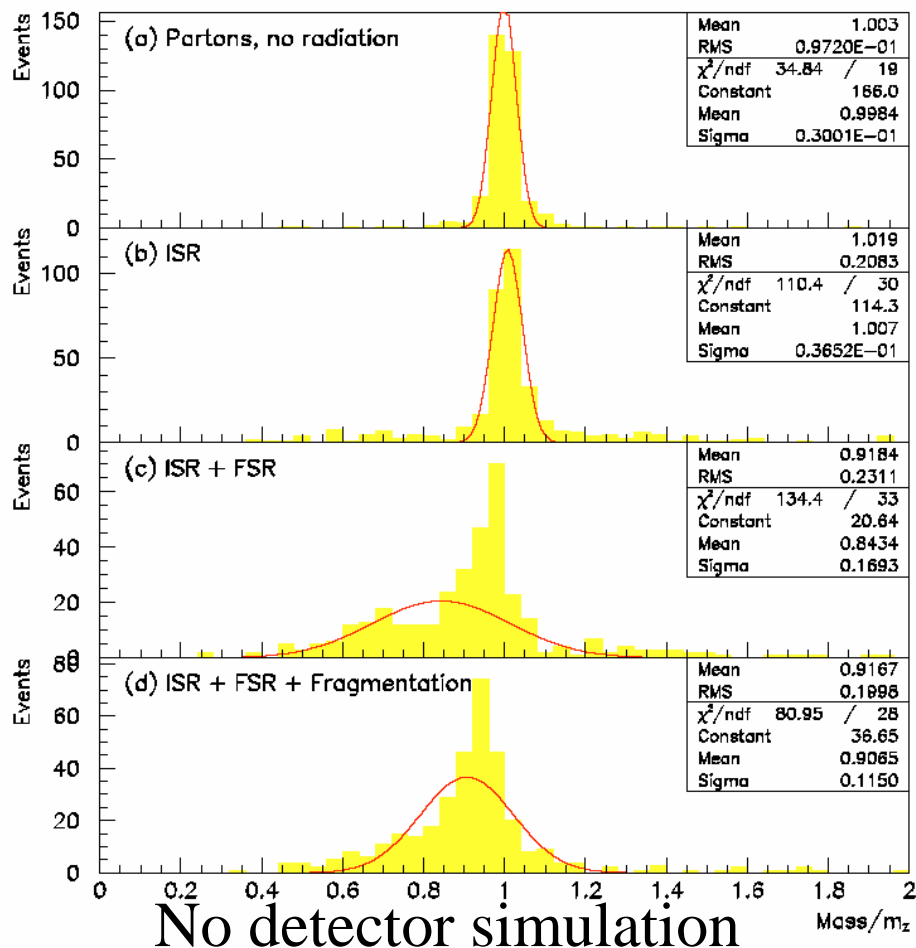
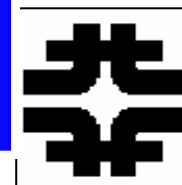


QIE pulse π 50 GeV (1ns)





Effects of Final State Radiation



Z's at the LHC in "CMS" detector



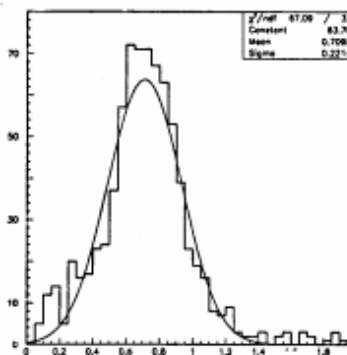
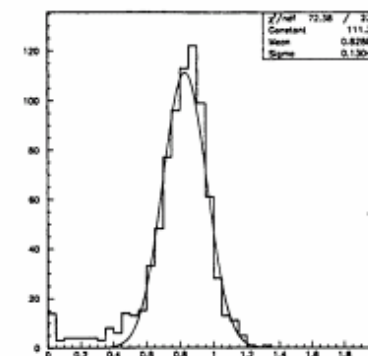
LHC – CMS Study of FSR



M_{JJ}/M_0 plots for dijets in CMS with and without FSR. The dominant effect of FSR is clear.

The $d(M/M_0)/(M/M_0)$ rms rises from ~ 11% to ~ 19%, the distribution shifts to smaller M/M_0 , and a radiative low mass tail becomes evident.

dM/M



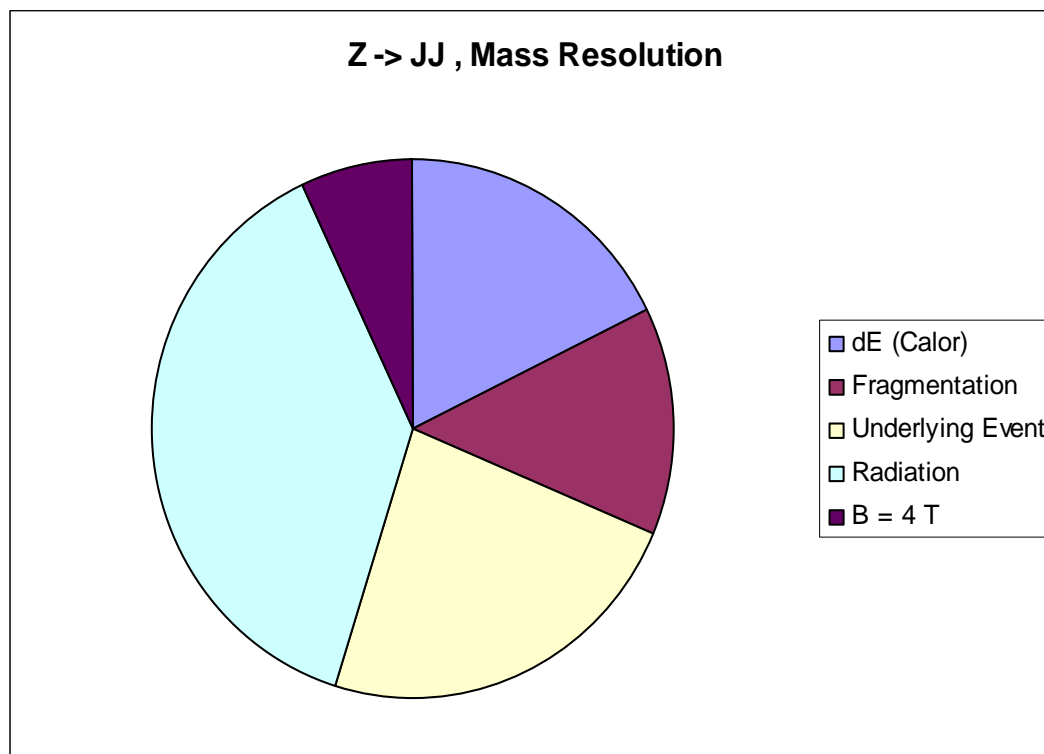
M/M_0



Hadron Collider- Dijet dM/M



A series of Monte Carlo studies were done in order to identify the elements contributing to the mass error. Events are low P_T , $Z \rightarrow JJ$. $dM/M \sim 13\%$ without FSR.



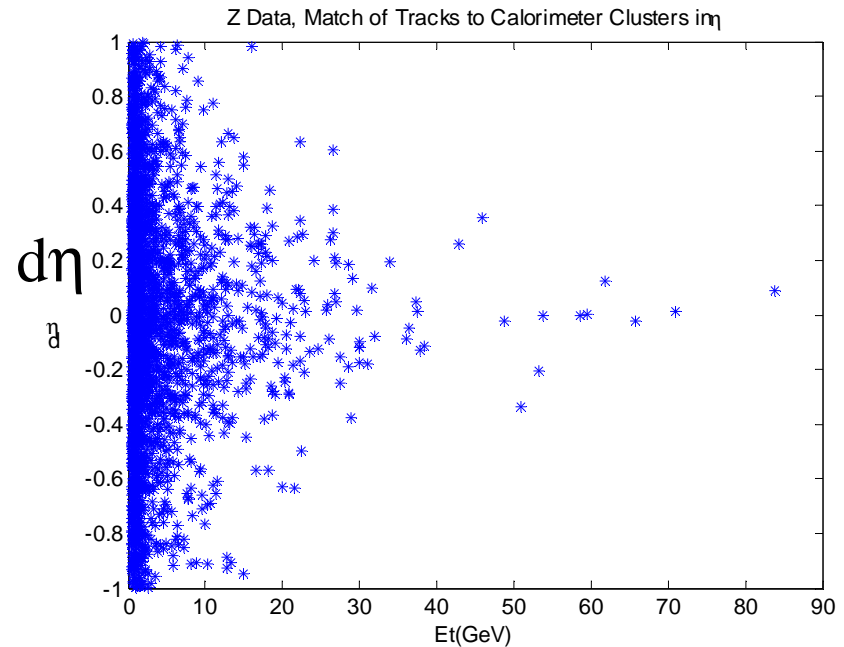
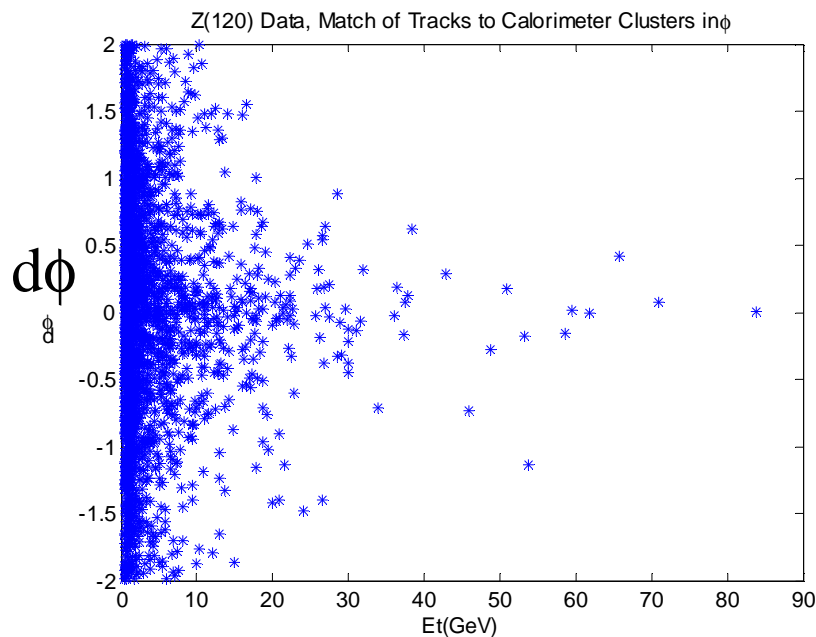
FSR is the biggest effect. The underlying event is the second largest error (if cone $R \sim 0.7$). Calorimeter resolution is a minor effect.



Track Matching



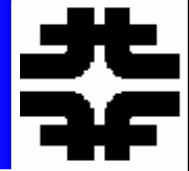
For a Monte Carlo sample of 120 GeV Z' match tracks in η and ϕ to “hadronic” clusters within the jet – cone size ~ 0.9 . Units are HCAL tower sizes.



ET

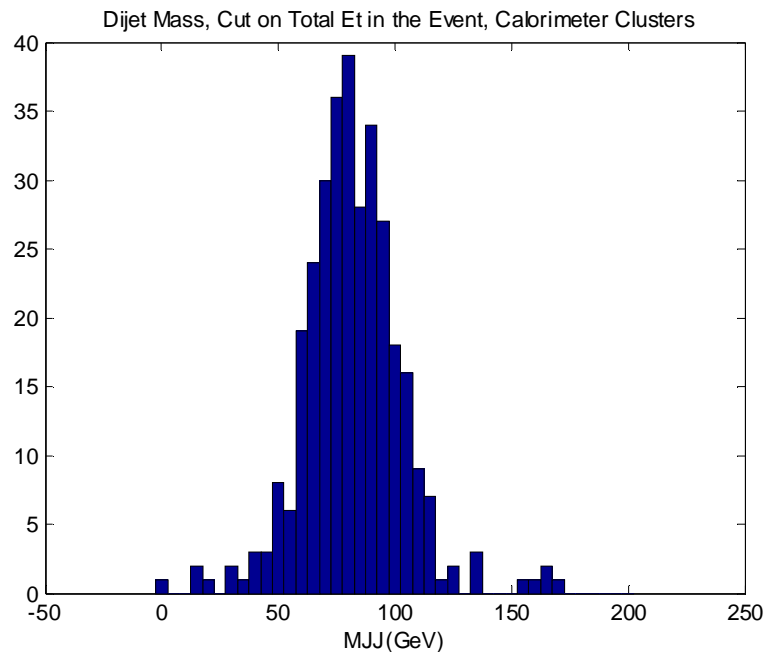


Improved Dijet Mass

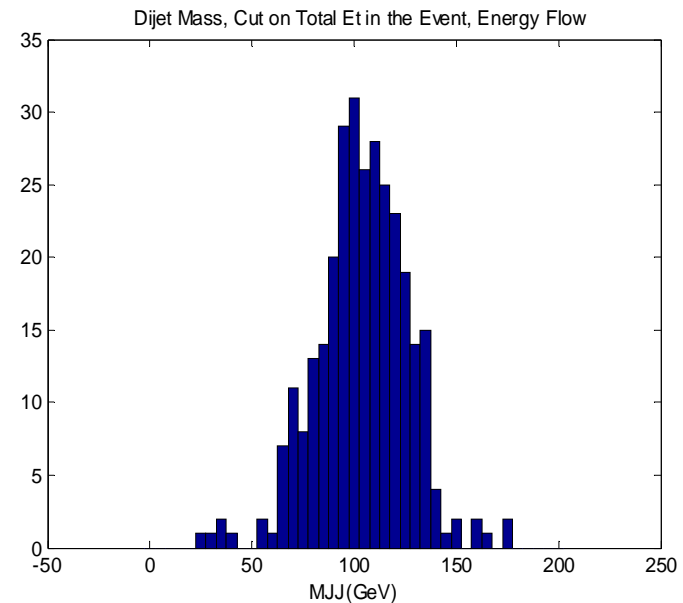


There is a ~ 22 % improvement in the dijet mass resolution.
This is welcome but clearly implies that calorimeter resolution is not the whole story.

Mean 81.7 GeV, (21%)

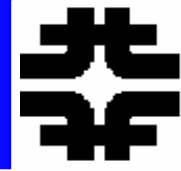


Mean 105.5 GeV, (17%)





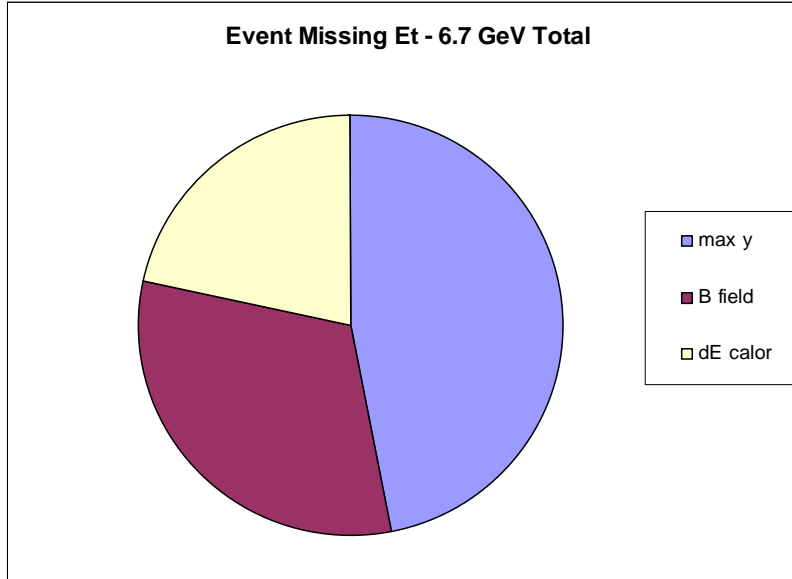
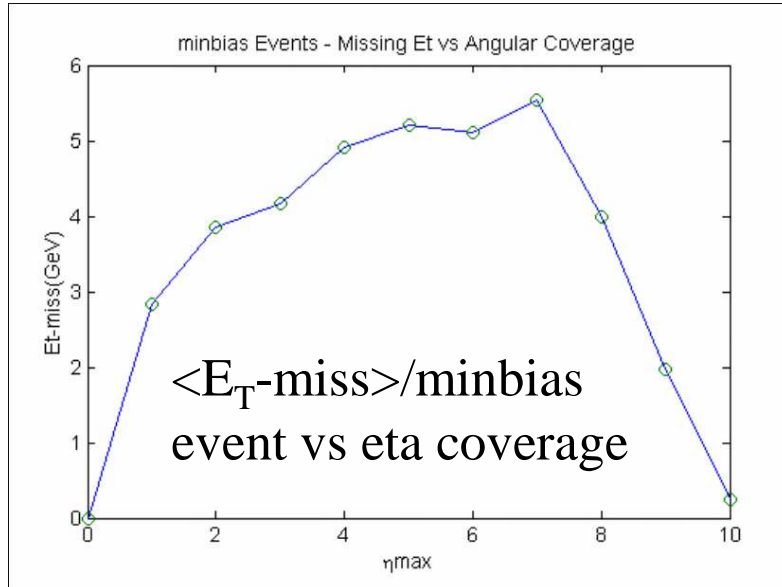
Pile-up Missing Et



Study done for CMS. Three major sources of detector induced missing E_T – incomplete angular coverage, B field “sweeping” to small angles and calorimetric energy resolution.

Clearly need radiation hard calorimetry to go to smaller angles – as C.M. energy increases particularly. Presently dose < 1 Grad at $|\eta| = 5$.

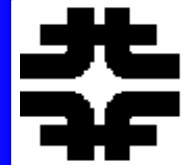
At SLHC, pileup events create a background of $\sim 5\text{GeV} * \text{sqrt}(62) = 40 \text{ GeV}$ E_T -miss / crossing. Fatal for W's, no problem for SUSY.



Contributions to E_T -miss for minbias events

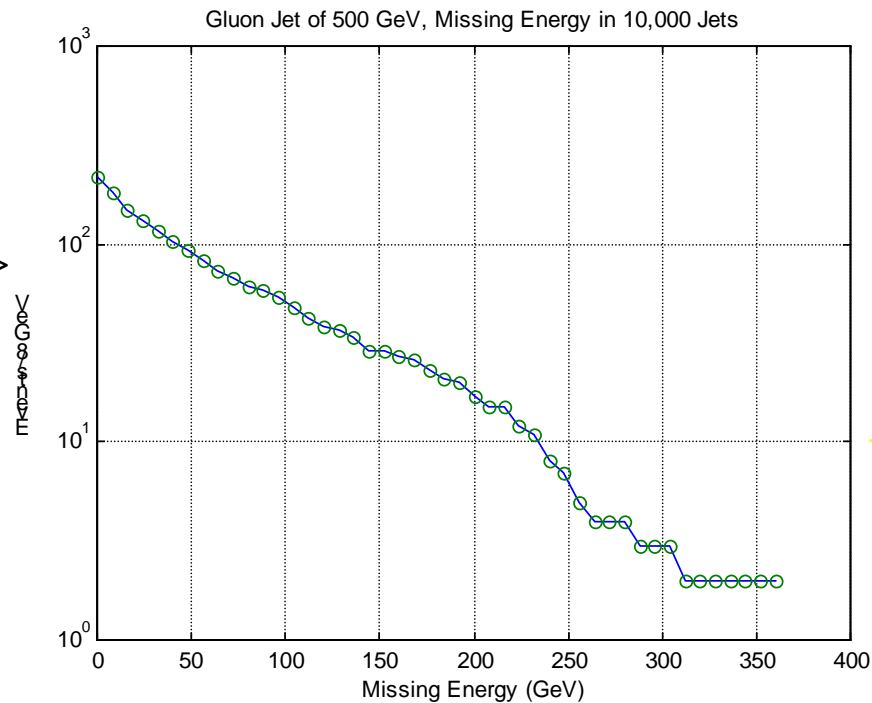


Intrinsic Limitations



Jet “splitting”, $g \rightarrow QQ$ and $Q \rightarrow q\ell\nu$, puts intrinsic limit on required depth. Jets themselves “leak”.

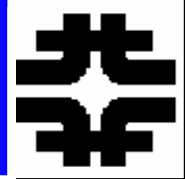
Jets
with
energy $>$
Missing
ET



**Jets “leak”
too – 0.1 %
will lose $>$
 $\frac{1}{2}$ of the
energy due
to splitting.**



Gluon Splitting



Gluon Splitting is a major source of real missing transverse energy

Require missing E_T to not point at a jet? OK but not very efficient.

